# Online Decision Mediation

**Daniel Jarrett**[1] **Alihan Hüyük**[1] **Mihaela van der Schaar**[1,2,3]

Department of Applied Mathematics and Theoretical Physics
[1]University of Cambridge, [2]UCLA, [3]Alan Turing Institute

[dkj25,ah2075,mv472]@cam.ac.uk

## Abstract

Consider learning a decision support assistant to serve as an intermediary between (oracle) expert behavior and (imperfect) human behavior: At each time, the algorithm observes an action chosen by a fallible agent, and decides whether to *accept* that agent's decision, *intervene* with an alternative, or *request* the expert's opinion. For instance, in clinical diagnosis, fully-autonomous machine behavior is often beyond ethical affordances, thus real-world decision support is often limited to monitoring and forecasting. Instead, such an intermediary would strike a prudent balance between the former (purely prescriptive) and latter (purely descriptive) approaches, while providing an efficient interface between human mistakes and expert feedback. In this work, we first formalize the sequential problem of *online decision mediation* —that is, of simultaneously learning and evaluating mediator policies from scratch with *abstentive feedback*: In each round, deferring to the oracle obviates the risk of error, but incurs an upfront penalty, and reveals the otherwise hidden expert action as a new training data point. Second, we motivate and propose a solution that seeks to trade off (immediate) loss terms against (future) improvements in generalization error; in doing so, we identify why conventional bandit algorithms may fail. Finally, through experiments and sensitivities on a variety of datasets, we illustrate consistent gains over applicable benchmarks on performance measures with respect to the mediator policy, the learned model, and the decision-making system as a whole.

## 1 Introduction

Research in data-driven decision support has burgeoned in recent years, with proposed applications in a wide variety of domains such as finance [1], psychology [2], and medicine [3]. Most work on machine learning for decision support falls into two categories: On one hand, *descriptive* approaches deal with monitoring, forecasting, and learning interpretable parameterizations of observed human behavior [4–8]. While such tools can help audit and debug decision-making, they play a limited role in directly guiding human behavior. On the other hand, *prescriptive* approaches deal with systems that behave autonomously, optimally, and with minimal manual control [9–12]. While such tools can reduce the need for expert input, they are often at odds with ethical considerations—especially in high-stakes settings such as healthcare [13–18]. Instead, we argue for a third: We believe machine learning decision support has a viable role as an *intermediary* between (oracle) expert behavior and (imperfect) human behavior—that is, as an "assistant", which would strike a prudent balance between the above two approaches, while providing an efficient interface between human mistakes and expert feedback.

**Online Decision Mediation** In this paper, we consider learning and evaluating *mediator policies* for online decision support from scratch: At each time step, upon observing the context vector of an incoming instance, the mediator policy decides whether to *accept* the human's action, *intervene* with its own output, or *request* the expert's opinion—and this determines which action is ultimately taken. Deferring to the oracle obviates the risk of error, but incurs an upfront penalty, and reveals the otherwise hidden expert action as a new training data point. As our running example, consider the task of

36th Conference on Neural Information Processing Systems (NeurIPS 2022).

early diagnosis in Alzheimer's disease, where the action is to diagnose each incoming patient as cognitively normal, mildly impaired, or at risk of dementia [19, 20]. Our problem setting is distinguished primarily by three key characteristics: (1) Instances—i.e. patients—arrive in a *streaming* process, and actions must be taken immediately and sequentially. (2) Feedback—i.e. true diagnoses—is only available in an *abstentive* manner, meaning ground truths are only revealed if the oracle is deferred to. (3) Evaluation—i.e. cumulative regret—is computed in an *online* fashion, without convenient separation into "training" versus "testing" phases. This setting is challenging but general, and applicable wherever domain experts are resource-constrained, e.g. if the costs of definitive examinations are high.

**Contributions** In the sequel, we first formalize this sequential problem of *online decision mediation* ("ODM"), and establish its unique challenges versus more conventional problem settings (Section 2). Second, we identify why conventional bandit algorithms may fail, and describe our proposed solution, *uncertainty-modulated policy for intervention and requisition* ("UMPIRE"), which seeks to trade off (immediate) loss terms against expected (future) improvements in generalization error (Section 3). Finally, through experiments and sensitivities on a variety of real-world datasets, we illustrate consistent gains over applicable benchmarks on a comprehensive set of performance measures with respect to the mediator policy, the learned model, and the entire decision-making system as a unit (Section 4).

**Implications** Humans are heterogeneous, and mistakes require timely correction. Machines are also fallible, and models require timely learning. The implications are clear: Rather than pitting computers *against* clinicians, an efficient mediator should *augment* clinician capabilities by leveraging costly but informative expert resources. By focusing on the (human-expert-mediator) decision-making system as a whole, we take a first step towards more methodical integration of machines "into the loop". Moreover, the technical problem itself combines diverse challenges from sequential decision-making, learning with rejection, and active learning, thus opening the door to multiple avenues of further work.

## 2 Online Decision Mediation

### 2.1 Problem Formulation

We use uppercase for random variables, and lowercase for specific values. Let $X$ denote the input variable, taking on values $x \in \mathcal{X}$, and let $Y$ denote the target variable, taking on values $y \in \mathcal{Y}$. In line with related fields, $X$ may synonymously be referred to as "contexts", "features", and "states" depending on the underlying task, and $Y$ may likewise be referred to as "actions", "decisions", and "labels". Per our motivating example, we shall adopt the "context-action" terminology for consistency, although our framework applies to any decision task that requires mapping inputs to specific outputs. Following most related settings, we focus on discrete action spaces, and leave continuous actions for future work.

**Human, Expert, and Mediator** Let $\rho(X)$ denote an exogenous distribution from which a streaming sequence of contexts $\{X_t\}_t$ is drawn and indexed by time step. We consider three decision-makers: a human, an expert, and a mediator. In each round, a human action is drawn as $\tilde{Y}_t \sim \tilde{\pi}(\cdot|X_t)$ from an (unknown and possibly stochastic) *human policy* $\tilde{\pi} \in \Pi$. For instance, this is the noisy diagnosis issued by an apprentice clinician. If prompted, an expert action may likewise be drawn as $Y_t \sim \pi_*(\cdot|X_t)$ from an (unknown and possibly stochastic) *expert policy* $\pi_* \in \Pi$. For instance, this is the final diagnosis issued by a senior doctor—that is, should they indeed be appointed to conduct a full examination of the patient. Finally, a "mediator" is identified by the tuple $(\hat{\pi}, \phi)$, consisting of a (learned) *model policy* $\hat{\pi} \in \Pi$—from which model actions $\hat{Y}_t \sim \hat{\pi}(\cdot|X_t)$ may be drawn—as well as a *mediator policy* $\phi \in \Phi$:

**Definition 1 (Decision System)** Let $\mathcal{S} := (\tilde{\pi}, \hat{\pi}, \pi_*, \phi)$ denote the *decision system* as a whole. Given an incoming $(X, \tilde{Y})$, the mediator policy defines a distribution $\phi(\cdot|X, \tilde{Y})$ over the space of mediator actions $\mathcal{Z} := \{0, 1, 2\}$, consisting of options *accept* ($z = 0$), *intervene* ($z = 1$), and *request* ($z = 2$). Let $\delta(Y - y)$ be the Dirac delta centered at $y$; drawing $Z \sim \phi(\cdot|X, \tilde{Y})$ induces the overall *system policy*:

$$\pi_{\mathcal{S}}(\cdot|X, \tilde{Y}) := \mathbb{1}_{[Z=0]}\delta(Y - \tilde{Y}) + \mathbb{1}_{[Z=1]}\delta(Y - \arg\max_y \hat{\pi}(y|X)) + \mathbb{1}_{[Z=2]}\pi_*(\cdot|X) \qquad (1)$$

Intervening incurs some cost $k_{\text{int}}$ (e.g. inconveniencing the apprentice clinician to reconsider/alter their decision). Requesting incurs some cost $k_{\text{req}}$ (e.g. appointing the senior doctor to provide their opinion), but also reveals the otherwise hidden ground-truth action: Let $D_t := \{(X_\tau, Y_\tau) : Z_\tau = 2\}_{\tau=1}^{t}$ denote the cumulative dataset of requested points, taking on values $d_t \in \mathcal{D}_t := \cup_t(\mathcal{X} \times \mathcal{Y})^t$, and constitutes the training set with which the model policy $\hat{\pi}$ is defined. Thus feedback (for learning) is "abstentive" in that it is only observable when the system "abstains" in favor of deferring the decision to the expert.

**Risk and Evaluation** Among other aspects, our objective of interest differs from supervised learning in two important ways: First, we are chiefly interested in the performance of the decision system $\mathcal{S}$, instead of the model $\hat{\pi}$ per se. Second, learning and evaluation are *both* conducted online. By way of contrast, consider first the familiar supervised learning objective, which is simply concerned with minimizing the *generalization error* of the model over the underlying data distribution, or the "model risk":

$$\mathcal{R}(\hat{\pi}) \coloneqq \mathbb{E}_{\substack{X\sim\rho \\ Y\sim\pi_*(\cdot|X)}} \ell(Y, \hat{\pi}(\cdot|X)) \tag{2}$$

where $\ell : \mathcal{Y} \times \Delta(\mathcal{Y}) \to \mathbb{R}$ is some choice of loss function. In decision problems, this most commonly takes the form of the zero-one loss $\ell(Y, \hat{\pi}(\cdot|x)) \coloneqq \ell_{01}(Y, \arg\max_y \hat{\pi}(y|x))$, or in some cases—if a surrogate loss is required—the cross-entropy $\ell(Y, \hat{\pi}(\cdot|x)) \coloneqq -\log \hat{\pi}(Y|x)$; we shall use the former to be consistent with comparable literature. Now, our main focus is not the model risk, but the "system risk":

**Definition 2 (System Risk)** Let $\mathcal{M} \coloneqq (\mathcal{X}, \mathcal{Y}, \tilde{\pi}, \pi_*, \rho, k_{\text{int}}, k_{\text{req}})$ denote the *mediation setting*. Given a mediator $(\hat{\pi}, \phi)$, the *system risk* in each round $t$ is the expected error of the induced system policy (i.e. having selected from human, model, and expert actions), plus the upfront cost of mediator actions:

$$\begin{aligned}\mathcal{R}_t(\hat{\pi}, \phi) \coloneqq \mathbb{E}_{\substack{X_t\sim\rho \\ \tilde{Y}_t\sim\tilde{\pi}(\cdot|X_t) \\ Y_t\sim\pi_*(\cdot|X_t)}} \big[\phi(Z_t\!=\!0|X_t, \tilde{Y}_t)\ell(Y_t, \delta(Y - \tilde{Y}_t)) +& \\ \phi(Z_t\!=\!1|X_t, \tilde{Y}_t)(\ell(Y_t, \hat{\pi}(\cdot|X_t)) + k_{\text{int}}) + \phi(Z_t\!=\!2|X_t, \tilde{Y}_t)k_{\text{req}}\big]&\end{aligned} \tag{3}$$

Then the *online decision mediation* ("ODM") problem is to select a mediator $(\hat{\pi}, \phi)$ to minimize (cumulative) *regret* over a possibly-unspecified horizon. Importantly, note that this is a more challenging objective than simply minimizing the generalization error of the model, system, or some asymptotic complexity thereof: Here we have no separation between "training" versus "testing", since losses begin accumulating from the very first step of the sequential process. The regret at any round $n$ is given by:

$$\textbf{Regret}(\boldsymbol{\hat{\pi}}, \boldsymbol{\phi})[n] \coloneqq \textstyle\sum_{t=0}^{n} \big(\mathcal{R}_t(\hat{\pi}_t, \phi_t) - \mathcal{R}_t(\pi_*, \phi_*)\big) \tag{4}$$

where we assume realizability such that the best-in-class mediator is defined as the tuple consisting of the expert policy $\pi_*$ and the greedy mediator policy $\phi_*$ (i.e. always choosing $Z$ to minimize each round's immediate system risk). Note the above notation makes it explicit that both the model policy and mediator policy evolve as sequences $\boldsymbol{\hat{\pi}} \coloneqq \{\hat{\pi}_t\}_t$ and $\boldsymbol{\phi} \coloneqq \{\phi_t\}_t$ that—in general—depend on $D_t$).

**Remark 1 (Assumptions)** For ease of exposition, we assume all mistakes are equally important, that $k_{\text{int}}, k_{\text{req}}$ are constants, and expert action classes are more or less balanced over the input distribution; allowing relaxations is straightforward and left for future work. To eliminate the more trivial cases, we assume $0 < k_{\text{int}} < k_{\text{req}}$, and operate in the common rejection regime where $k_{\text{req}} = \frac{m}{m-1} - \gamma$ for some small $\gamma > 0$, with $m$ being the number of actions in $\mathcal{Y}$; this induces the most interesting tradeoff setting where abstention is neither excessive nor immediately ruled out by the greedy policy. (In our experiments, we shall empirically consider a range of sensitivities). We assume nothing about $\tilde{\pi}$, for instance if it is even stationary. Lastly, we assume $D_0$ is randomly seeded with one example per action class.

### 2.2 Related Work

The ODM problem lies at the confluence of three classes of learning problems while being distinct from all: (i) learning with rejection, (ii) stream-based active learning, and (iii) stochastic contextual bandits. As before, we employ generic notation and make note of synonymous terminology as appropriate.

**Learning with Rejection** Compared to standard supervised learning, *learning with rejection* is a problem setting that endows the algorithm—during test time—with the option to "reject" their own prediction in favor of expert advice [21–26]. This is variously referred to as the option to "abstain" from a decision, or to "defer" to an oracle. Exercising it incurs an *abstention cost* $k_{\text{abs}}$, but enables avoiding misclassification when the model is uncertain. Typically, a solution consists of a model policy $\hat{\pi}$ and a *rejection policy* $\psi$ defining a distribution $\psi(U|X)$ over the space of actions $\mathcal{U} \coloneqq \{1, 2\}$, consisting of the options *not abstain* ($u\!=\!1$) and *abstain* ($u\!=\!2$). While the rejection option is similar to that in ODM, learning proceeds from a static dataset, evaluation focuses on model risk, and—like supervised learning—labels in the batch are always available. An *online* variant of this setting shares more similarity with the ODM problem by focusing on minimizing the cumulative loss over the course of learning, instead of simply minimizing the held-out performance of the algorithm [27–30]. However, a key distinction from us is that feedback is *not* an active choice, and expert labels are always streamed (or when the model does *not* defer to the expert, which is exactly the opposite of our setting).

Table 1: *Online Decision Mediation vs. Related Work.* The ODM problem is distinguished by three key factors: (1) Learning is stream-based (so exploratory considerations cannot benefit from any pool-based comparison). (2) Feedback is abstentive (so some exploitative actions—precisely, $z \in \{0, 1\}$—yield no learning signal at all). (3) Evaluation is online (so the exploration-exploitation tradeoff is explicitly measured by the cumulative loss). Subscripts $t$ are omitted from policy terms. Shaded terms denote those evaluated by the risk function, "a.s.c." denotes asymptotic sample complexity, "feedback condition" indicates when ground-truths are revealed for learning, and "multi-class" indicates whether each setting is not restricted (theoretically or empirically) to binary decisions.

| **Problem Setting** | **Stream-based** | **Abstain Option** | **Active Request** | **Components** ( Evaluated ) | **Risk Function of Interest** | **Minimization of Interest** | **Feedback Condition** | **Online Eval.** | **Multi-class** |
|---|---|---|---|---|---|---|---|---|---|
| Supervised Learning | ✗ | ✗ | ✗ | $\pi_*, \hat{\pi}$ | $\mathcal{R} = \mathbb{E}_{\substack{X\sim\rho \\ Y\sim\pi_*(\cdot\mid X)}} \ell(Y, \hat{\pi}(\cdot\mid X))$ | $\mathcal{R}(\hat{\pi})$ | (n/a) | ✗ | ✓ |
| Learning with Rejection [21–26] | ✗ | ✓ | ✗ | $\pi_*, \hat{\pi}, \psi$ | $\mathcal{R} = \mathbb{E}_{\substack{X\sim\rho \\ Y\sim\pi_*(\cdot\mid X)}} [\psi(1\mid X)\ell(Y, \hat{\pi}(\cdot\mid X)) + \psi(2\mid X)k_{\text{abs}}]$ | $\mathcal{R}(\hat{\pi}, \psi)$ | (n/a) | ✗ | ✓ |
| Online Learning with Rejection [27–30] | ✓ | ✓ | ✗ | $\pi_*, \hat{\pi}, \psi$ | $\mathcal{R}_t = \mathbb{E}_{\substack{X_t\sim\rho \\ Y_t\sim\pi_*(\cdot\mid X_t)}} [\psi(1\mid X_t)\ell(Y_t, \hat{\pi}(\cdot\mid X_t)) + \psi(2\mid X_t)k_{\text{abs}}]$ | $\sum_t(\mathcal{R}_t(\hat{\pi}, \psi) - \mathcal{R}_t(\pi_*, \psi_*))$ | (always) | ✓ | ✗ |
| (Stream-based) Active Learning [31–36] | ✓ | ✗ | ✓ | $\pi_*, \hat{\pi}, \phi$ | $\mathcal{R} = \mathbb{E}_{\substack{X\sim\rho \\ Y\sim\pi_*(\cdot\mid X)}} \ell(Y, \hat{\pi}(\cdot\mid X))$ | $\mathcal{R}(\hat{\pi})$ a.s.c. | $Z=2$ | ✗ | ✗ |
| Active Learning with Abstention [37–40] | ✓ | ✓ | ✓ | $\pi_*, \hat{\pi}, \psi, \phi$ | $\mathcal{R} = \mathbb{E}_{\substack{X\sim\rho \\ Y\sim\pi_*(\cdot\mid X)}} [\psi(1\mid X)\ell(Y, \hat{\pi}(\cdot\mid X)) + \psi(2\mid X)k_{\text{abs}}]$ | $\mathcal{R}(\hat{\pi}, \psi)$ a.s.c. | $Z=2$ | ✗ | ✗ |
| Dual Purpose Learning [41] | ✓ | ✓ | ✓ | $\pi_*, \hat{\pi}, \phi{=}\psi$ | $\mathcal{R} = \mathbb{E}_{\substack{X\sim\rho \\ Y\sim\pi_*(\cdot\mid X)}} [\ell(Y, \hat{\pi}(\cdot\mid X))\mid Z = 1]$ | $\mathcal{R}(\hat{\pi}, \phi)$ a.s.c. | $Z=2$ | ✗ | ✗ |
| (Stochastic Contextual) Bandits [42–48] | ✓ | ✗ | ✗ | $\upsilon, \hat{\pi}$ | $\mathcal{R}_t = -\mathbb{E}_{\substack{X_t\sim\rho \\ \hat{Y}_t\sim\hat{\pi}(\cdot\mid X_t)}} \upsilon(X_t, \hat{Y}_t)$ | $\sum_t(\mathcal{R}_t(\hat{\pi}) - \mathcal{R}_t(\pi_*))$ | (always) | ✓ | ✓ |
| Bandits with Active Learning [49–52] | ✓ | ✗ | ✓ | $\upsilon, \hat{\pi}, \phi$ | $\mathcal{R}_t = \mathbb{E}_{\substack{X_t\sim\rho \\ \hat{Y}_t\sim\hat{\pi}(\cdot\mid X_t)}} [\phi(2\mid X_t)k_{\text{req}} - \upsilon(X_t, \hat{Y}_t)]$ | $\sum_t(\mathcal{R}_t(\hat{\pi}) - \mathcal{R}_t(\pi_*))$ | $Z=2$ | ✓ | ✓ |
| Apple Tasting with Context [53–55] | ✓ | ✗ | ✓ | $\upsilon, \phi = \hat{\pi}$ | $\mathcal{R}_t = \mathbb{E}_{X_t\sim\rho}[\phi(2\mid X_t)(k_{\text{req}} - \upsilon(X_t))]$ | $\sum_t(\mathcal{R}_t(\phi) - \mathcal{R}_t(\phi_*))$ | $Z=2$ | ✓ | ✗ |
| Reinforced Active Learning [56–58] | ✓ | ✗ | ✓ | $\pi_*, \hat{\pi}, \phi$ | $\mathcal{R}_t = \mathbb{E}_{\substack{X_t\sim\rho \\ Y_t\sim\hat{\pi}(\cdot\mid X_t)}} [\phi(2\mid X_t)\ell(Y, \hat{\pi}(\cdot\mid X))]$ | $\sum_t(\mathcal{R}_t(\phi) - \mathcal{R}_t(\phi_*))$ | (always) | ✓ | ✓ |
| **Online Decision Mediation** | ✓ | ✓ | ✓ | $\pi_*, \tilde{\pi}, \hat{\pi}, \phi{=}\psi$ | $\mathcal{R}_t = \mathbb{E}_{\substack{X_t\sim\rho \\ \tilde{Y}_t\sim\tilde{\pi}(\cdot\mid X_t) \\ Y_t\sim\pi_*(\cdot\mid X_t)}} [\phi(0\mid X_t, \tilde{Y}_t)\ell(Y_t, \delta(Y - \tilde{Y}_t)) +$ $\phi(1\mid X_t, \tilde{Y}_t)(\ell(Y_t, \hat{\pi}(\cdot\mid X_t)) + k_{\text{int}}) + \phi(2\mid X_t, \tilde{Y}_t)k_{\text{req}}]$ | $\sum_t(\mathcal{R}_t(\hat{\pi}, \phi) - \mathcal{R}_t(\pi_*, \phi_*))$ | $Z=2$ | ✓ | ✓ |

**Stream-based Active Learning** In contrast with standard incremental learning, ground truths in *stream-based active learning* are unobserved unless actively "acquired" by the algorithm during training [31–36]. This is variously referred to as the option to "request" or "query" the oracle for its decision. Like supervised learning, the goal is to minimize test-time model risk, but with emphasis on reducing labeled and/or unlabeled asymptotic sample complexity. Typically, a solution consists of a model $\hat{\pi}$ and an *acquisition policy* $\phi$ defining a distribution $\phi(Z|X)$ over the space of actions $\mathcal{Z} := \{1, 2\}$, consisting of the options *not request* ($z = 1$) and *request* ($z = 2$). While the active request aspect is similar to that in ODM, evaluation focuses on model risk, so $\phi$ is not evaluated in the objective itself; moreover, the model has no ability to abstain from a prediction. One variant includes *abstention* to enable the algorithm—during test time—to reject their own prediction [37–40]. However, the objective remains to minimize test-time loss and its asymptotic complexity, which contrasts with our focus on evaluating cumulative losses over the entire process. A second variant called *dual purpose learning* is perhaps more similar in that the model abstains from a decision just when the expert is queried for its decision [41] (i.e. the acquisition policy $\phi$ coincides with the rejection policy $\psi$, and $\mathcal{Z} = \mathcal{U}$). But the risk function of interest is still like the usual test-time model risk, but now conditioned on $Z = 1$, so $\phi$ only enters the objective as a conditioning term to omit points where the model abstains.

**Stochastic Contextual Bandits** Lastly, ODM bears resemblance to stochastic contextual bandits, a class of sequential decision problems with the goal of minimizing (cumulative) *regret* defined in terms of an arbitrary "reward" function $\upsilon : \mathcal{X} \times \mathcal{Y} \rightarrow \mathbb{R}$ [42–48]. A main difference from ODM is that bandit rewards and are always observed as feedback for learning after each round, but no "expert" actions (viz. best-in-class policy) are available to be queried. One variant incorporates elements of *active learning* by stipulating that feedback must be requested at some cost $k_{\text{req}}$ [49–52]; in a special case dubbed *apple tasting*, model decisions are tied to acquisition decisions (i.e. the acquisition policy $\phi$ coincides with the model policy $\hat{\pi}$, and $\mathcal{Z} = \mathcal{Y}$) [53–55]. But unlike ODM, the model has no option to abstain, and there is no tradeoff between requesting information and making predictions. A second variant turns around and treats active learning itself as a bandit problem [56–58]; in the streaming, contextual case [56], the model policy $\hat{\pi}$ itself is actually not evaluated at all: Instead, the acquisition policy $\phi$ is rewarded positively just when querying the expert turns out to be "useful" (i.e. $Y \neq \hat{Y}$), and punished just when querying the expert turns out to be "redundant" (i.e. $Y = \hat{Y}$); moreover, feedback (for $\phi$, in this setting) is always observed. While these works are similar to ODM in focusing on the online evaluation objective of cumulative regret, the essential element of abstentive feedback—which is central to our motivation for a solution to ODM to mediate *efficiently* using expert resources—is missing.

Table 1 contextualizes ODM versus related work: Our setting combines the challenges from each, and is uniquely characterized by the three key aspects alluded to in Section 1: streaming instances, abstentive feedback, and online evaluation. In Section 3, we argue that a good algorithm must appropriately account for these challenges simultaneously. In Section 4, we verify empirically that neglecting any of them results in poor performance. (Additionally, since we are motivated from the perspective of decision support as an intermediary between humans, models, and experts, note that—as another practical component—ODM also extends $\mathcal{Z}$ with the option to accept human decisions $\tilde{Y} \sim \tilde{\pi}(\cdot|X)$).

# 3 Mediator Policies

In light of the preceding discussion, it is clear a good mediator should satisfy the following criteria. The first deals with immediate loss, the second with future loss, and the third with trading off the two:

- It should accept or intervene only when *errors* are thereby unlikely (cf. learning with rejection).
- It should acquire ground truths when *uncertainty* may thereby be reduced (cf. active learning).
- It should balance such exploration and exploitation *adaptively* over time (cf. contextual bandits).

**Greedy Mediator** It is instructive to first examine the greedy policy. Given any model policy $\hat{\pi}$, the greedy mediator policy $\phi_*$ simply chooses $Z$ to minimize the immediate (i.e. one-step) system risk, which balances immediate probabilities of error with immediate costs of intervention/requisition:

$$\begin{aligned}\phi_*(Z|X,\tilde{Y}) \coloneqq \delta\big(Z - \arg\min\nolimits_z \big(&\mathbb{1}_{[z=0]}(1-\hat{\pi}(\tilde{Y}|X)) \\ &+ \mathbb{1}_{[z=1]}(1-\hat{\pi}(\hat{Y}|X)+k_{\text{int}}) + \mathbb{1}_{[z=2]}k_{\text{req}}\big)\big)\end{aligned} \tag{5}$$

where $\delta(Z-z)$ denotes the Dirac delta centered at $z$, and $\hat{Y} \coloneqq \arg\max_y \hat{\pi}(y|X)$. It is clear that such a mediator policy is optimal in terms of regret if the model policy were already perfect (i.e. if $\hat{\pi}=\pi_*$), or if the model policy were otherwise fixed (e.g. if $Z=2$ no longer provided any feedback for learning).

**Passive Exploration** But what if the model is not perfect, and must incorporate new data points for learning? Actually, the greedy policy already "inadvertently" performs a sort of *passive* exploration: Whenever the target probabilities $[\hat{\pi}(y=1|X),...,\hat{\pi}(y=m|X)]$ for a context $X$ are not sufficiently concentrated, $\phi_*$ would request from the expert, which may reduce uncertainty for points similar to $X$. However, $\phi_*$ may learn too slowly: If—at any point—the model is even *slightly* erroneously confident (e.g. $\hat{\pi}(y'|X) \geq 1-k_{\text{req}}+\varepsilon$ for any $y' \neq y$, for any $\varepsilon > 0$), then it would simply not query the expert, and may commit similar mistakes again later. This is because it fails to distinguish between *aleatoric* and *epistemic* uncertainty: Not only do we wish to defer (viz. abstain) when the former is high at $X$, but we also wish to defer (viz. learn) when the latter may be reduced by knowing the ground truth at $X$. So the question is: Can we explore in a manner that better balances these (present vs. future) demands?

## 3.1 Bandit Mediator Policies

Prima facie, this resembles a bandit tradeoff, so the immediate question becomes: Can we simply formulate this as a specific instance of contextual bandits? Consider an ODM problem with $m$ actions in $\mathcal{Y}$: This gives $m+2$ "arms" in total (i.e. an *accept*, a *request*, and an *intervene* arm for each of the $m$ underlying actions). However, precisely due to the nature of abstentive feedback, the answer is *no*:

**Loss vs. Feedback** In conventional bandit problems, there is no distinction between the notions "loss" and "feedback". In each round, when an arm $y_t$ is pulled in response to a context $x_t$, the negative reward $-v(x_t, y_t)$ serves dual purposes: It is always *incurred* into the performance measure (viz. regret), and it is always *observed* as a new data point for learning (viz. reinforcement). In ODM, however, "loss" and "feedback" are distinct quantities: In each round, when a mediator action $z_t$ is chosen in response to a context-action pair $(x_t, \tilde{y}_t)$, the resulting loss is always *incurred* (viz. Definition 2), but no information whatsoever (i.e. not even the loss) is *observed* as feedback for learning unless $z_t = 2$.

**Exploring without Learning** It should now be apparent why bandit algorithms may suffer in ODM. The crux of the issue here is that *only one arm can actually provide any new information* (i.e. the *request* arm). So the role of "exploration" here is very different: Bandit strategies would "explore" different arms pointlessly with no learning occurring most of the time. It is easy to see that this applies to all manner of algorithms such as $\epsilon$-greedy policies, posterior sampling, and strategies that rely on optimism in the face of uncertainty (the latter actually leading to strictly *fewer* request arms being pulled!). In Appendix C, we formally show that ODM is actually a distinct and concretely "harder" problem than contextual bandits (Definition 3)—precisely due to the nature of abstentive feedback.

### 3.2 UMPIRE Mediator Policy

Given the previous discussion, a simple "$\epsilon$-request" mediator policy may seem promising: It executes the greedy policy $\phi$, but with probability $\epsilon$ opts to request from the expert. Learning thus occurs more frequently, and there are no exploratory actions that yield no learning. But an important problem is that *not all exploratory actions are equally useful*: The value of any requested information surely depends on the context $x_t$; by randomizing "indiscriminately", an $\epsilon$-request strategy does not account for this.

We propose a more principled basis for interpolating between exploration and exploitation that we term *uncertainty-modulated policy for intervention and requisition* ("UMPIRE"). The main idea is that we might be willing to pay more to request an oracle action now, if it means we can more confidently rely on model predictions in the future (i.e. by accepting or intervening autonomously). So our motivation is to explicitly trade off (immediate) *system risk* with expected improvements in the (future) *model risk*.

To do so, we need a method that allows us to estimate the latter. Operating in the probabilistic setting, let $W$ denote the parameter variable, taking on values in $w \in \mathcal{W}$, such that we can write $\hat{\pi}_w(Y|X) := p(Y|X, w)$, and can also speak of the marginal $p(Y|D, X) = \mathbb{E}_{W \sim p(\cdot|D)} p(Y|X, W)$. Now, denote the *expected model risk* with $\bar{\mathcal{R}}(D) := \mathbb{E}_{W \sim p(\cdot|D)} \mathcal{R}(\hat{\pi}_W)$; note that this is itself a random variable due to its dependence on $D$. Consider the $t$-th round of play: If the mediator chooses $z \in \{0, 1\}$, then $d_t = d_{t-1}$ so we have $\bar{\mathcal{R}}(d_t) = \bar{\mathcal{R}}(d_{t-1})$. But in deciding whether to choose $z = 2$, we wish to capture a measure of how much this risk might possibly improve—that is, if we were to reveal (and learn from) the ground-truth label $Y_t$. So we are interested in how far $\bar{\mathcal{R}}(D_t)$ can end up relative to $\bar{\mathcal{R}}(d_{t-1})$, where $Y_t \sim p(\cdot|d_{t-1}, x_t)$. The following result gives such an upper bound on expected improvement:

**Theorem 1 (Expected Improvement)** Let $\mathcal{R}$ be bounded as $[-b, b]$—for instance, by centering $\ell_{01}$. Let $\mathbb{I}[W; Y_t|d_{t-1}, x_t]$ denote the mutual information between $W$ and $Y_t$ conditioned on $d_{t-1}$ and $x_t$, and let $W_0$ denote the principal branch of the product logarithm function. Then (proof in Appendix C):

$$\bar{\mathcal{R}}(d_{t-1}) - \mathbb{E}_{Y_t \sim p(\cdot|d_{t-1}, x_t)}[\bar{\mathcal{R}}(D_t)|d_{t-1}, x_t, Z_t = 2] \leq 2b(e^{W_0\left(\frac{1}{e}(\mathbb{I}[W; Y_t|d_{t-1}, x_t] - 1)\right) + 1} - 1) \quad (6)$$

This motivates a straightforward technique: Define $g : v \mapsto g(v) = 2b(e^{W_0(\frac{1}{e}(v-1))+1} - 1)$, and let $\kappa$ denote some tradeoff coefficient. Then we can designate $\bar{k}_{\text{req}} := (1 - \kappa g(\mathbb{I}[W; Y_t|d_{t-1}, x_t])) k_{\text{req}}$, and simply use $\bar{k}_{\text{req}}$ in place of $k_{\text{req}}$ wherever it appears—but keeping the greedy mediator otherwise intact. UMPIRE thus has one hyperparameter $\kappa$; in our experiments we simply set its value as the normalizing constant $\kappa_0 := (2b(e^{W_0((\log m - 1)/e)+1} - 1))^{-1}$, which has the effect of keeping all costs non-negative.

**Interpretation** Since $g$ is monotonically increasing, Theorem 1 is naturally interpreted as translating an information-theoretic criterion (i.e. the mutual information) into a decision-theoretic criterion (i.e. the expected improvement in posterior risk)—which is what we require. In particular, the argument to $g$ expands as $\mathbb{I}[W; Y_t|d_{t-1}, x_t] = \mathbb{H}[W|d_{t-1}] - \mathbb{E}_{Y_t \sim p(\cdot|d_{t-1}, x_t)} \mathbb{H}[W|d_{t-1}, x_t, Y_t]$, which has the interpretation of how much the (epistemic) *uncertainty* in the model policy is expected to decrease if $Y_t \sim p(\cdot|d_{t-1}, x_t)$ is revealed; this view is reminiscent of entropy-based approaches to active learning [59, 60]. Observe that when deployed, $G_t := g(\mathbb{I}[W; Y_t|D_{t-1}, X_t])$ is large in the beginning, so $\bar{k}_{\text{req}}$ is small and UMPIRE behaves like standard incremental learning. In the limit of a perfect model, $G_t$ goes to zero, so $\bar{k}_{\text{req}} = k_{\text{req}}$ and UMPIRE behaves the same as the (optimal) greedy mediator $(\pi_*, \phi_*)$.

### 3.3 Practical Implementation

Some practical remarks deserve mention. First, UMPIRE is compatible with any choice of probabilistic modeling technique, such as Gaussian processes, Bayesian neural networks, and dropout-based approximations. Second, since integration over parameter posteriors is generally intractable, we use standard Monte-Carlo sampling to compute expectations: Let $s$ denote the number of samples taken from the posterior, and let $\{w_{i,t}\}_{i=1}^{s}$ indicate the set of samples drawn from $p(W|d_t)$. In computing the value of $g_t$, observe that the inner expression $\mathbb{E}_{Y_t \sim p(\cdot|d_{t-1}, x_t)} \mathbb{H}[W|d_{t-1}, x_t, Y_t]$ requires retraining the model policy on every possible value of $Y_t$. Instead, we can rely on the symmetry of mutual information and expand $\mathbb{I}[Y_t; W|d_{t-1}, x_t] = \mathbb{H}[Y_t|d_{t-1}, x_t] - \mathbb{E}_{W \sim p(\cdot|d_{t-1})} \mathbb{H}[Y_t|x_t, W]$, so we can write:

$$\hat{\mathbb{I}}[W; Y_t|d_{t-1}, x_t] := H[\tfrac{1}{s} \textstyle\sum_{i=1}^{s} p(Y_t|x_t, w_{i,t-1})] - \tfrac{1}{s} \textstyle\sum_{i=1}^{s} H[p(Y_t|x_t, w_{i,t-1})] \quad (7)$$

where we define $H[p(Y)] := -\sum_{y \in \mathcal{Y}} p(y) \log p(y)$, giving us a more efficient way to compute the expression without such retraining (see Appendix C for detail). Lastly, to guarantee consistency we can easily still request from the expert with some small probability $\epsilon$ (i.e. in the same way the "$\epsilon$-request" policy above does so over the greedy policy). Algorithm 1 summarizes UMPIRE as applied to ODM.

**Algorithm 1** UMPIRE Mediator ▷ for Online Decision Mediation

```
**Hyperparameters**: tradeoff coefficient $\kappa$, Monte-Carlo samples $s$
**Input**: initial dataset $d_0$, cost of intervention $k_{\text{int}}$, cost of requisition $k_{\text{req}}$
**for** each round $t = 1, \ldots$ **do**
    $x_t \leftarrow X_t \sim \rho$
    $\tilde{y}_t \leftarrow \tilde{Y}_t \sim \tilde{\pi}(\cdot|x_t)$                                                ▷ human action
    $\hat{\pi}(Y|x_t) \coloneqq \frac{1}{s}\sum_{i=1}^{s} p(Y|x_t, w_{i,t-1})$
    $\hat{y}_t \leftarrow \arg\max_y \hat{\pi}(y|x_t)$                                              ▷ model action
    $\hat{\mathbb{I}}[W;Y_t|d_{t-1},x_t] \leftarrow H[\frac{1}{s}\sum_{i=1}^{s} p(Y_t|x_t, w_{i,t-1})] - \frac{1}{s}\sum_{i=1}^{s} H[p(Y_t|x_t, w_{i,t-1})]$
    $\phi(Z|x_t,\tilde{y}_t) \coloneqq \delta(Z - \arg\min_z(\mathbb{1}_{[z=0]}(1-\hat{\pi}(\tilde{y}_t|x_t)) + \mathbb{1}_{[z=1]}(1-\hat{\pi}(\hat{y}_t|x_t)+k_{\text{int}}) + \mathbb{1}_{[z=2]}(1-\kappa g(\hat{\mathbb{I}}[W;Y_t|d_{t-1},x_t]))k_{\text{req}}))$
    $z_t \leftarrow Z_t \sim \phi(\cdot|x_t,\tilde{y}_t)$
    **if** $z_t = 2$ **then**
        $y_t \leftarrow Y_t \sim \pi_*(\cdot|x_t)$                                              ▷ expert action
        $d_t \leftarrow d_{t-1} \cup \{(x_t, y_t)\}$
    **else** $d_t \leftarrow d_{t-1}$
    **Output**: $\bar{y}_t \leftarrow \mathbb{1}_{[z_t=0]}\tilde{y}_t + \mathbb{1}_{[z_t=1]}\hat{y}_t + \mathbb{1}_{[z_t=2]}y_t$              ▷ (final) system action
```

## 4 Empirical Results

Three aspects of UMPIRE deserve investigation: **(a) Performance**: *Does it work?* Section 4.1 compares it to existing methods, validating its role in decision support by most consistently improving decisions. **(b) Source of Gain**: *Why does it work?* Section 4.2 deconstructs the key characteristics of UMPIRE, verifying the importance of each. **(c) Sensitivity Analysis**: Finally, Section 4.3 assesses the sensitivity of UMPIRE and benchmarks to the expert's stochasticity, costs of request, and number of samples used.

**Datasets** We experiment with six environments. In **`GaussSine`**, synthetic points are generated in three categories by rounding a sinusoidal latent function on 2D Gaussian input [61]. In **`HighEnergy`**, the task is to identify signals in high energy particles registered in a Cherenkov gamma telescope [62]. In **`MotionCapture`**, the task is to recognize hand postures from data recorded by glove markers on users [63]. In **`LunarLander`**, the task is to perform actions in the OpenAI gym [64] Atari environment, with the expert defined as a PPO2 agent [65,66] trained on the true reward. In **`Alzheimers`**, the task is to perform early diagnosis of patients in the Alzheimer's Disease Neuroimaging Initiative study [67] as cognitively normal, mildly impaired, or at risk of dementia [19,20]. Lastly, in **`CysticFibrosis`**, the task is to perform diagnosis of patients enrolled in the UK Cystic Fibrosis registry [68] as to their GOLD grading in chronic obstructive pulmonary disease [69]. See Appendix B for additional detail.

**Benchmarks** We consider adaptations of algorithms from related work. First as our minimal baseline, **`Human`** always accepts $z = 0$, thus constituting the starting point for performance comparison. **`Random`** draws $z$ at random. **`Supervised`** picks $z \in \{0, 1\}$ based solely on $\hat{\pi}$'s output, and $z = 2$ w.p. $\epsilon$, and thus resembles supervised learning. **`Cost-Sensitive`** is the greedy $(\hat{\pi}, \phi_*)$ from Section 3, which additionally accounts for costs $k_{\text{int}}, k_{\text{req}}$. **`Thompson Sampling`** [46] draws from the posterior $p(W|d)$ and selects $z$ greedily using $(\hat{\pi}_W, \phi_*)$; the **`Full`** version also uses that sampled model when predicting. **`Epsilon-Greedy`** [47] is greedy but draws $z$ at random w.p. $\epsilon$; the **`Request`** version is the smarter "$\epsilon$-request" from Section 3.2. **`Pessimistic Bayesian Sampling`** adapts OBS [44] to ODM by reversing the direction of optimism such that the tendency to request actually *increases*. **`Bayesian Active Request`** adapts Bayesian active learning [60] to ODM by requesting w.p. $\sim$ expected reduction in entropy. To further highlight the advantage of our proposed criterion, **`Matched Decaying Request`** is an artificially boosted benchmark that is similar to $\epsilon$-request—but where $\epsilon$ is a decay function that has the benefit of matching the effective request rate of UMPIRE: This is done *post-hoc* by searching for a polynomial function that best models UMPIRE's request pattern. See Appendix B for additional detail.

**Experiment Setup** Each experiment run consists of $n = 2000$ rounds of interactions (except for the synthetic `GaussSine`, for which $n = 500$), and this is repeated for a total of 10 runs with random seeds. For all algorithms, the underlying model policy is implemented identically using Dirichlet-based Gaussian process classifiers [61,70–72]. We simulate fallible human decisions as random perturbations of the ground truth with some probability $\alpha$. As mentioned in Section 2.1, we let $k_{\text{req}} = \frac{m}{m-1} - \gamma$ for some small $\gamma > 0$: To do so, we simply set $k_{\text{req}}$ to $\frac{m}{m-1}$ rounded down to the nearest decimal point. However, we shall perform additional sensitivities on this below. In all experiments, we set $k_{\text{int}} = 0.1$, $\alpha = \frac{1}{2}$, $\epsilon = 10\%$ where applicable, and $\kappa = \kappa_0$ as noted in Section 3.2. Regret is defined with respect to the oracle mediator $(\pi_*, \phi_*)$, for which $\pi_*$ is approximated by training on the full dataset in advance. Performance metrics for each benchmark are reported as means and standard deviations across all runs.

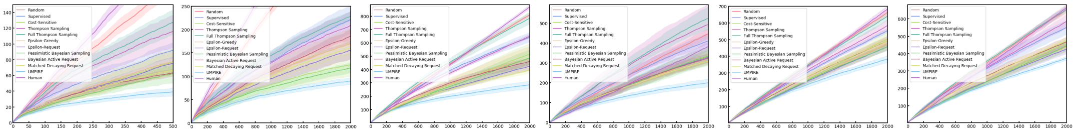

(a) **`GaussSine`** (b) **`HighEnergy`** (c) **`MotionCapture`** (d) **`LunarLander`** (e) **`Alzheimers`** (f) **`CysticFibrosis`**

Figure 1: *Performance (System)*: Regrets. Numbers are plotted as cumulative sums of system loss less oracle loss.

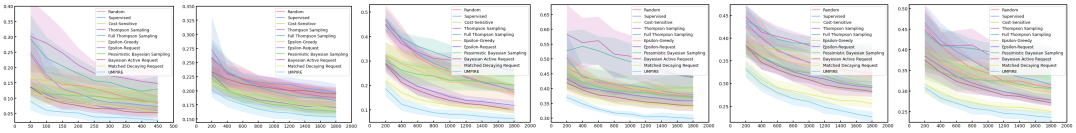

(a) **`GaussSine`** (b) **`HighEnergy`** (c) **`MotionCapture`** (d) **`LunarLander`** (e) **`Alzheimers`** (f) **`CysticFibrosis`**

Figure 2: *Performance (Model)*: Heldout Mistakes. Models are evaluated on heldout data once every $n/10$ rounds.

| | **`GaussSine`** | | | **`HighEnergy`** | | | **`MotionCapture`** | | | **`LunarLander`** | | | **`Alzheimers`** | | | **`CysticFibrosis`** | | |
|---|---|---|---|---|---|---|---|---|---|---|---|---|---|---|---|---|---|---|
| Benchmark | *Err. Acc.* | *Exc. Int.* | *Abs. Shf.* | *Err. Acc.* | *Exc. Int.* | *Abs. Shf.* | *Err. Acc.* | *Exc. Int.* | *Abs. Shf.* | *Err. Acc.* | *Exc. Int.* | *Abs. Shf.* | *Err. Acc.* | *Exc. Int.* | *Abs. Shf.* | *Err. Acc.* | *Exc. Int.* | *Abs. Shf.* |
| `Random` | 116±8 | 131±7 | 37±8 | 452±17 | 545±19 | 199±11 | 454±18 | 572±24 | 260±21 | 449±18 | 634±21 | 386±26 | 448±22 | 615±30 | 326±22 | 448±22 | 616±23 | 325±20 |
| `Supervised` | 19±8 | 47±7 | 34±7 | 204±17 | 201±20 | 203±18 | 39±8 | 485±34 | 256±14 | 114±18 | 661±39 | 388±27 | 201±29 | 466±22 | 330±14 | 155±23 | 536±46 | 344±22 |
| `Cost-Sensitive` | 33±14 | 36±11 | 37±11 | 176±15 | 139±16 | 176±15 | 101±36 | 352±48 | 232±41 | 166±20 | 607±36 | 403±18 | 305±29 | 333±21 | 333±21 | 265±16 | 299±19 | 296±11 |
| `Thompson Sampling` | 44±10 | 90±18 | 50±10 | 229±24 | 226±17 | 194±20 | 118±14 | 622±18 | 303±10 | 202±39 | 882±79 | 502±63 | 275±20 | 603±19 | 379±24 | 284±13 | 628±32 | 374±21 |
| `Full Thompson Sampling` | 41±7 | 105±14 | 64±7 | 231±10 | 252±14 | 219±9 | 119±18 | 728±32 | 415±28 | 205±28 | 907±43 | 552±31 | 277±24 | 665±35 | 430±17 | 273±24 | 714±33 | 450±13 |
| `Epsilon-Greedy` | 29±9 | 42±11 | 28±11 | 196±20 | 177±28 | 174±20 | 95±28 | 319±66 | 194±47 | 172±19 | 587±24 | 385±21 | 260±31 | 337±21 | 290±20 | 226±24 | 315±23 | 267±19 |
| `Epsilon-Request` | 16±7 | 25±7 | 22±4 | 162±13 | 124±14 | 162±13 | 32±6 | 220±31 | 132±15 | 129±19 | 523±42 | 342±26 | 220±21 | 284±13 | 265±15 | 167±22 | 275±27 | 234±12 |
| `Pessimistic Bayesian Sampling` | 16±7 | 45±9 | 26±7 | 139±14 | 147±10 | 143±14 | 41±19 | 441±39 | 194±31 | 111±18 | 704±47 | 364±30 | 177±22 | 449±25 | 275±17 | 136±19 | 429±22 | 248±21 |
| `Bayesian Active Request` | 12±6 | 25±7 | 19±4 | 191±14 | 192±18 | 192±13 | 19±6 | 232±26 | 125±14 | 87±11 | 532±26 | 304±19 | 143±16 | 351±18 | 238±16 | 114±26 | 371±24 | 232±20 |
| `Matched Decaying Request` | 15±6 | 23±8 | 20±4 | 154±11 | 122±12 | 154±11 | 21±4 | 158±23 | 93±13 | 102±12 | 449±23 | 291±16 | 128±12 | 211±17 | 175±14 | 93±11 | 198±21 | 155±12 |
| **UMPIRE** | 4±3 | 6±3 | 6±4 | 112±15 | 86±9 | 112±15 | 13±5 | 67±28 | 42±17 | 64±12 | 343±16 | 212±15 | 90±12 | 130±18 | 125±11 | 80±13 | 132±12 | 119±15 |

Table 2: *Performance (Mediator)*: Erroneous acceptance, excessive intervention, and abstention shortfall at $t = n$.

### 4.1 Performance

Recall from Section 1 we motivated ODM from the view of *decision support*: To best improve decision-making by the (human-expert-mediator) system as a whole. Primarily, then, we evaluate the performance of the *decision system*—that is, in terms of system regret (Equation 4). Figure 1 shows results for all algorithms, with `Human` (i.e. without support) also shown for comparison: UMPIRE consistently accumulates lower regret. This is our objective function, and this is the main takeaway. Secondarily, we can also assess the (heldout) performance of the *model policy*—that is, if it were tasked with acting autonomously at any point. Figure 2 shows the rate of heldout mistakes: UMPIRE appears to induce more efficient learning. As another auxiliary, we can also consider how the *mediator policy* behaves—that is, if it accepts erroneously ($z = 0$ but $\tilde{y} \neq y$), intervenes excessively ($z = 1$ but oracle $z_* \in \{0, 2\}$), or abstains not conservatively enough ($z \in \{0, 1\}$ while $\tilde{y} \neq y$ and $\hat{y} \neq y$). Table 2 shows the results, likewise with UMPIRE as best. (Note that this is not simply due to more frequent requests, since `Matched Decaying Request` selects $z = 2$ just as often as UMPIRE using a dynamic $\epsilon_t$ tuned post-hoc). For more comprehensive measures of the system (loss, regret, mistakes) and model (heldout cross entropy, mistakes, AUROC, and AUPRC), see Figures 8, 9, 10, 11, 12, 13, and 14 in Appendix A.

### 4.2 Source of Gain

| *Setting* | **CS** | **DE** | **UA** |
|---|---|---|---|
| `No Request` | ✗ | ✗ | ✗ |
| `Passive Request` | ✓ | ✗ | ✗ |
| `Epsilon-Request w/o CS` | ✗ | ✓ | ✗ |
| `Epsilon-Request with CS` | ✓ | ✓ | ✗ |
| `Dynamic-Request w.p. KG` | ✗ | ✓ | ✓ |
| `Dynamic-Request with ME` | ✓ | ✓ | ✗ |
| **UMPIRE** | ✓ | ✓ | ✓ |

Table 3: *Source-of-Gain Legend*.

Recall from Section 2 that ODM combines the challenges from all three related settings, and from Section 3 that UMPIRE is designed with three corresponding desiderata in mind. We now examine each aspect's contribution to final performance. Table 3 enumerates some settings to isolate the following: (i) Does it act exploit $\hat{\pi}$ in a cost-sensitive manner ("CS"), like in learning with rejection? (ii) Does it attempt to explore deliberately in addition ("DE"), like in bandit algorithms? (iii) Does it leverage uncertainty awareness in decision-making ("UA"), similar to active learning? (Abbreviations: `Dynamic-Request w.p. KG` requests w.p. $\kappa G_t$, and `Dynamic-Request with ME` requests with matched $\epsilon_t$, i.e. same as `Matched Decaying Request` from above). Figure 3 shows results for the decision system in terms of system regret, and secondarily Figure 4 shows results for the learned model in terms of heldout mistakes: It is apparent that all three aspects are crucial for performance, and cannot be neglected. For more comprehensive source-of-gain evaluation metrics for the system, model, and mediator, see Figures 15, 16, 17, 18, 19, 20, and 21, and Table 5 in Appendix A.

### 4.3 Sensitivity Analysis

Lastly, we examine UMPIRE's sensitivity to several factors. First, the expert might be more or less stochastic depending on the environment. We simulate this by progressively injecting additional noise to the latent function in `GaussSine`. Figure 5 shows the results: The advantage of UMPIRE is most

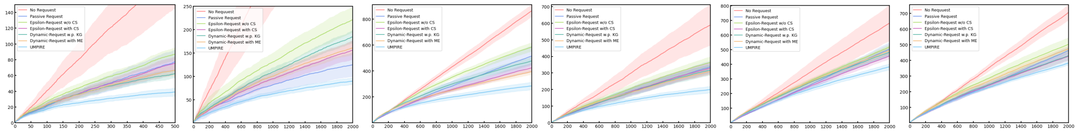

(a) `GaussSine` (b) `HighEnergy` (c) `MotionCapture` (d) `LunarLander` (e) `Alzheimers` (f) `CysticFibrosis`

Figure 3: *Source of Gain (System)*: Regrets. Numbers plotted as cumulative sums of system loss less oracle loss.

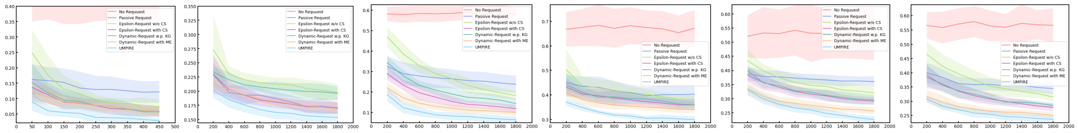

(a) `GaussSine` (b) `HighEnergy` (c) `MotionCapture` (d) `LunarLander` (e) `Alzheimers` (f) `CysticFibrosis`

Figure 4: *Source of Gain (Model)*: Heldout Mistakes. Models evaluated on heldout data once every $n/10$ rounds.

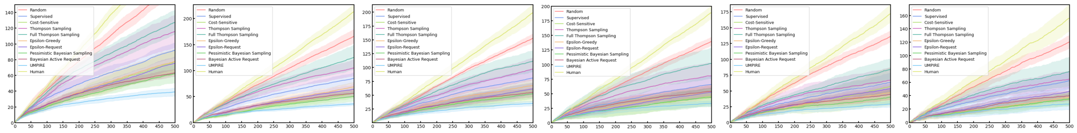

(a) `+0% Noise` (b) `+10% Noise` (c) `+20% Noise` (d) `+30% Noise` (e) `+40% Noise` (f) `+50% Noise`

Figure 5: *Expert Stochasticity vs. Performance*: Regret at various noise levels added to ground truths (`GaussSine`).

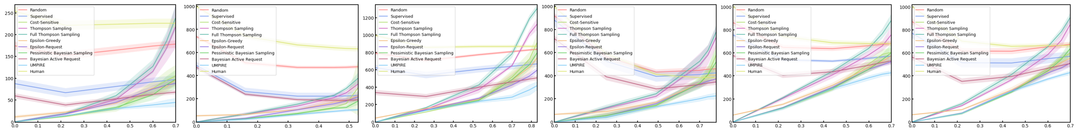

(a) `GaussSine` (b) `HighEnergy` (c) `MotionCapture` (d) `LunarLander` (e) `Alzheimers` (f) `CysticFibrosis`

Figure 6: *Cost of Request vs. Performance*: Episodic cumulative regret at round $t = n$ at various costs of request.

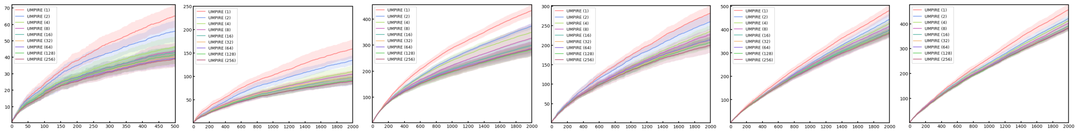

(a) `GaussSine` (b) `HighEnergy` (c) `MotionCapture` (d) `LunarLander` (e) `Alzheimers` (f) `CysticFibrosis`

Figure 7: *Number of Samples vs. Performance*: Regret using various numbers of posterior samples $s$ in UMPIRE.

pronounced at lower noise levels, and decreases as noise levels rise; this makes sense, as our estimates of uncertainty become more entangled with noise. For more comprehensive results, see Figures 22, 23, 24, and 25 in Appendix A. Second, we examine the consequence of different costs of request. Recall that we have been operating in the regime where $k_{\text{req}} = \frac{m}{m-1} - \gamma$ for some small $\gamma > 0$ [22, 25, 37, 40]. We now allow the cost of request to vary from $k_{\text{req}} = 0$ to $\frac{m}{m-1}$ as sensitivities. (For completeness, we actually go slightly beyond the standard threshold and go as high as $\gamma = -0.05 < 0$). Figure 6 shows the results: The advantage of UMPIRE appears most pronounced at higher costs, and decreases in the opposite direction; this makes sense, as cheaper costs mean abstention becomes a more trivial decision. For more comprehensive results, see Figures 26, 27, 28, and 29 in Appendix A. Finally, recall that Equation 7 requires estimating the mutual information by Monte-Carlo samples. Figure 7 shows the sensitivity of performance to the practical choice of sample size $s$: Observe that performance appears to stabilize with reasonable choices of $s \approx 64$ and above. See Appendix A for additional detail.

**Additional Sensitivities** In the above experiments, the imperfect human decisions are simulated with $\alpha = \frac{1}{2}$. However, it should be clear that the specific pattern or frequency of mistakes does not affect the basic structure of the problem, as long as the imperfect decisions stochastically deviate from the expert's with some probability between zero and one. Appendices E.3–E.4 perform a complete re-run of all experiments under the same conditions as before—but now setting $\alpha = \frac{9}{10}$. Similarly, we can verify that our intuitions still hold when the cost of intervention $k_{\text{int}} = 0.0$, which corresponds to the special case where the machine behaves "autonomously" for all intents and purposes, except where it requests input from the expert. Appendices E.5–E.6 perform experiments for the cartesian product of settings $\alpha \in \{0.5, 0.7, 0.9, 1.0\}$ and $k_{\text{int}} \in \{0.0, 0.1\}$, using the `GaussSine` environment. Across all sensitivities, it is easy to see that UMPIRE still consistently accumulates lower regret (our primary metric of interest), as well as outperforming comparators with respect to to the rest of the performance measures.

# 5 Discussion

Research in machine learning for decision-making is proliferating, such as in data-driven clinical decision support—but much focus is exclusively placed on comparing computers *versus* clinicians [73]: Less explored is how machines can serve as adjuncts to make decision systems more efficient *as a unit*. In this work, we take a first step by formalizing ODM as a sequential problem, proposing UMPIRE as a potential solution, and demonstrating the importance of considering all aspects of this unique setting. While this perspective is general, the ethical responsibility for a decision—e.g. signing off on a diagnosis—often must ultimately fall on humans: To remain vigilant of potential bias in societal impact, it is thus crucial to examine the complementary problem of "closing the loop" by considering how humans themselves may in turn interpret feedback to modify their own behavior [74]. Moreover, future work may explore generalizing ODM and its solutions—such as to settings with differential costs of mistake or class imbalances, or to consider aspects of interpretability in model policies for human feedback.

**Applications** In addition to clinical decision support, the ODM problem setting is applicable to any scenario where "imperfect" decision-makers are the front-line decision-makers, and "oracle" decision-makers are available as expert supervision—albeit with limited availability, and where learning feedback is abstentive. This situation arises in many settings where the responsibility for a decision must ultimately fall on a *person* (i.e. the imperfect human or the expert), but a *machine* is available for learning and issuing recommendations. The following are some potential examples of such:

- *Product Inspection*: Suppose a junior employee signs off on the quality of a product batch. The mediator can decide to (1) accept the sign-off *as is*, or (2) recommend a re-inspection for the batch, due to a disagreeing autonomous prediction as to the product quality, or (3) recommend that a more senior employee take over and issue their more qualified assessment.
- *Content Moderation*: Suppose users in a social network can report suspected content violations in real time. The mediator can decide to (1) accept and act on a user's report *as is*, or (2) recommend that the user re-classify the content due to a disagreeing assessment as to its appropriateness, or (3) recommend that an internal moderator take over and issue their judgement.
- *Spoken-Dialog System*: Suppose a customer selects a possibly-nonsensical option in a spoken-dialog system. The mediator can decide to (1) accept and act on the user's option *as is*, or (2) recommend that the user re-select an option from the same menu, or (3) re-route the customer to a phone conversation with an actual (human) customer representative to continue the work.

Finally, note that ODM is also applicable in settings where there is no imperfect human involved, so the machine simply makes decisions autonomously and learns from selective expert feedback; this is simply the setting where $k_{\text{int}}=0$. Importantly, however, this does not alter the basic structure of the ODM problem, whose hardness is distinguished by the fact that expert feedback is costly and abstentive.

**Limitations** There are two main limitations of our analysis: First, ODM is an *online learning* framework. In general, it is known that online learning may not perform well during early time steps when the learner's decisions are largely exploratory, especially if learning proceeds "from scratch"—which is the setting we operate in. In this sense, UMPIRE as a solution is also not immune to this challenge. Therefore, future work would benefit from examining the potential to *not* learn from scratch—e.g. to "warm-start" a learner using existing data, which can be done using a variety of methods from the extensive literature on imitation learning. Second, we must recognize that there are *two sides* to human-machine interactions: While ODM focuses on how machines should best propose recommendations to humans, there is also the complementary aspect of how/whether humans actually incorporate such recommendations into their behavior. Ignoring this second aspect may lead to models that are accurate but not necessarily best at proposing recommendations that are most likely to be complied with—which would severely undermine the practical utility of such a model. Therefore, future work would also benefit from *jointly* studying how humans and machines should behave in a "mutually-aware" fashion.

## Acknowledgments

We would like to thank the reviewers for their comments, suggestions, and generous feedback. This work was supported by Alzheimer's Research UK, The Alan Turing Institute under EPSRC grant number EP/N510129/1, the United States Office of Naval Research (ONR), as well as the National Science Foundation (NSF) under grant numbers 1407712, 1462245, 1524417, 1533983, and 1722516.

# References

[1] Gernmanno Teles, Joel JPC Rodrigues, Kashif Saleem, Sergei Kozlov, and Ricardo AL Rabêlo. Machine learning and decision support system on credit scoring. *Neural Computing and Applications*, 32(14):9809–9826, 2020.

[2] Bernhard Kratzwald, Suzana Ilić, Mathias Kraus, Stefan Feuerriegel, and Helmut Prendinger. Deep learning for affective computing: Text-based emotion recognition in decision support. *Decision Support Systems*, 115:24–35, 2018.

[3] Alistair EW Johnson, Mohammad M Ghassemi, Shamim Nemati, Katherine E Niehaus, David A Clifton, and Gari D Clifford. Machine learning and decision support in critical care. *Proceedings of the IEEE*, 104(2):444–466, 2016.

[4] Daniel Jarrett, Alihan Hüyük, and Mihaela Van Der Schaar. Inverse decision modeling: Learning interpretable representations of behavior. *International Conference on Machine Learning (ICML)*, 2021.

[5] Alihan Hüyük, Daniel Jarrett, Cem Tekin, and Mihaela van der Schaar. Explaining by imitating: Understanding decisions by interpretable policy learning. *International Conference on Learning Representations (ICLR)*, 2021.

[6] Constantin A Rothkopf and Christos Dimitrakakis. Preference elicitation and inverse reinforcement learning. *Joint European conference on machine learning and knowledge discovery in databases (ECML)*, 2011.

[7] Iván Sánchez Fernández, Arnold J Sansevere, Marina Gaínza-Lein, Kush Kapur, and Tobias Loddenkemper. Machine learning for outcome prediction in electroencephalograph (eeg)-monitored children in the intensive care unit. *Journal of child neurology*, 33(8):546–553, 2018.

[8] Bryan Lim and Mihaela van der Schaar. Disease-atlas: Navigating disease trajectories using deep learning. In *Machine Learning for Healthcare Conference*, pages 137–160. PMLR, 2018.

[9] Ahmad EL Sallab, Mohammed Abdou, Etienne Perot, and Senthil Yogamani. Deep reinforcement learning framework for autonomous driving. *Electronic Imaging*, 2017(19):70–76, 2017.

[10] Tim Lustberg, Johan van Soest, Mark Gooding, Devis Peressutti, Paul Aljabar, Judith van der Stoep, Wouter van Elmpt, and Andre Dekker. Clinical evaluation of atlas and deep learning based automatic contouring for lung cancer. *Radiotherapy and Oncology*, 126(2):312–317, 2018.

[11] Katerina Lepenioti, Minas Pertselakis, Alexandros Bousdekis, Andreas Louca, Fenareti Lampathaki, Dimitris Apostolou, Gregoris Mentzas, and Stathis Anastasiou. Machine learning for predictive and prescriptive analytics of operational data in smart manufacturing. In *International Conference on Advanced Information Systems Engineering*, pages 5–16. Springer, 2020.

[12] Eyke Hüllermeier. Prescriptive machine learning for automated decision making: Challenges and opportunities. *arXiv preprint arXiv:2112.08268*, 2021.

[13] Samuele Lo Piano. Ethical principles in machine learning and artificial intelligence: cases from the field and possible ways forward. *Nature*, 7(1):1–7, 2020.

[14] Nina Schwalbe and Brian Wahl. Artificial intelligence and the future of global health. *The Lancet*, 395(10236):1579–1586, 2020.

[15] Emanuele Neri, Francesca Coppola, Vittorio Miele, Corrado Bibbolino, and Roberto Grassi. Artificial intelligence: Who is responsible for the diagnosis?, 2020.

[16] Abdullah Awaysheh, Jeffrey Wilcke, François Elvinger, Loren Rees, Weiguo Fan, and Kurt L Zimmerman. Review of medical decision support and machine-learning methods. *Veterinary pathology*, 56(4):512–525, 2019.

[17] Daniel Jarrett, Eleanor Stride, Katherine Vallis, and Mark J Gooding. Applications and limitations of machine learning in radiation oncology. *The British journal of radiology*, 92(1100):20190001, 2019.

[18] Saif Khairat, David Marc, William Crosby, Ali Al Sanousi, et al. Reasons for physicians not adopting clinical decision support systems: critical analysis. *JMIR medical informatics*, 6(2):e8912, 2018.

[19] Bennett P Leifer. Early diagnosis of alzheimer's disease: clinical and economic benefits. *Journal of the American Geriatrics Society*, 51(5s2):S281–S288, 2003.

[20] Susanne G Mueller, Michael W Weiner, Leon J Thal, Ronald C Petersen, Clifford R Jack, William Jagust, John Q Trojanowski, Arthur W Toga, and Laurel Beckett. Ways toward an early diagnosis in alzheimer's disease: the alzheimer's disease neuroimaging initiative (adni). *Alzheimer's & Dementia*, 1(1):55–66, 2005.

[21] Corinna Cortes, Giulia DeSalvo, and Mehryar Mohri. Learning with rejection. In *International Conference on Algorithmic Learning Theory*, pages 67–82. Springer, 2016.

[22] Harish G Ramaswamy, Ambuj Tewari, and Shivani Agarwal. Consistent algorithms for multiclass classification with an abstain option. *Electronic Journal of Statistics*, 12(1):530–554, 2018.

[23] Chenri Ni, Nontawat Charoenphakdee, Junya Honda, and Masashi Sugiyama. On the calibration of multiclass classification with rejection. *Advances in Neural Information Processing Systems*, 32, 2019.

[24] Hussein Mozannar and David Sontag. Consistent estimators for learning to defer to an expert. In *International Conference on Machine Learning*, pages 7076–7087. PMLR, 2020.

[25] Nontawat Charoenphakdee, Zhenghang Cui, Yivan Zhang, and Masashi Sugiyama. Classification with rejection based on cost-sensitive classification. In *International Conference on Machine Learning*, pages 1507–1517. PMLR, 2021.

[26] Kilian Hendrickx, Lorenzo Perini, Dries Van der Plas, Wannes Meert, and Jesse Davis. Machine learning with a reject option: A survey. *arXiv preprint arXiv:2107.11277*, 2021.

[27] Gergely Neu and Nikita Zhivotovskiy. Fast rates for online prediction with abstention. In *Conference on Learning Theory*, pages 3030–3048. PMLR, 2020.

[28] Amin Sayedi, Morteza Zadimoghaddam, and Avrim Blum. Trading off mistakes and don't-know predictions. *Advances in Neural Information Processing Systems*, 23, 2010.

[29] Corinna Cortes, Giulia DeSalvo, Claudio Gentile, Mehryar Mohri, and Scott Yang. Online learning with abstention. In *international conference on machine learning*, pages 1059–1067. PMLR, 2018.

[30] Chicheng Zhang and Kamalika Chaudhuri. The extended littlestone's dimension for learning with mistakes and abstentions. In *Conference on Learning Theory*, pages 1584–1616. PMLR, 2016.

[31] Les Atlas, David Cohn, and Richard Ladner. Training connectionist networks with queries and selective sampling. *Advances in neural information processing systems*, 2, 1989.

[32] David Cohn, Les Atlas, and Richard Ladner. Improving generalization with active learning. *Machine learning*, 15(2):201–221, 1994.

[33] Sanjoy Dasgupta, Daniel J Hsu, and Claire Monteleoni. A general agnostic active learning algorithm. *Advances in neural information processing systems*, 20, 2007.

[34] Alina Beygelzimer, Sanjoy Dasgupta, and John Langford. Importance weighted active learning. In *Proceedings of the 26th annual international conference on machine learning*, pages 49–56, 2009.

[35] Burr Settles. Active learning, 2012.

[36] Giulia DeSalvo, Claudio Gentile, and Tobias Sommer Thune. Online active learning with surrogate loss functions. *Advances in Neural Information Processing Systems*, 34, 2021.

[37] Shubhanshu Shekhar, Mohammad Ghavamzadeh, and Tara Javidi. Active learning for binary classification with abstention. *arXiv preprint arXiv:1906.00303*, 2019.

[38] Nikita Puchkin and Nikita Zhivotovskiy. Exponential savings in agnostic active learning through abstention. In *Conference on Learning Theory*, pages 3806–3832. PMLR, 2021.

[39] Shubhanshu Shekhar, Mohammad Ghavamzadeh, and Tara Javidi. Active learning for classification with abstention. *IEEE Journal on Selected Areas in Information Theory*, 2(2):705–719, 2021.

[40] Yinglun Zhu and Robert Nowak. Efficient active learning with abstention. *arXiv preprint arXiv:2204.00043*, 2022.

[41] Kareem Amin, Giulia DeSalvo, and Afshin Rostamizadeh. Learning with labeling induced abstentions. *Advances in Neural Information Processing Systems*, 34, 2021.

[42] Wei Chu, Lihong Li, Lev Reyzin, and Robert Schapire. Contextual bandits with linear payoff functions. In *Proceedings of the Fourteenth International Conference on Artificial Intelligence and Statistics*, pages 208–214. JMLR Workshop and Conference Proceedings, 2011.

[43] Emilie Kaufmann, Olivier Cappé, and Aurélien Garivier. On bayesian upper confidence bounds for bandit problems. In *Artificial intelligence and statistics*, pages 592–600. PMLR, 2012.

[44] Benedict C May, Nathan Korda, Anthony Lee, and David S Leslie. Optimistic bayesian sampling in contextual-bandit problems. *Journal of Machine Learning Research*, 13:2069–2106, 2012.

[45] Shipra Agrawal and Navin Goyal. Thompson sampling for contextual bandits with linear payoffs. In *International conference on machine learning*, pages 127–135. PMLR, 2013.

[46] Daniel J Russo, Benjamin Van Roy, Abbas Kazerouni, Ian Osband, Zheng Wen, et al. A tutorial on thompson sampling. *Foundations and Trends® in Machine Learning*, 11(1):1–96, 2018.

[47] Tor Lattimore and Csaba Szepesvári. *Bandit algorithms*. Cambridge University Press, 2020.

[48] Alihan Hüyük, Daniel Jarrett, and Mihaela van der Schaar. Inverse contextual bandits: Learning how behavior evolves over time. *arXiv preprint arXiv:2107.06317*, 2021.

[49] Linqi Song and Jie Xu. A contextual bandit approach for stream-based active learning. *arXiv preprint arXiv:1701.06725*, 2017.

[50] András Antos, Varun Grover, and Csaba Szepesvári. Active learning in multi-armed bandits. In *International conference on algorithmic learning theory*. Springer, 2009.

[51] Alexandra Carpentier, Alessandro Lazaric, Mohammad Ghavamzadeh, Rémi Munos, and Peter Auer. Upper-confidence-bound algorithms for active learning in multi-armed bandits. In *International Conference on Algorithmic Learning Theory*. Springer, 2015.

[52] Linqi Song, Jie Xu, and Congduan Li. Active learning for streaming data in a contextual bandit framework. In *Proceedings of the 2019 5th International Conference on Computing and Data Engineering*, pages 29–35, 2019.

[53] David P Helmbold, Nick Littlestone, and Philip M Long. Apple tasting and nearly one-sided learning. In *Proceedings., 33rd Annual Symposium on Foundations of Computer Science*, pages 493–502. IEEE Computer Society, 1992.

[54] David P Helmbold, Nicholas Littlestone, and Philip M Long. Apple tasting. *Information and Computation*, 161(2):85–139, 2000.

[55] James A Grant and David S Leslie. Apple tasting revisited: Bayesian approaches to partially monitored online binary classification. *arXiv preprint arXiv:2109.14412*, 2021.

[56] Sarah Wassermann, Thibaut Cuvelier, and Pedro Casas. Ral-improving stream-based active learning by reinforcement learning. In *European Conference on Machine Learning and Principles and Practice of Knowledge Discovery in Databases (ECML-PKDD) Workshop on Interactive Adaptive Learning (IAL)*, 2019.

[57] Ravi Ganti and Alexander G Gray. Building bridges: Viewing active learning from the multi-armed bandit lens. *arXiv preprint arXiv:1309.6830*, 2013.

[58] Djallel Bouneffouf, Romain Laroche, Tanguy Urvoy, Raphael Féraud, and Robin Allesiardo. Contextual bandit for active learning: Active thompson sampling. In *International Conference on Neural Information Processing*, pages 405–412. Springer, 2014.

[59] David JC MacKay. Information-based objective functions for active data selection. *Neural computation*, 4(4):590–604, 1992.

[60] Neil Houlsby, Ferenc Huszár, Zoubin Ghahramani, and Máté Lengyel. Bayesian active learning for classification and preference learning. *arXiv preprint arXiv:1112.5745*, 2011.

[61] Geoff Pleiss, Jacob R. Gardner, Kilian Q. Weinberger, Andrew Gordon Wilson, and Max Balandat. Exact gp regression on classification labels. *GPyTorch Examples*, 2020.

[62] RK Bock, A Chilingarian, M Gaug, F Hakl, Th Hengstebeck, M Jiřina, J Klaschka, E Kotrč, P Savický, S Towers, et al. Methods for multidimensional event classification: a case study using images from a cherenkov gamma-ray telescope. *Nuclear Instruments and Methods in Physics Research Section A: Accelerators, Spectrometers, Detectors and Associated Equipment*, 516(2-3):511–528, 2004.

[63] Andrew Gardner, Jinko Kanno, Christian A Duncan, and Rastko Selmic. Measuring distance between unordered sets of different sizes. In *Proceedings of the IEEE conference on computer vision and pattern recognition*, pages 137–143, 2014.

[64] Greg Brockman, Vicki Cheung, Ludwig Pettersson, Jonas Schneider, John Schulman, Jie Tang, and Wojciech Zaremba. Openai gym. *OpenAI*, 2016.

[65] John Schulman, Sergey Levine, Pieter Abbeel, Michael Jordan, and Philipp Moritz. Trust region policy optimization. *International Conference on Machine Learning (ICML)*, 2015.

[66] Antonin Raffin. Rl baselines zoo: A collection of pre-trained reinforcement learning agents. `https://github.com/araffin/rl-baselines-zoo`, 2018.

[67] Laurel A Beckett, Michael C Donohue, Cathy Wang, et al. The alzheimer's disease neuroimaging initiative phase 2: Increasing the length, breadth, and depth of our understanding. *Alzheimer's & Dementia*, 11(7):823–831, 2015.

[68] David Taylor-Robinson, Olia Archangelidi, Siobhán B Carr, Rebecca Cosgriff, Elaine Gunn, Ruth H Keogh, Amy MacDougall, Simon Newsome, Daniela K Schlüter, Sanja Stanojevic, et al. Data resource profile: the uk cystic fibrosis registry. *International journal of epidemiology*, 47(1):9–10e, 2018.

[69] Federico P Gómez and Roberto Rodriguez-Roisin. Global initiative for chronic obstructive lung disease (gold) guidelines for chronic obstructive pulmonary disease. *Current opinion in pulmonary medicine*, 8(2):81–86, 2002.

[70] Carl Edward Rasmussen and Christopher KI Williams. Gaussian processes for machine learning. 2006. *Cited on*, page 95, 2014.

[71] Jacob R Gardner, Geoff Pleiss, David Bindel, Kilian Q Weinberger, and Andrew Gordon Wilson. Gpytorch: Blackbox matrix-matrix gaussian process inference with gpu acceleration. In *Advances in Neural Information Processing Systems*, 2018.

[72] Dimitrios Milios, Raffaello Camoriano, Pietro Michiardi, Lorenzo Rosasco, and Maurizio Filippone. Dirichlet-based gaussian processes for large-scale calibrated classification. *Advances in Neural Information Processing Systems*, 31, 2018.

[73] Baptiste Vasey, Stephan Ursprung, Benjamin Beddoe, Elliott H Taylor, Neale Marlow, Nicole Bilbro, Peter Watkinson, and Peter McCulloch. Association of clinician diagnostic performance with machine learning–based decision support systems: a systematic review. *JAMA network open*, 4(3):e211276–e211276, 2021.

[74] Yuchao Qin, Fergus Imrie, Alihan Hüyük, Daniel Jarrett, Mihaela van der Schaar, et al. Closing the loop in medical decision support by understanding clinical decision-making: A case study on organ transplantation. *Advances in Neural Information Processing Systems*, 34, 2021.

[75] Yarin Gal, Riashat Islam, and Zoubin Ghahramani. Deep bayesian active learning with image data. In *International Conference on Machine Learning*, pages 1183–1192. PMLR, 2017.

[76] Andreas Kirsch, Joost Van Amersfoort, and Yarin Gal. Batchbald: Efficient and diverse batch acquisition for deep bayesian active learning. *Advances in neural information processing systems*, 32, 2019.

[77] Andrew Jesson, Panagiotis Tigas, Joost van Amersfoort, Andreas Kirsch, Uri Shalit, and Yarin Gal. Causal-bald: Deep bayesian active learning of outcomes to infer treatment-effects from observational data. *Advances in Neural Information Processing Systems*, 34, 2021.

[78] Hideaki Ishibashi and Hideitsu Hino. Stopping criterion for active learning based on deterministic generalization bounds. In *International Conference on Artificial Intelligence and Statistics*, pages 386–397. PMLR, 2020.

[79] Gábor Bartók and Csaba Szepesvári. Partial monitoring with side information. In *International Conference on Algorithmic Learning Theory*, pages 305–319. Springer, 2012.

[80] Johannes Kirschner, Tor Lattimore, and Andreas Krause. Information directed sampling for linear partial monitoring. In *Conference on Learning Theory*, pages 2328–2369. PMLR, 2020.

[81] Hongju Park and Mohamad Kazem Shirani Faradonbeh. Analysis of thompson sampling for partially observable contextual multi-armed bandits. *IEEE Control Systems Letters*, 6:2150–2155, 2021.

[82] Guy Tennenholtz, Uri Shalit, Shie Mannor, and Yonathan Efroni. Bandits with partially observable confounded data. In *Uncertainty in Artificial Intelligence*, pages 430–439. PMLR, 2021.

[83] Rohin Shah, Pedro Freire, Neel Alex, Rachel Freedman, Dmitrii Krasheninnikov, Lawrence Chan, Michael D Dennis, Pieter Abbeel, Anca Dragan, and Stuart Russell. Benefits of assistance over reward learning. 2020.

[84] Allan Dafoe, Edward Hughes, Yoram Bachrach, Tantum Collins, Kevin R McKee, Joel Z Leibo, Kate Larson, and Thore Graepel. Open problems in cooperative ai. *arXiv preprint arXiv:2012.08630*, 2020.

[85] Dorsa Sadigh, Anca D Dragan, Shankar Sastry, and Sanjit A Seshia. *Active preference-based learning of reward functions*. 2017.

[86] Sören Mindermann, Rohin Shah, Adam Gleave, and Dylan Hadfield-Menell. Active inverse reward design. *arXiv preprint arXiv:1809.03060*, 2018.

[87] Erdem Bıyık, Malayandi Palan, Nicholas C Landolfi, Dylan P Losey, and Dorsa Sadigh. Asking easy questions: A user-friendly approach to active reward learning. *arXiv preprint arXiv:1910.04365*, 2019.

[88] Nils Wilde, Dana Kulić, and Stephen L Smith. Active preference learning using maximum regret. In *2020 IEEE/RSJ International Conference on Intelligent Robots and Systems (IROS)*, pages 10952–10959. IEEE, 2020.

[89] Dylan Hadfield-Menell, Stuart J Russell, Pieter Abbeel, and Anca Dragan. Cooperative inverse reinforcement learning. *Advances in neural information processing systems*, 29, 2016.

[90] Dhruv Malik, Malayandi Palaniappan, Jaime Fisac, Dylan Hadfield-Menell, Stuart Russell, and Anca Dragan. An efficient, generalized bellman update for cooperative inverse reinforcement learning. In *International Conference on Machine Learning*, pages 3394–3402. PMLR, 2018.

[91] Mark Woodward, Chelsea Finn, and Karol Hausman. Learning to interactively learn and assist. In *Proceedings of the AAAI conference on artificial intelligence*, volume 34, pages 2535–2543, 2020.

[92] Dylan Hadfield-Menell. The principal-agent alignment problem in artificial intelligence. 2021.

[93] Umaa Rebbapragada, Carla E Brodley, Damien Sulla-Menashe, and Mark A Friedl. Active label correction. In *2012 IEEE 12th International Conference on Data Mining*, pages 1080–1085. IEEE, 2012.

[94] Ruth Urner, Shai Ben David, and Ohad Shamir. Learning from weak teachers. In *Artificial intelligence and statistics*, pages 1252–1260. PMLR, 2012.

[95] Jan Kremer, Fei Sha, and Christian Igel. Robust active label correction. In *International conference on artificial intelligence and statistics*, pages 308–316. PMLR, 2018.

[96] Mattia Zeni, Wanyi Zhang, Enrico Bignotti, Andrea Passerini, and Fausto Giunchiglia. Fixing mislabeling by human annotators leveraging conflict resolution and prior knowledge. *Proceedings of the ACM on Interactive, Mobile, Wearable and Ubiquitous Technologies*, 3(1):1–23, 2019.

[97] Andrea Bontempelli, Stefano Teso, Fausto Giunchiglia, and Andrea Passerini. Learning in the wild with incremental skeptical gaussian processes. *arXiv preprint arXiv:2011.00928*, 2020.

[98] Stefano Teso, Andrea Bontempelli, Fausto Giunchiglia, and Andrea Passerini. Interactive label cleaning with example-based explanations. *Advances in Neural Information Processing Systems*, 34, 2021.

[99] Chicheng Zhang and Kamalika Chaudhuri. Active learning from weak and strong labelers. *Advances in Neural Information Processing Systems*, 28, 2015.

[100] Songbai Yan, Kamalika Chaudhuri, and Tara Javidi. Active learning from imperfect labelers. *Advances in Neural Information Processing Systems*, 29, 2016.

[101] Shalmali Joshi, Sonali Parbhoo, and Finale Doshi-Velez. Pre-emptive learning-to-defer for sequential medical decision-making under uncertainty. *arXiv preprint arXiv:2109.06312*, 2021.

[102] Hussein Mozannar, Arvind Satyanarayan, and David Sontag. Teaching humans when to defer to a classifier via exemplars. In *Proceedings of the AAAI Conference on Artificial Intelligence*, volume 36, pages 5323–5331, 2022.

[103] Gagan Bansal, Besmira Nushi, Ece Kamar, Eric Horvitz, and Daniel S Weld. Is the most accurate ai the best teammate? optimizing ai for teamwork. In *Proceedings of the AAAI Conference on Artificial Intelligence*, volume 35, pages 11405–11414, 2021.

[104] Gagan Bansal, Besmira Nushi, Ece Kamar, Daniel S Weld, Walter S Lasecki, and Eric Horvitz. Updates in human-ai teams: Understanding and addressing the performance/compatibility tradeoff. In *Proceedings of the AAAI Conference on Artificial Intelligence*, volume 33, pages 2429–2437, 2019.

# A Additional Results

Sections A.1–A.3 present more comprehensive empirical results organized to correspond with Sections 4.1–4.3. The objective of ODM is to minimize the *system regret*, so that should be the primary measure of performance; however, we also provide a variety of other metrics to give a broader picture of how UMPIRE and benchmarks behave. In order of appearance in the sequel: The **system loss** is defined by Equation 3: $\mathcal{R}_t(\hat{\pi},\phi) := \mathbb{E}_{X_t\sim\rho}\mathbb{E}_{\tilde{Y}_t\sim\tilde{\pi}(\cdot|X_t)}\mathbb{E}_{Y_t\sim\pi_*(\cdot|X_t)}[\phi(Z_t=0|X_t,\tilde{Y}_t)\ell(Y_t,\delta(Y-\tilde{Y}_t)) +\phi(Z_t=1|X_t,\tilde{Y}_t)(\ell(Y_t,\hat{\pi}(\cdot|X_t))+k_{\text{int}})+\phi(Z_t=2|X_t,\tilde{Y}_t)k_{\text{req}}]$, where we approximate the expectations over multiple samples by averaging over the ten runs of each experiment; loss values are taken as the moving average of a rolling window of width $n/5$. The **system regret** is defined by Equation 4: $\text{Regret}[t] := \sum_{\tau=0}^{t}(\mathcal{R}_\tau(\hat{\pi},\phi)-\mathcal{R}_\tau(\pi_*,\phi_*))$; that is, regret values are the cumulative sums of system loss less oracle loss (with the oracle mediator policy being the greedy policy $\phi_*$ and the oracle model policy $\pi_*$ approximated by training on the full dataset in advance), where we similarly approximate the expectations over multiple trajectories by averaging over the ten runs of each experiment. The **system mistake** at each time $t$ is defined as whether or not the decision system $\mathcal{S}$ as a whole outputs a final decision $\bar{Y}_t\sim\pi_{\mathcal{S}}(\cdot|X,\tilde{Y})$ that is a mistake; that is, if $\bar{Y}_t$ is different from the (observed or unobserved) decision of the expert $Y_t$: $\mathbb{E}_{X_t\sim\rho}\mathbb{E}_{\tilde{Y}_t\sim\tilde{\pi}(\cdot|X_t)}\mathbb{E}_{Y_t\sim\pi_*(\cdot|X_t)}\ell(Y_t,\bar{\pi}_{\mathcal{S}}(\cdot|X_t,\tilde{Y}_t))$, where we again likewise approximate the expectations over multiple samples by averaging over the ten runs of each experiment; as with system loss, numbers are computed as the moving average of a rolling window of width $n/5$. Across all evaluation measures, UMPIRE consistently performs better than applying existing methods.

Secondarily, heldout metrics measure how well the learned model policy $\hat{\pi}$ would do if asked to make decisions $\hat{Y}\sim\hat{\pi}(\cdot|X)$ autonomously. These compute the *model risk* as in Equation 2: Model-Risk$[t]$ $:=\mathbb{E}_{X\sim\rho}\mathbb{E}_{Y\sim\pi_*(\cdot|X)}\ell(Y,\hat{\pi}_t(\cdot|X))$ where $\hat{\pi}_t$ is the model policy at the end of round $t$ (i.e. learned on the dataset $D_t := \{(X_\tau,Y_\tau) : Z_\tau = 2\}_{\tau=1}^{t}$), where we approximate the expectations by averaging over heldout datasets of size $n=2000$. This is computed once every $n/10$ rounds to show its evolution across $t$, and a different heldout dataset is randomly drawn for every run. The **heldout mistakes** metric uses the zero-one loss; the **heldout cross entropy** uses the cross entropy between expert and model policies; the **heldout AUROC** refers to the area under the receiver operating characteristic curve; and the **heldout AUPRC** refers to the area under the precision-recall curve. Lastly, measures of the mediator policy include the cumulative numbers of erroneous acceptances, excessive interventions, and abstention shortfalls throughout each trajectory, as defined as in Section 4.1, again averaged over ten runs. As before, across all measures, UMPIRE consistently performs better than applying existing methods.

Section A.2 presents the **source-of-gain** analysis, which follows a similar format to Section A.1, but now comparing UMPIRE against different versions of itself—with various (combinations of) characteristics removed (viz. Table 3), incl. cost-sensitivity, deliberate exploration, and uncertainty awareness. As noted in the manuscript, it is apparent that all three aspects of UMPIRE are crucial for performance.

Section A.3 presents various sensitivity analyses, likewise following a similar format to Section 4.3 but including additional results. First, we look at the effect of **expert stochasticity** on the performance of UMPIRE and benchmarks: This is accomplished by injecting additional noise to the latent function in `GaussSine`: Since ground-truth labels are generated as $y=$ round$(f(x_1,x_2))$ for some latent function $f$ (see Section B), we add additional noise by setting $y=$ round$(f(x_1,x_2)+$uniform$(-\frac{q}{2},\frac{q}{2}))$ for $q\in\{0.0,0.1,0.2,0.3,0.4,0.5\}$. Results for sensitivities are computed and presented in relation with benchmark comparators, as well as with source-of-gain comparators. In both cases, the advantage of UMPIRE appears the most pronounced at lower noise levels, and decreases with higher noise levels.

Second, we look at the effect of **cost of request** on performance: This is achieved by executing the entire experiment procedure at various values of $k_{\text{req}}$. As above, results are presented in relation to benchmark comparators and source-of-gain comparators. As noted in the manuscript, in this work we focus on the most common regime where $k_{\text{req}}=\frac{m}{m-1}-\gamma$ for some $\gamma>0$ [22,23,25,37,40]; as in [25], we refer to [22] for a discussion on how the case $\gamma\leq 0$ yields a fundamentally different class of problems. (However, for completeness we do go beyond the cutoff and experiment with up to $\gamma=-0.05<0$). To show how results change across the range of values for $k_{\text{req}}$, we report the *episodic average loss* (across all $n$ rounds) versus the cost of request, as well as the (cumulative) *system regret* (at round $t=n$) versus the cost of request. Both metrics are reported for both benchmark comparators and source-of-gain comparators. The advantage of UMPIRE is the most pronounced at higher costs (where the passive exploration induced by the greedy policy plays a smaller role), and decreases in the opposite direction.

Finally, in all experiments so far we used $s=256$ **Monte-Carlo samples** in our UMPIRE implementation. We can look at the effect of $s$: Performance appears to be reasonably good at $s\approx 64$ and above.

## A.1 Performance

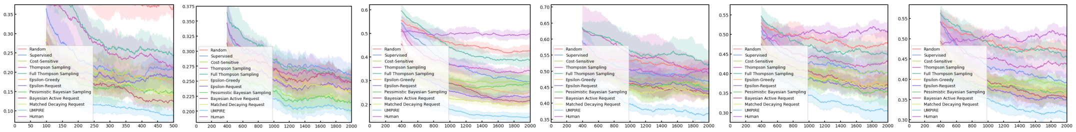

(a) **GaussSine** (b) **HighEnergy** (c) **MotionCapture** (d) **LunarLander** (e) **Alzheimers** (f) **CysticFibrosis**

Figure 8: *System Performance*: Losses. Numbers are plotted as moving average of rolling window of width $n/5$.

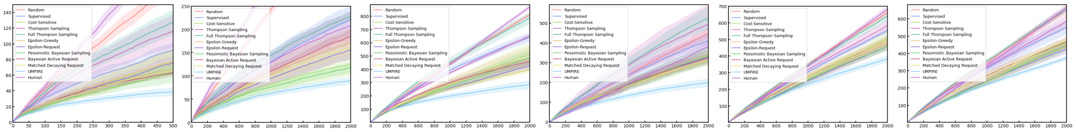

(a) **GaussSine** (b) **HighEnergy** (c) **MotionCapture** (d) **LunarLander** (e) **Alzheimers** (f) **CysticFibrosis**

Figure 9: *System Performance*: Regrets. Numbers are plotted as cumulative sums of system loss less oracle loss.

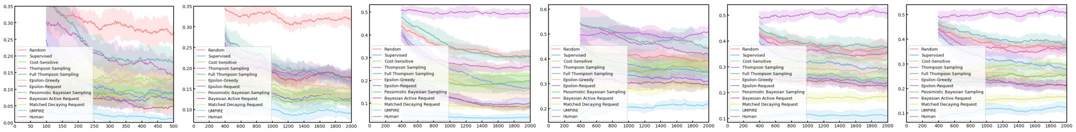

(a) **GaussSine** (b) **HighEnergy** (c) **MotionCapture** (d) **LunarLander** (e) **Alzheimers** (f) **CysticFibrosis**

Figure 10: *System Performance*: Mistakes. Numbers are plotted as moving average of rolling window of width $n/5$.

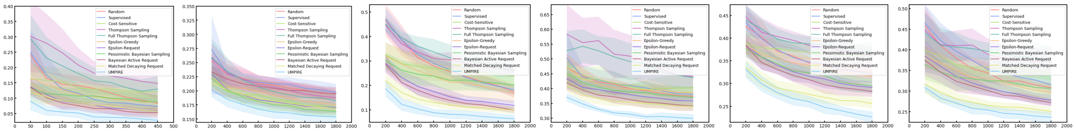

(a) **GaussSine** (b) **HighEnergy** (c) **MotionCapture** (d) **LunarLander** (e) **Alzheimers** (f) **CysticFibrosis**

Figure 11: *Model Performance*: Heldout Mistakes. Models are evaluated on heldout data once every $n/10$ rounds.

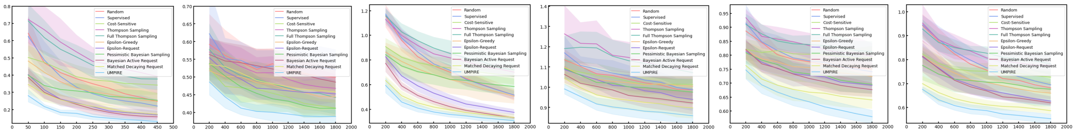

(a) **GaussSine** (b) **HighEnergy** (c) **MotionCapture** (d) **LunarLander** (e) **Alzheimers** (f) **CysticFibrosis**

Figure 12: *Model Performance*: Heldout CrossEnt. Models are evaluated on heldout data once every $n/10$ rounds.

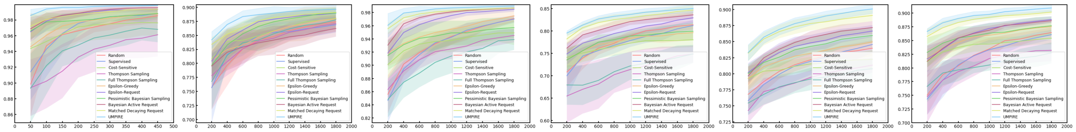

(a) **GaussSine** (b) **HighEnergy** (c) **MotionCapture** (d) **LunarLander** (e) **Alzheimers** (f) **CysticFibrosis**

Figure 13: *Model Performance*: Heldout AUROC. Models are evaluated on heldout data once every $n/10$ rounds.

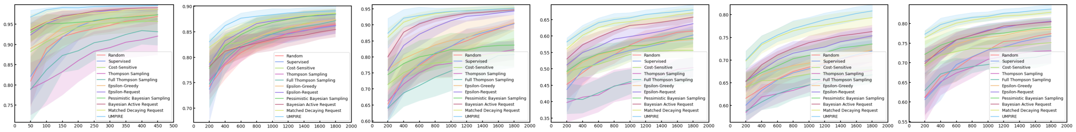

(a) **GaussSine** (b) **HighEnergy** (c) **MotionCapture** (d) **LunarLander** (e) **Alzheimers** (f) **CysticFibrosis**

Figure 14: *Model Performance*: Heldout AUPRC. Models are evaluated on heldout data once every $n/10$ rounds.

| | GaussSine | | | HighEnergy | | | MotionCapture | | | LunarLander | | | Alzheimers | | | CysticFibrosis | | |
|---|---|---|---|---|---|---|---|---|---|---|---|---|---|---|---|---|---|---|
| Benchmark | *Err. Acc.* | *Exc. Int.* | *Abs. Shf.* | *Err. Acc.* | *Exc. Int.* | *Abs. Shf.* | *Err. Acc.* | *Exc. Int.* | *Abs. Shf.* | *Err. Acc.* | *Exc. Int.* | *Abs. Shf.* | *Err. Acc.* | *Exc. Int.* | *Abs. Shf.* | *Err. Acc.* | *Exc. Int.* | *Abs. Shf.* |
| Random | 116±8 | 131±7 | 37±8 | 452±17 | 545±19 | 199±11 | 454±18 | 572±24 | 260±21 | 449±18 | 634±21 | 386±26 | 448±22 | 615±30 | 326±22 | 448±22 | 616±23 | 325±20 |
| Supervised | 19±8 | 47±7 | 34±7 | 204±17 | 201±20 | 203±18 | 39±8 | 485±34 | 256±14 | 114±18 | 661±39 | 388±27 | 201±29 | 466±22 | 330±14 | 155±23 | 536±46 | 344±22 |
| Cost-Sensitive | 33±14 | 36±11 | 37±11 | 176±15 | 139±16 | 176±15 | 101±36 | 352±48 | 232±41 | 166±20 | 607±36 | 403±18 | 305±29 | 333±21 | 333±21 | 265±16 | 299±19 | 296±11 |
| Thompson Sampling | 44±10 | 90±18 | 50±10 | 229±24 | 226±17 | 194±20 | 118±14 | 622±18 | 303±10 | 202±39 | 882±79 | 502±63 | 275±20 | 603±19 | 379±24 | 284±13 | 628±32 | 374±21 |
| Full Thompson Sampling | 41±7 | 105±14 | 64±7 | 231±10 | 252±14 | 219±9 | 119±18 | 728±32 | 415±28 | 205±28 | 907±43 | 552±31 | 277±24 | 665±35 | 430±17 | 273±24 | 714±33 | 450±13 |
| Epsilon-Greedy | 29±9 | 42±11 | 28±11 | 196±20 | 177±28 | 174±20 | 95±28 | 319±66 | 194±47 | 172±19 | 587±24 | 385±21 | 260±31 | 337±21 | 290±20 | 226±24 | 315±23 | 267±19 |
| Epsilon-Request | 16±7 | 25±7 | 22±4 | 162±13 | 124±14 | 162±13 | 32±6 | 220±31 | 132±15 | 129±19 | 523±42 | 342±26 | 220±21 | 284±13 | 265±15 | 167±22 | 275±27 | 234±12 |
| Pessimistic Bayesian Sampling | 16±7 | 45±9 | 26±7 | 139±14 | 147±10 | 143±14 | 41±19 | 441±39 | 194±31 | 111±18 | 704±47 | 364±30 | 177±22 | 449±25 | 275±17 | 136±19 | 429±22 | 248±21 |
| Bayesian Active Request | 12±6 | 25±7 | 19±4 | 191±14 | 192±18 | 192±13 | 19±6 | 232±26 | 125±14 | 87±11 | 532±26 | 304±19 | 143±16 | 351±18 | 238±16 | 114±26 | 371±24 | 232±20 |
| Matched Decaying Request | 15±6 | 23±8 | 20±4 | 154±11 | 122±12 | 154±11 | 21±4 | 158±23 | 93±13 | 102±12 | 449±23 | 291±16 | 128±12 | 211±17 | 175±14 | 93±11 | 198±21 | 155±12 |
| **UMPIRE** | 4±3 | 6±3 | 6±4 | 112±15 | 86±9 | 112±15 | 13±5 | 67±28 | 42±17 | 64±12 | 343±16 | 212±15 | 90±12 | 130±18 | 125±11 | 80±13 | 132±12 | 119±15 |

Table 4: *Mediator Performance*: Erroneous acceptance, excessive intervention, and abstention shortfall at $t = n$.

## A.2 Source of Gain

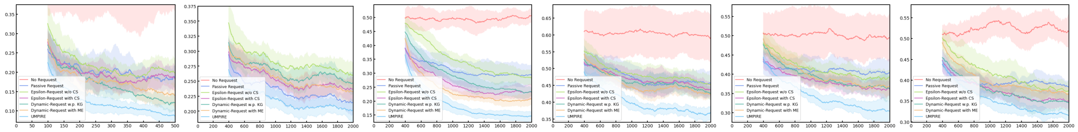

(a) **GaussSine** (b) **HighEnergy** (c) **MotionCapture** (d) **LunarLander** (e) **Alzheimers** (f) **CysticFibrosis**

Figure 15: *System Performance*: Losses. Numbers are plotted as moving average of rolling window of width $n/5$.

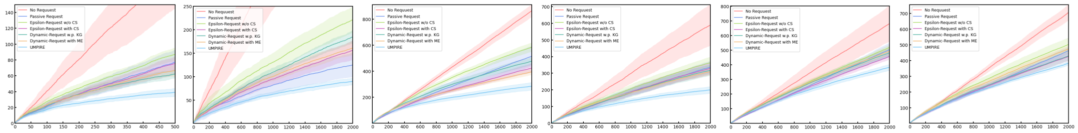

(a) **GaussSine** (b) **HighEnergy** (c) **MotionCapture** (d) **LunarLander** (e) **Alzheimers** (f) **CysticFibrosis**

Figure 16: *System Performance*: Regrets. Numbers are plotted as cumulative sums of system loss less oracle loss.

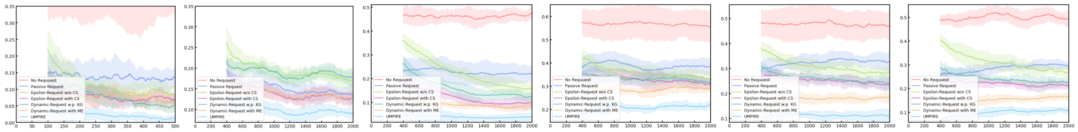

(a) **GaussSine** (b) **HighEnergy** (c) **MotionCapture** (d) **LunarLander** (e) **Alzheimers** (f) **CysticFibrosis**

Figure 17: *System Performance*: Mistakes. Numbers are plotted as moving average of rolling window of width $n/5$.

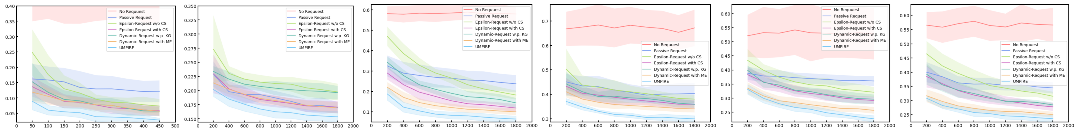

(a) **GaussSine** (b) **HighEnergy** (c) **MotionCapture** (d) **LunarLander** (e) **Alzheimers** (f) **CysticFibrosis**

Figure 18: *Model Performance*: Heldout Mistakes. Models are evaluated on heldout data once every $n/10$ rounds.

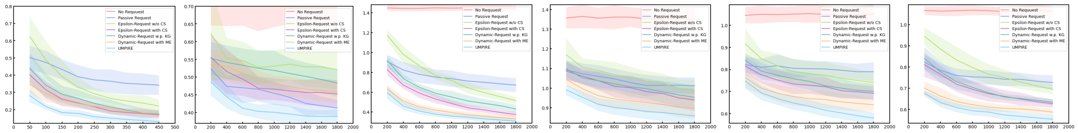

(a) **GaussSine** (b) **HighEnergy** (c) **MotionCapture** (d) **LunarLander** (e) **Alzheimers** (f) **CysticFibrosis**

Figure 19: *Model Performance*: Heldout CrossEnt. Models are evaluated on heldout data once every $n/10$ rounds.

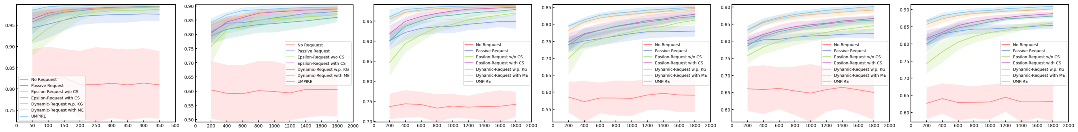

(a) **GaussSine** (b) **HighEnergy** (c) **MotionCapture** (d) **LunarLander** (e) **Alzheimers** (f) **CysticFibrosis**

Figure 20: *Model Performance*: Heldout AUROC. Models are evaluated on heldout data once every $n/10$ rounds.

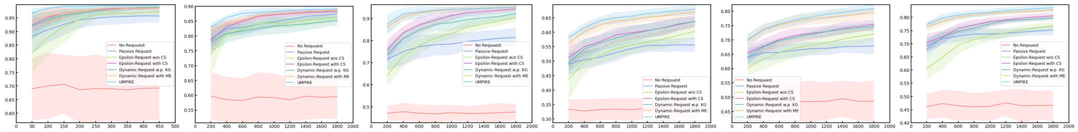

(a) **GaussSine** (b) **HighEnergy** (c) **MotionCapture** (d) **LunarLander** (e) **Alzheimers** (f) **CysticFibrosis**

Figure 21: *Model Performance*: Heldout AUPRC. Models are evaluated on heldout data once every $n/10$ rounds.

| | **GaussSine** | | | **HighEnergy** | | | **MotionCapture** | | | **LunarLander** | | | **Alzheimers** | | | **CysticFibrosis** | | |
|---|---|---|---|---|---|---|---|---|---|---|---|---|---|---|---|---|---|---|
| Benchmark | *Err. Acc.* | *Exc. Int.* | *Abs. Shf.* | *Err. Acc.* | *Exc. Int.* | *Abs. Shf.* | *Err. Acc.* | *Exc. Int.* | *Abs. Shf.* | *Err. Acc.* | *Exc. Int.* | *Abs. Shf.* | *Err. Acc.* | *Exc. Int.* | *Abs. Shf.* | *Err. Acc.* | *Exc. Int.* | *Abs. Shf.* |
| No Requeust | 124±33 | 84±40 | 120±34 | 581±65 | 400±140 | 493±106 | 530±60 | 397±71 | 589±40 | 596±171 | 538±165 | 681±79 | 706±83 | 250±114 | 541±96 | 714±53 | 285±78 | 580±48 |
| Passive Request | 33±14 | 36±11 | 37±11 | 176±15 | 139±16 | 176±15 | 101±36 | 352±48 | 232±41 | 166±20 | 607±36 | 403±18 | 305±29 | 333±21 | 333±21 | 265±16 | 299±19 | 296±11 |
| Epsilon-Request w/o CS | 29±10 | 32±7 | 34±7 | 227±16 | 176±17 | 203±18 | 81±12 | 386±32 | 256±14 | 161±21 | 568±37 | 388±27 | 258±33 | 375±27 | 330±14 | 264±27 | 374±52 | 344±22 |
| Epsilon-Request with CS | 16±7 | 25±7 | 22±4 | 162±13 | 124±14 | 162±13 | 32±6 | 220±31 | 132±15 | 129±19 | 523±42 | 342±26 | 220±21 | 284±13 | 265±15 | 167±22 | 275±27 | 234±12 |
| Dynamic-Request w.p. KG | 19±5 | 21±6 | 23±5 | 212±13 | 174±14 | 194±12 | 48±11 | 290±31 | 187±18 | 130±19 | 540±26 | 345±27 | 198±14 | 333±23 | 265±15 | 180±28 | 313±26 | 256±19 |
| Dynamic-Request with ME | 15±6 | 23±8 | 20±4 | 154±11 | 122±12 | 154±11 | 21±4 | 158±23 | 93±13 | 102±12 | 449±23 | 291±16 | 128±12 | 211±17 | 175±14 | 93±11 | 198±21 | 155±12 |
| **UMPIRE** | 4±3 | 6±3 | 6±4 | 112±15 | 86±9 | 112±15 | 13±5 | 67±28 | 42±17 | 64±12 | 343±16 | 212±15 | 90±12 | 130±18 | 125±11 | 70±11 | 120±11 | 106±12 |

Table 5: *Mediator Performance*: Erroneous acceptance, excessive intervention, and abstention shortfall at $t = n$.

### A.3 Sensitivity Analysis

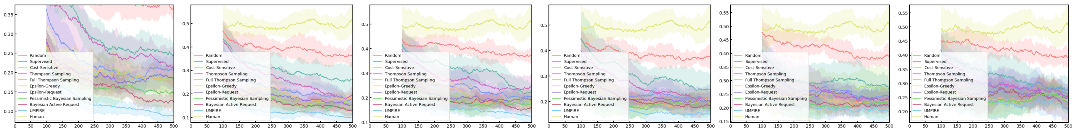

(a) **+0% Noise** (b) **+10% Noise** (c) **+20% Noise** (d) **+30% Noise** (e) **+40% Noise** (f) **+50% Noise**

Figure 22: *Expert Stochasticity vs. Performance*: Loss at various noise levels added to ground truths (`GaussSine`).

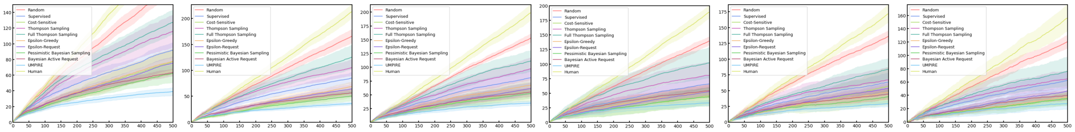

(a) **+0% Noise** (b) **+10% Noise** (c) **+20% Noise** (d) **+30% Noise** (e) **+40% Noise** (f) **+50% Noise**

Figure 23: *Expert Stochasticity vs. Performance*: Regret at various noise levels added to ground truths (`GaussSine`).

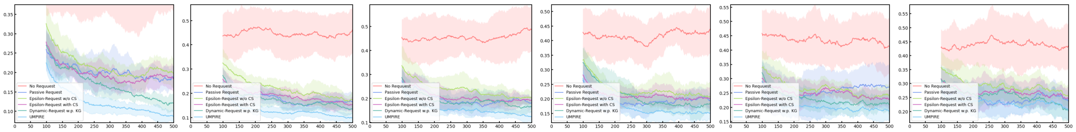

(a) **+0% Noise** (b) **+10% Noise** (c) **+20% Noise** (d) **+30% Noise** (e) **+40% Noise** (f) **+50% Noise**

Figure 24: *Expert Stochast. vs. Source of Gain*: Loss at various noise levels added to ground truths (`GaussSine`).

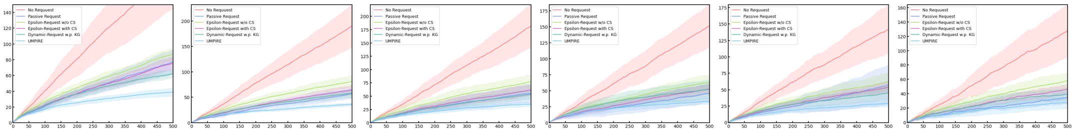

(a) **+0% Noise** (b) **+10% Noise** (c) **+20% Noise** (d) **+30% Noise** (e) **+40% Noise** (f) **+50% Noise**

Figure 25: *Expert Stochast. vs. Source of Gain*: Regret at various noise levels added to ground truths (`GaussSine`).

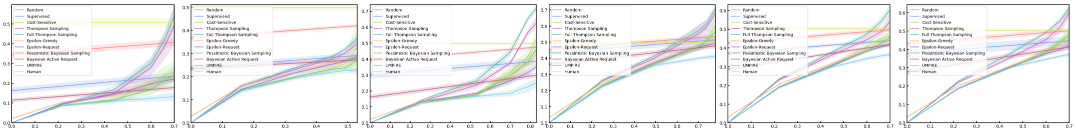

(a) **GaussSine** (b) **HighEnergy** (c) **MotionCapture** (d) **LunarLander** (e) **Alzheimers** (f) **CysticFibrosis**

Figure 26: *Cost of Request vs. Performance*: Episodic average loss across all $n$ rounds at various costs of request.

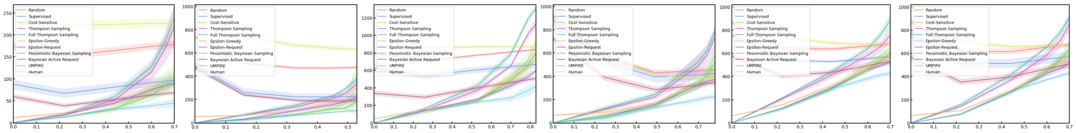

(a) **GaussSine** (b) **HighEnergy** (c) **MotionCapture** (d) **LunarLander** (e) **Alzheimers** (f) **CysticFibrosis**

Figure 27: *Cost of Request vs. Performance*: Episodic cumulative regret at round $t = n$ at various costs of request.

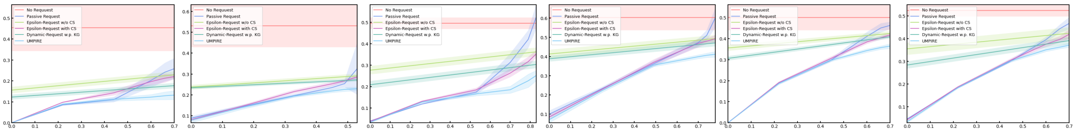

(a) **GaussSine** (b) **HighEnergy** (c) **MotionCapture** (d) **LunarLander** (e) **Alzheimers** (f) **CysticFibrosis**

Figure 28: *Cost of Request vs. Source of Gain*: Episodic average loss across all $n$ rounds at various costs of request.

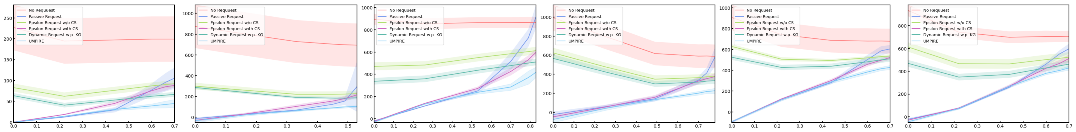

(a) **GaussSine** (b) **HighEnergy** (c) **MotionCapture** (d) **LunarLander** (e) **Alzheimers** (f) **CysticFibrosis**

Figure 29: *Cost of Request vs. Source of Gain*: Episodic cumulative regret at round $t = n$ at various costs of request.

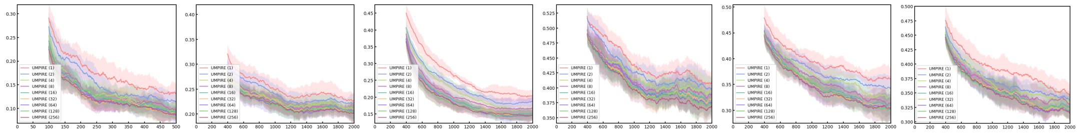

(a) **`GaussSine`** (b) **`HighEnergy`** (c) **`MotionCapture`** (d) **`LunarLander`** (e) **`Alzheimers`** (f) **`CysticFibrosis`**

Figure 30: *Number of Samples vs. Performance*: Loss using various numbers of posterior samples $s$ in UMPIRE.

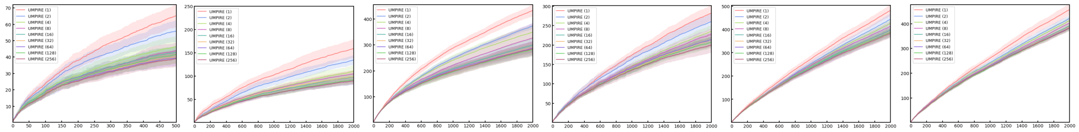

(a) **`GaussSine`** (b) **`HighEnergy`** (c) **`MotionCapture`** (d) **`LunarLander`** (e) **`Alzheimers`** (f) **`CysticFibrosis`**

Figure 31: *Number of Samples vs. Performance*: Regret using various numbers of posterior samples $s$ in UMPIRE.

# B Experiment Details

## B.1 Dataset Details

All datasets used are publicly available. **`GaussSine`** is a synthetic environment that generates points by first constructing a smooth underlying latent function applied to two-dimensional iid. Gaussian input, and then setting decision boundaries by rounding the latent function to the nearest integer: $y = \text{round}(f(x_1, x_2))$ where $f(x_1, x_2) = \sin(0.15\pi u + x_1 + x_2) + 1$ with $u \sim \text{uniform}(0, 1)$; this is implemented exactly as given in the example in [61]. **`HighEnergy`** is a UCI dataset, and the task is to identify patterns caused by primary gammas (signal) from cosmic rays in the upper atmosphere (background), where the patterns are generated by simulated registration of high energy particles in an atmospheric Cherenkov gamma telescope [62]: There are $\approx 19000$ data points in total, from which $n = 2000$ are sampled for each randomly seeded run of experiments; the context space consists of 11 attributes, and the decision space is binary (signal vs. background). **`MotionCapture`** is a UCI dataset, and the task is to recognize different hand postures from data recorded by glove markers attached to users performing different movements using a Vicon motion capture camera system [63]: There are $\approx 78000$ data points in total, from which $n = 2000$ are sampled for each randomly seeded run of experiments; the context space consists of 38 attributes, and the decision space consists of 5 hand postures. In **`LunarLander`**, the task is to perform actions in the OpenAI gym [64] Atari environment "Lunar Lander": Given any game state, the expert action is defined as the action chosen by a PPO2 agent [65, 66] pre-trained on the environment using the true reward function. We generate $\approx 24000$ data points in total, from which $n = 2000$ are sampled for each randomly seeded run of experiments; the context space consists of 8 attributes, and the decision space consists of 4 rocket actions. The **`Alzheimers`** dataset records patients in the Alzheimer's Disease Neuroimaging Initiative study [67], including a range of demographic variables (age, education level, marital status, etc.), biomarkers (entorhinal, fusiform, hippocampus, etc.), and cognitive test scores (ADAS, CRD sum of boxes, mini mental state, etc.), and where the task is to perform early diagnosis of those patients as cognitively normal, mildly impaired, or at risk of dementia [19, 20]. There are $\approx 12000$ data points in total, from which $n = 2000$ are sampled for each randomly seeded run of experiments; the context space consists of 22 attributes, and the decision space consists of 3 diagnostic actions. The **`CysticFibrosis`** dataset records a cohort of patients enrolled in the UK Cystic Fibrosis registry [68], including a range of demographic variables (age, weight, smoking status, etc.), bacterial infections (burkholderia cepacia, pseudomonas aeruginosa, haemophilus influenza, etc.), and comorbidities (liver disease, hypertension, osteopenia, etc.), and where the task is to perform diagnosis of patients as to their GOLD grading in chronic obstructive pulmonary disease [69] (precisely, "severe" is up to 49% of predicted FEV1 value, "moderate" is between 50–79% of predicted FEV1 value, and "mild" otherwise). There are $\approx 31000$ data points in total, from which $n = 2000$ are sampled for each randomly seeded run of experiments; the context space consists of 34 attributes, and the decision space consists of 3 diagnostic actions.

## B.2 Benchmark Details

In the following, we note where algorithms previously studied for related fields in Table 1 are applicable to ODM or not. We implement the **`Supervised`** benchmark as picking $z \in \{0, 1\}$ based solely on $\hat{\pi}$'s output, and $z = 2$ w.p. $\epsilon$, which makes it resemble "supervised learning" in that incoming data points for learning are not related to the algorithm's decisions whatsoever. The **`Cost-Sensitive`** benchmark is the greedy $(\hat{\pi}, \phi_*)$ from Section 3, which is a straightforward method for solving the "learning with rejection" problem [21–26], and does account for costs ($k_{\text{int}}$ and) $k_{\text{req}}$. However, any such approach has the obvious shortcoming that exploration is entirely passive, as noted in Section 3. Note that algorithms for "online learning with rejection" [27–30] cannot be applied to ODM since they require feedback that is always observed, whereas we work in a setting with abstentive feedback (moreover, existing algorithms are specialized to the binary case). In terms of active learning, note that the majority of related work is specialized to the binary setting in the interest of providing guarantees under specific assumptions; this is similar in environments without the rejection option [31–36] as well as with the rejection option [37–40]. However, a popular and practically applicable paradigm for active learning in the batch learning setting is the Bayesian active learning technique [60], which has since been extended to operate in a variety of other settings [75–77]. In this (pool-based) active learning setting, points are selected for query by ranking the expected reduction in entropy of the available points. Our **`Bayesian Active Request`** benchmark is implemented so as to most straightforwardly adapt this technique to the (stream-based) ODM problem by requesting w.p. $\sim$ expected reduction in entropy. Lastly, as noted in Section 2, the learning setting of [41] somewhat resembles ODM; however, their algorithm requires solving an intractable optimization problem over the version space, and is only applied to binary classification problems, which is not compatible with our more general requirement.

The class of algorithms most readily applicable—prima facie, at least—to ODM is stochastic contextual bandits. We implement the **`Thompson Sampling`** [46] benchmark straightforwardly: First, we draw a sample from the posterior $p(W|d)$, then we select $z$ greedily using the policy $(\hat{\pi}_W, \phi_*)$. There are two versions to consider: When $z=1$ is chosen (i.e. when the model policy is asked to predict), we can either switch to using the marginal $p(Y|D,X)=\mathbb{E}_{W\sim p(\cdot|D)}p(Y|X,W)$ (which would be lower-variance), or still use the sample $\hat{\pi}_W$ (which would be canonical Thompson sampling); the latter is what we refer to as the **`Full`** version. Likewise, we implement the **`Epsilon-Greedy`** [47] benchmark straightforwardly: It acts exactly as the greedy mediator, but draws $z$ at random w.p. $\epsilon$. Given the discussion in Section 3.1, it should be clear that randomly exploring arms $z\in\{0,1\}$ may be wasteful, therefore we also implement a **`Request`** version, which corresponds to the "$\epsilon$-request" described in Section 3.2: It acts exactly as the greedy mediator, but chooses $z=2$ w.p. $\epsilon$. In addition to posterior sampling and epsilon-greedy policies, a third class of strategies in bandit settings is "optimism in the face of uncertainty". However, naively applying these (e.g. the UCB algorithm) would mean that arms $z\in\{0,1\}$ are pulled *more* than in the greedy policy, and thus the request arm is pulled *less* (because model uncertainty is only involved in arms $z\in\{0,1\}$, whereas there is no uncertainty when the request arm is pulled)—which is the exact opposite of what we want. Instead, we implement the **`Pessimistic Bayesian Sampling`** benchmark, which adapts OBS [44] to ODM by reversing the direction of optimism such that the tendency to request actually *increases*. Finally, to highlight the advantage of our proposed criterion, **`Matched Decaying Request`** is an artificially boosted benchmark that is similar to $\epsilon$-request—but where $\epsilon$ is a decay function that has the benefit of matching the effective request rate of UMPIRE: First, the behavior of UMPIRE is observed throughout its 10 runs of experiments for each environment. Second, we plot the curve containing the cumulative number of requests made by UMPIRE as a function of time, averaged across those 10 runs. Third, we search for a polynomial function $\epsilon_t$ of $t$ that—when used to define an $\epsilon_t$-request mediator—produces a request curve that best matches UMPIRE's request curve. (Thus we note that this benchmark is artificial in the sense that it has the benefit of hindsight knowledge).

# C Proofs and Derivations

## C.1 Expected Improvement

Our proof technique is inspired by the strategy used to derive a deterministic generalization bound in [78]. However, there are several key differences: While they use a similar argument to derive a stopping criterion in the conventional active learning problem, we do so to derive a proxy for determining which mediator action to take in UMPIRE for the ODM problem. More importantly, their result gives a bound having observed both $x_t$ and $y_t$, whereas we work with only $x_t$ having been observed, with $y_t$ not yet observed. Furthermore, they explicitly compute KL divergences between parameter posteriors, whereas—with the expectation over $Y_t \sim p(\cdot|d_{t-1}, x_t)$ around the KL-term—we obtain an expression for mutual information instead, which allows us to expand it in the opposite direction to be amenable to computation, and does not require explicit KL divergences between parameter posteriors.

**Theorem 1** Let the model risk $\mathcal{R}$ be bounded as $[-b, b]$—for instance, by centering the loss $\ell_{01}$. Let $\mathbb{I}[W; Y_t|d_{t-1}, x_t]$ denote the mutual information between $W$ and $Y_t$ conditioned on $d_{t-1}$ and $x_t$, and let $W_0$ denote the principal branch of the product logarithm function. Then we have the following:

$$\bar{\mathcal{R}}(d_{t-1}) - \mathbb{E}_{Y_t \sim p(\cdot|d_{t-1}, x_t)}[\bar{\mathcal{R}}(D_t)|d_{t-1}, x_t, Z_t = 2] \leq 2b(e^{W_0\left(\frac{1}{e}(\mathbb{I}[W;Y_t|d_{t-1},x_t]-1)\right)+1} - 1) \quad (6)$$

*Proof.* Let $f\!:\!\mathcal{W}\!\to\![-b, b]$ and $c$ be a constant that satisfies $\mathbb{E}_{W\sim p(\cdot|d)} f(W)^2 \!\leq\! c$ for any $d \in \mathcal{D}$:

$$\begin{aligned}
&\mathbb{E}_{\substack{Y_t\sim p(\cdot|d_{t-1},x_t)\\ W\sim p(\cdot|d_{t-1},x_t,Y_t)}} f(W) - \mathbb{E}_{W\sim p(\cdot|d_{t-1})} f(W) && (8)\\
&\leq \tfrac{1}{\lambda}\big(\mathbb{E}_{Y_t\sim p(\cdot|d_{t-1},x_t)} \log \mathbb{E}_{W\sim p(\cdot|d_{t-1})} e^{\lambda f(W)} - \mathbb{E}_{W\sim p(\cdot|d_{t-1})} \lambda f(W)\\
&\quad + \mathbb{E}_{Y_t\sim p(\cdot|d_{t-1},x_t)} D_{\text{KL}}\big(p(W|d_{t-1}, x_t, Y_t)\|p(W|d_{t-1})\big)\big) && (9)\\
&\leq \tfrac{1}{\lambda}\big((e^{2b\lambda} - 2b\lambda - 1)\mathbb{E}_{W\sim p(\cdot|d_{t-1})} \tfrac{f(W)^2}{4b^2}\\
&\quad + \mathbb{E}_{Y_t\sim p(\cdot|d_{t-1},x_t)} D_{\text{KL}}\big(p(W|d_{t-1}, x_t, Y_t)\|p(W|d_{t-1})\big)\big) && (10)\\
&\leq \tfrac{1}{\lambda}\big(\tfrac{c}{4b^2}(e^{2b\lambda} - 2b\lambda - 1) + \mathbb{I}[W; Y_t|d_{t-1}, x_t]\big) && (11)
\end{aligned}$$

where the first inequality uses Lemma 2, the second Lemma 3, and the third the fact that:

$$\mathbb{I}[W; Y_t|d_{t-1}, x_t] = \mathbb{E}_{Y_t\sim p(\cdot|d_{t-1},x_t)} D_{\text{KL}}(p(W|d_{t-1}, x_t, Y_t)\|p(W|d_{t-1})) \quad (12)$$

Minimizing Expression 11 with respect to $\lambda$ by setting the derivative to zero:

$$\begin{aligned}
2be^{2b\lambda} - 2b &= \tfrac{1}{\lambda}\big(e^{2b\lambda} - 2b\lambda - 1 + \tfrac{4b^2}{c}\mathbb{I}[W; Y_t|d_{t-1}, x_t]\big) && (13)\\
(2b\lambda - 1)e^{2b\lambda-1} &= \tfrac{4b^2}{ec}\big(\mathbb{I}[W; Y_t|d_{t-1}, x_t] - \tfrac{c}{4b^2}\big) && (14)\\
\lambda &= \tfrac{1}{2b}\big(W_0\big(\tfrac{4b^2}{ec}\mathbb{I}[W; Y_t|d_{t-1}, x_t] - \tfrac{1}{e}\big) + 1\big) && (15)
\end{aligned}$$

Substituting this $\lambda$ back into Expression 11:

$$\begin{aligned}
&\tfrac{1}{\lambda}\big(e^{2b\lambda} - 2b\lambda - 1 + \mathbb{I}[W; Y_t|d_{t-1}, x_t]\big) && (16)\\
&\qquad = \tfrac{2b}{W_0(h)+1}\big(e^{W_0(h)+1} - (W_0(h) + 1) + \mathbb{I}[W; Y_t|d_{t-1}, x_t] - 1\big) && (17)\\
&\qquad = \tfrac{2b}{W_0(h)+1}\big(e^{W_0(h)+1} + W_0(h)e^{W_0(h)+1} - (W_0(h) + 1)\big) && (18)\\
&\qquad = 2b\big(e^{W_0(\frac{1}{e}\mathbb{I}[W;Y_t|d_{t-1},x_t]-\frac{1}{e})+1} - 1\big) && (19)
\end{aligned}$$

where we define $h\!:=\!\frac{1}{e}\mathbb{I}[W; Y_t|d_{t-1}, x_t]\!-\!\frac{1}{e}$ and let $c\!=\!4b^2$. Now let $f\!:=\!-\mathcal{R}$:

$$\begin{aligned}
&\bar{\mathcal{R}}(d_{t-1}) - \mathbb{E}_{Y_t\sim p(\cdot|d_{t-1},x_t)}[\bar{\mathcal{R}}(D_t)|d_{t-1}, x_t, Z_t = 2]\\
&\qquad = \mathbb{E}_{W\sim p(\cdot|d_{t-1})}\mathcal{R}(W) - \mathbb{E}_{\substack{Y_t\sim p(\cdot|d_{t-1},x_t)\\ W\sim p(\cdot|d_{t-1},x_t,Y_t)}} \mathcal{R}(W) && (20)\\
&\qquad \leq g\big(\mathbb{I}[W; Y_t|d_{t-1}, x_t]\big)
\end{aligned}$$

where we define $g\!:\!v\!\mapsto\! g(v) = 2b(e^{W_0(\frac{1}{e}(v-1))+1}\!-\!1)$, which concludes the proof. □

**Lemma 2** For any $f\!:\!\mathcal{W}\!\to\!\mathbb{R}$:

$$\mathbb{E}_{W\sim p(\cdot|d_{t-1},x_t,y_t)} f(W) \leq \log \mathbb{E}_{W\sim p(\cdot|d_{t-1})} e^{f(W)} + D_{\text{KL}}\big(p(W|d_{t-1}, x_t, y_t)\|p(W|d_{t-1})\big) \quad (21)$$

*Proof.* Use any argument for Donsker-Varadhan's variational representation of the KL divergence, e.g.

$$\begin{aligned}
&D_{\text{KL}}\big(p(W|d_{t-1}, x_t, y_t)\|p(W|d_{t-1})\big) && (22)\\
&\quad = \sup_{f':\mathcal{W}\to\mathbb{R}} \big\{\mathbb{E}_{W\sim p(\cdot|d_{t-1},x_t,y_t)} f'(W) - \log \mathbb{E}_{W\sim p(\cdot|d_{t-1})} e^{f'(W)}\big\} && (23)\\
&\quad \geq \mathbb{E}_{W\sim p(\cdot|d_{t-1},x_t,y_t)} f(W) - \log \mathbb{E}_{W\sim p(\cdot|d_{t-1})} e^{f(W)} && (24)
\end{aligned}$$

Or, to the same effect:

$$\begin{aligned}
&\log \mathbb{E}_{W\sim p(\cdot|d_{t-1})} e^{f(W)} && (25)\\
&\qquad = \sup_{p'\in\Delta(\mathcal{W})} \big\{\mathbb{E}_{W\sim p'} f(W) - D_{\text{KL}}\big(p'\|p(W|d_{t-1})\big)\big\} && (26)\\
&\qquad \geq \mathbb{E}_{W\sim p(\cdot|d_{t-1},x_t,y_t)} f(W) - D_{\text{KL}}\big(p(W|d_{t-1}, x_t, y_t)\|p(W|d_{t-1})\big) && (27)
\end{aligned}$$

**Lemma 3** For any $\lambda > 0$, $f : \mathcal{W} \to [-b, b]$:

$$\log \mathbb{E}_{W\sim p(\cdot|d_{t-1})} e^{\lambda f(W)} - \mathbb{E}_{W\sim p(\cdot|d_{t-1})} \lambda f(W) \leq (e^{2b\lambda} - 2b\lambda - 1)\mathbb{E}_{W\sim p(\cdot|d_{t-1})} \tfrac{f(W)^2}{4b^2} \tag{28}$$

*Proof.* Note that $\frac{1}{u^2}(e^u - u - 1)$ is a nondecreasing function of $u$, so:

$$e^{\lambda f(W)} - \lambda f(W) - 1 \leq (e^{2b\lambda} - 2b\lambda - 1)\tfrac{f(W)^2}{4b^2} \tag{29}$$

$$\mathbb{E}_{W\sim p(\cdot|d_{t-1})}[e^{\lambda f(W)} - \lambda f(W) - 1] \leq (e^{2b\lambda} - 2b\lambda - 1)\mathbb{E}_{W\sim p(\cdot|d_{t-1})} \tfrac{f(W)^2}{4b^2} \tag{30}$$

$$\log \mathbb{E}_{W\sim p(\cdot|d_{t-1})} e^{\lambda f(W)} - \mathbb{E}_{W\sim p(\cdot|d_{t-1})} \lambda f(W) \leq (e^{2b\lambda} - 2b\lambda - 1)\mathbb{E}_{W\sim p(\cdot|d_{t-1})} \tfrac{f(W)^2}{4b^2} \tag{31}$$

### C.2 Practical Implementation

We briefly elaborate here on the derivation for Equation 7. Let $\{w_{i,t}\}_{i=1}^{s}$ indicate the set of samples drawn from posterior $p(W|d_t)$. To compute the value of $\mathbb{I}[W; Y_t|d_{t-1}, x_t]$ at each round, we can write:

$$\begin{aligned} \mathbb{I}[W; Y_t|d_{t-1}, x_t] &= \mathbb{E}_{Y_t\sim p(\cdot|d_{t-1},x_t)} D_{\text{KL}}\big(p(W|d_{t-1}, x_t, Y_t) \| p(W|d_{t-1})\big) && (32)\\ &= \mathbb{H}[W|d_{t-1}] - \mathbb{E}_{Y_t\sim p(\cdot|d_{t-1},x_t)} \mathbb{H}[W|d_{t-1}, x_t, Y_t] && (33) \end{aligned}$$

which is the expected—over $Y_t \sim p(\cdot|d_{t-1}, x_t)$—reduction in entropy of $W$, i.e. how much the $Y_t$'s "inform" on $W$ given $x_t$. However, computing this term requires retraining on every possible $Y_t$ value:

$$H[p(W|d_{t-1})] - \textstyle\sum_{y_t\in\mathcal{Y}} \mathbb{E}_{W\sim p(\cdot|d_{t-1})} p(y_t|x_t, W) H[\underbrace{p(W'|d_{t-1}, x_t, y_t)}_{\text{retrain}}] \tag{34}$$

where $H[p(W)] := -\frac{1}{s}\sum_{i=1}^{s} \log p(w_i)$. However, if we expand mutual information the opposite way:

$$\begin{aligned} \mathbb{I}[Y_t; W|d_{t-1}, x_t] &= \mathbb{E}_{W\sim p(\cdot|d_{t-1})} D_{\text{KL}}\big(p(Y_t|x_t, W) \| p(Y_t|d_{t-1}, x_{t-1})\big) && (35)\\ &= \mathbb{H}[Y_t|d_{t-1}, x_t] - \mathbb{E}_{W\sim p(\cdot|d_{t-1})} \mathbb{H}[Y_t|x_t, W] && (36) \end{aligned}$$

which is the expected—over $W \sim p(\cdot|d_{t-1})$—reduction in entropy of $Y_t|x_t$, i.e. how much the $W$'s "disagree" on $Y_t|x_t$ given $d_{t-1}$. Computing this term does not require retraining on every possible $Y_t$:

$$H[\tfrac{1}{s}\textstyle\sum_{i=1}^{s} p(Y_t|x_t, w_{i,t-1})] - \tfrac{1}{s}\sum_{i=1}^{s} H[p(Y_t|x_t, w_{i,t-1})] \tag{37}$$

where $H[p(Y)] := -\sum_{y\in\mathcal{Y}} p(y) \log p(y)$. Therefore this is the implementation we use in Algorithm 1.

### C.3 Abstentive Feedback

In Section 3.1, we argued that abstentive feedback is the primary ingredient distinguishing ODM from bandits. To precisely highlight this, consider a more abstract formalism of a learner interacting with an environment. Let $\mathcal{X}$ be the space of contexts, $\mathcal{A}$ of actions, and $\mathcal{O}$ of outcomes, and let $\Sigma$ be some alphabet of feedback signals. Let $\mathbf{R} \in \mathbb{R}^{|\mathcal{A}|\times|\mathcal{O}|}$ denote the reward matrix, $\mathbf{F} \in \Sigma^{|\mathcal{A}|\times|\mathcal{O}|}$ the feedback matrix, and $\mathcal{H} := \Delta(\mathcal{O})^{\mathcal{X}}$ a class of functions mapping contexts to distributions of outcomes. Then:

**Definition 3** A *contextual partial monitoring* game [79, 80] between a learner and an environment is specified by $(\mathbf{R}, \mathbf{F}, \mathcal{H})$, which is given to the learner, and $h \in \mathcal{H}$, which is not. At the beginning of each round, a context $x_t \in \mathcal{X}$ is drawn exogenously, upon which the learner selects $a_t \in \mathcal{A}$ and the environment selects $o_t \in \mathcal{O}$. Then the learner receives the *unobservable* reward $\mathbf{R}_{a_t,o_t}$, as well as the *observable* feedback $\mathbf{F}_{a_t,o_t}$. The goal of the learner is to minimize the (unobserved) cumulative losses.

- Bandit Feedback: In this formalism, contextual bandit problems are characterized by the property that $\mathbf{F} = \mathbf{R}$: The feedback received for learning is identical to the loss incurred at every round. Therefore *some amount of learning always occurs*, regardless of which arm is ultimately pulled.
- Abstentive Feedback: In contrast, ODM is characterized by the fact that every row (i.e. action) of $\mathbf{F}$ contains the same (null) symbol for all columns (i.e. outcomes), except the row corresponding to requesting the expert decision. Writing out the matrices for ODM with mediator $(\hat{\pi}, \phi)$ as the learner:

$$\mathbf{R} = \begin{bmatrix} -\ell(y^{(0)}, \delta(Y - \tilde{y}_t)) & \ldots & -\ell(y^{(m-1)}, \delta(Y - \tilde{y}_t)) \\ -k_{\text{int}} & \ldots & -\ell(y^{(m-1)}, \delta(Y - y^{(0)})) - k_{\text{int}} \\ -\ell(y^{(0)}, \delta(Y - y^{(1)})) - k_{\text{int}} & \ldots & -\ell(y^{(m-1)}, \delta(Y - y^{(1)})) - k_{\text{int}} \\ \vdots & \ldots & \vdots \\ -\ell(y^{(0)}, \delta(Y - y^{(m-2)})) - k_{\text{int}} & \ldots & -\ell(y^{(m-1)}, \delta(Y - y^{(m-2)})) - k_{\text{int}} \\ -\ell(y^{(0)}, \delta(Y - y^{(m-1)})) - k_{\text{int}} & \ldots & -k_{\text{int}} \\ -k_{\text{req}} & \ldots & -k_{\text{req}} \end{bmatrix} \quad \mathbf{F} = \begin{bmatrix} \perp & \ldots & \perp \\ \perp & \ldots & \perp \\ \perp & \ldots & \perp \\ \vdots & \ldots & \vdots \\ \perp & \ldots & \perp \\ \perp & \ldots & \perp \\ y^{(0)} & \ldots & y^{(m-1)} \end{bmatrix} \tag{38}$$

where $y^{(i)}$ denotes the $i^{\text{th}}$ element in $\mathcal{Y}$ (containing $m$ elements), indexed from zero upwards. (The first row in each matrix corresponds to accepting the human decision, the last row requesting from the expert, and intermediate rows intervening with a model output; the columns correspond to the $m$ possible values that the oracle $Y$ can take.[1]) Thus *no learning occurs for all except one action*—which is why the role of "exploration" is very different in that most arms pulled for the sake of exploration yield no learning. Therefore we would not expect naively applying bandit algorithms in ODM to perform well.

Note that there does exist a rich literature on variations on the bandit problem—e.g. combinatorial bandits, bandits with side information, etc.—in which the feedback received at each round is *more* informative than the loss incurred. However, that only means the learner has strictly more information to work with. The point here is that contextual bandits never provide feedback with *less* information than the loss, which is the case for ODM. Also, note that while Definition 3 is general, only some special cases have been studied, such as apple tasting with a logistic model [55], locally-observable games with linear/logistic models [79], or where both rewards and observations are linear [80]. Future work may consider analyzing ODM under more general contextual partial monitoring settings. Lastly, note that partial monitoring is not to be confused with partially-observable bandits (see e.g. [81, 82]): The latter deals with partially-observed *contexts*, while the former deals with partially-observed *feedback*.

# D Further Related Work

Section 2.2 described the context and challenges of ODM, paying particular attention to the three primary strands of related problem settings: *learning with rejection* [21–30], *stream-based active learning* [31–36], *stochastic contextual bandits* [42–48], as well as some variations thereof [37–41, 49–58]. For completeness, we now describe some additional domains of—more tangentially—related work.

There is a wide-ranging field of research dedicated to studying various aspects of "assistive learning" and "cooperative learning", where the overarching goal is to use machines to help humans achieve their goals [83, 84]. For instance, *active reward learning* seeks to infer a human's goals, preferences, or reward functions by observing their behavior and choosing particular questions to ask the human for targeted feedback [85–88]. A typical solution consists of a question policy and a policy decision function to maximize the expected reward. On a different note, *assistance games* model humans as part of the environment with some latent goal, and the agent's goal is to balance between actions that learn about this goal and actions that achieve the learned goal [83,89–91]. This leads to a two-agent POMDP with the goal of finding pairs of strategies for humans and machines that maximize expected reward, with human actions and machine actions observable to both. In either case, while the high-level idea is similar to ours—that is, to seek some notion of "principal-agent alignment" [92] between humans and machines—their formalisms, objectives, and solution strategies are entirely distinct from ODM.

In the supervised learning setting, *active label correction* deals with interactive methods for cleaning an established training dataset of possibly-mislabeled examples by using the assistance of a domain expert [93–95]. Since cleaned labels are only obtainable at a cost, the goal is to identify training patterns for which knowing the true labels best improves the learning algorithm's performance. For instance, [94] leverages the assumption of class-conditional noise, and [95] takes advantage of the assumption that noise is concentrated near decision boundaries. In the incremental learning setting, *skeptical learning* deals with learning from a stream of possibly-mislabeled examples, where the algorithm has the opportunity to ask the human to double-check their annotations before learning from each incoming data point [96–98]. For instance, [96] uses an estimate of confidence about both the model and the user in order to decide whether or not an example is worth double-checking, and [97] uses Gaussian processes to supply explicit uncertainty estimates regarding each incoming sample. In either case, a pitfall is that noisy labels may sometimes be admitted and erroneously learned from, which means that incorrect data accumulates over time with high probability. The idea of label correction has also been applied to *active learning from weak labelers*, either given the ability to query from a pool of samples [99], or the ability to query anywhere in the input space [100]. In all these fields, while the high-level idea of interacting with strong (oracle) and weak (human) agents bears some resemblance to our setting, their formalisms, objectives, and solution strategies are entirely distinct from ODM.

[1] Here, the space $\mathcal{A}$ contains the $m+2$ "arms" (i.e. one *accept* arm, one *request* arm, and one *intervene* arm for each of the $m$ underlying actions), the space $\mathcal{O}=\mathcal{Y}$ contains the $m$ possible expert ground-truths, and the alphabet $\Sigma=\mathcal{Y}\cup\{\perp\}$ contains the $m$ possible labels, as well as including the null symbol to denote the lack of feedback.

# E Further Discussions and Sensitivities

## E.1 Why keep the imperfect human in the loop?

Our choice to keep the imperfect human in the loop is motivated by real-world ethical considerations: In many high-stakes settings, concrete attribution of *responsibility* is an absolute requirement. For instance, in most healthcare systems, the responsibility for a cancer diagnosis must be traceable to the *person* (not a *machine*) who actually ordered it—and is therefore legally/ethically/financially accountable for it (see e.g. [13, 15]).

Our formulation of the ODM problem reflects this consideration. In our framework, an imperfect human first attempts to make a decision, which is observed. Then, the *mediator* decides which of the following happens: (1) "Accept": The imperfect human's decision goes through. So the *imperfect human* is responsible for that decision. (2) "Intervene": The mediator proposes an alternative to the imperfect human. This immediately incurs a cost ($k_{\text{int}}$), representing the fact that the imperfect human is now asked to spend time/resources in reconsidering/altering their original decision in light of the proposal. But the *imperfect human* is still responsible for the decision, regardless of whether or not they comply with the proposal.[2] (3) "Request": The expert is invited to make the decision instead. So the *expert* is now responsible for that decision.

If we "remove" the imperfect human from the loop, then all decisions would be made autonomously by the machine unless the expert is queried—which is strongly at odds with societal notions of ethical responsibility/accountability for high-stakes decisions. (To be clear, the "intervene" option is not autonomously "overriding" the imperfect human's decision: It is simply proposing an alternative!)

## E.2 Can the model interact only with the expert?

Many existing works operate in a framework where the *machine* itself is directly allowed to make decisions autonomously, and selectively query the expert (e.g. when it is uncertain). Given the above discussion, we would expect that this setting is generally applicable to non-high-stakes decisions (i.e. where notions of responsibility are not legally/ethically/financially required to be tied to a *person*).

That being said, the ODM framework is simply a *generalization* of this. Consider setting $k_{\text{int}} = 0$ in ODM: This effectively recovers the simpler setting where a machine interacts with an expert (i.e. the imperfect human would indeed become "redundant"). Importantly, however, in general the human is *not* "redundant" whenever $k_{\text{int}} > 0$, as long as the imperfect human has non-zero probability of being correct. Precisely, the mediator policy needs to decide if the human is likely already correct, so it can choose to "accept" (instead of "intervene") in order to avoid incurring the cost $k_{\text{int}}$.

Finally, it is worth reiterating that the ODM problem is also distinguished by the fact that feedback is *abstentive*. Whereas, existing works in machine-expert interaction (including [24] and [101]) operate in settings where feedback is *not* abstentive. That is to say, even if we set $k_{\text{int}} = 0$, the ODM setting is still fundamentally more challenging to tackle, as discussed throughout the manuscript.

### Preface to further results in Appendices E.3–E.6

In our experiments, the imperfect human's decisions are simulated with $\alpha = 0.5$, although the specific frequency of human mistakes does not affect the basic structure/hardness of the problem. Our motivation is simply to simulate decisions that stochastically deviate from the expert's with some probability between zero and one. Appendices E.3–E.4 perform a complete re-run of our main experiments under the same conditions as before—but now setting $\alpha = 0.9$. For completeness, we can additionally ask how performance varies for different levels of $\alpha$, and if $k_{\text{int}} = 0.0$ instead of $k_{\text{int}} = 0.1$. Appendices E.5–E.6 perform experiments for the cartesian product of settings $\alpha \in \{0.5, 0.7, 0.9, 1.0\}$ and $k_{\text{int}} \in \{0.0, 0.1\}$, using the GaussSine environment. Across all sensitivities, it is easy to verify that UMPIRE still consistently accumulates lower regret (our primary metric of interest), as well as outperforming comparators with respect to to the rest of the performance measures.

[2] Whether or not they comply with the proposal is beyond the scope of our work: There may be a variety of reasons why they do/don't comply downstream. Importantly, however, from the perspective of the *mediator*, it has already done its job—and the correctness of its proposed alternative can be evaluated (and on the basis of which we can define concrete notions of model regret and system regret, which is what we do).

### E.3 Sensitivity on Human Error (Performance)

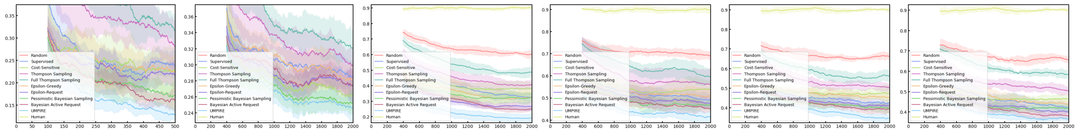

(a) **GaussSine** (b) **HighEnergy** (c) **MotionCapture** (d) **LunarLander** (e) **Alzheimers** (f) **CysticFibrosis**

Figure 32: *System Performance*: Losses. Numbers are plotted as moving average of rolling window of width $n/5$.

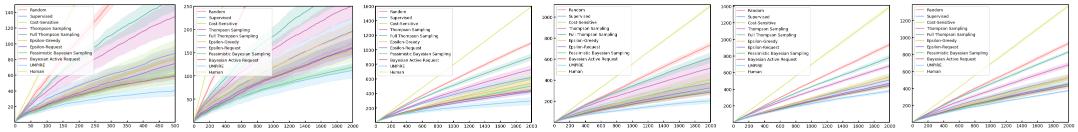

(a) **GaussSine** (b) **HighEnergy** (c) **MotionCapture** (d) **LunarLander** (e) **Alzheimers** (f) **CysticFibrosis**

Figure 33: *System Performance*: Regrets. Numbers are plotted as cumulative sums of system loss less oracle loss.

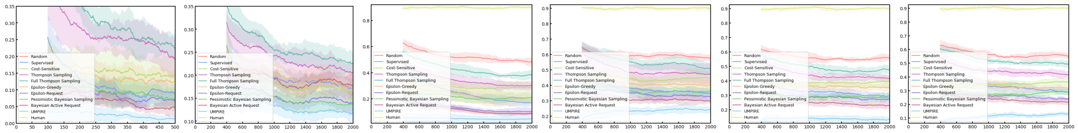

(a) **GaussSine** (b) **HighEnergy** (c) **MotionCapture** (d) **LunarLander** (e) **Alzheimers** (f) **CysticFibrosis**

Figure 34: *System Performance*: Mistakes. Numbers are plotted as moving average of rolling window of width $n/5$.

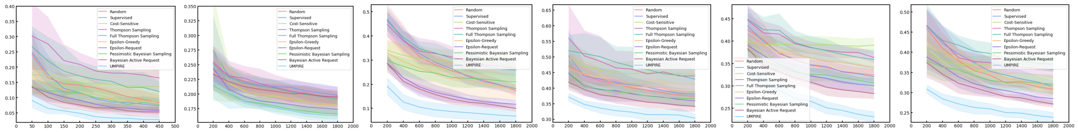

(a) **GaussSine** (b) **HighEnergy** (c) **MotionCapture** (d) **LunarLander** (e) **Alzheimers** (f) **CysticFibrosis**

Figure 35: *Model Performance*: Heldout Mistakes. Models are evaluated on heldout data once every $n/10$ rounds.

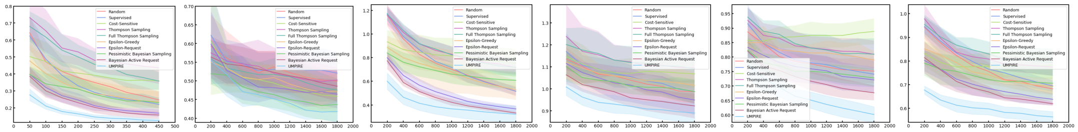

(a) **GaussSine** (b) **HighEnergy** (c) **MotionCapture** (d) **LunarLander** (e) **Alzheimers** (f) **CysticFibrosis**

Figure 36: *Model Performance*: Heldout CrossEnt. Models are evaluated on heldout data once every $n/10$ rounds.

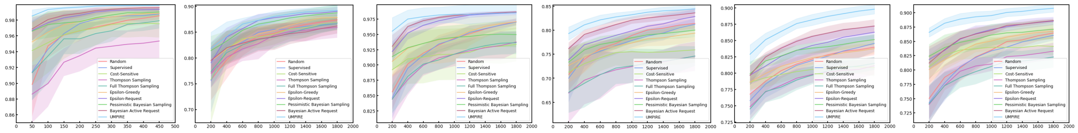

(a) **GaussSine** (b) **HighEnergy** (c) **MotionCapture** (d) **LunarLander** (e) **Alzheimers** (f) **CysticFibrosis**

Figure 37: *Model Performance*: Heldout AUROC. Models are evaluated on heldout data once every $n/10$ rounds.

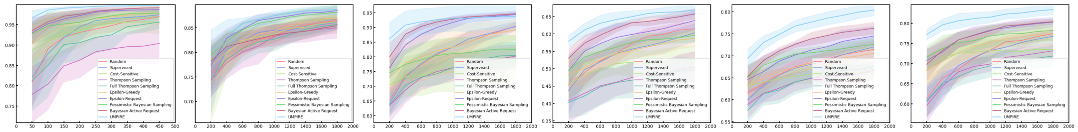

(a) **GaussSine** (b) **HighEnergy** (c) **MotionCapture** (d) **LunarLander** (e) **Alzheimers** (f) **CysticFibrosis**

Figure 38: *Model Performance*: Heldout AUPRC. Models are evaluated on heldout data once every $n/10$ rounds.

| | **GaussSine** | | | **HighEnergy** | | | **MotionCapture** | | | **LunarLander** | | | **Alzheimers** | | | **CysticFibrosis** | | |
|---|---|---|---|---|---|---|---|---|---|---|---|---|---|---|---|---|---|---|
| Benchmark | *Err. Acc.* | *Exc. Int.* | *Abs. Shf.* | *Err. Acc.* | *Exc. Int.* | *Abs. Shf.* | *Err. Acc.* | *Exc. Int.* | *Abs. Shf.* | *Err. Acc.* | *Exc. Int.* | *Abs. Shf.* | *Err. Acc.* | *Exc. Int.* | *Abs. Shf.* | *Err. Acc.* | *Exc. Int.* | *Abs. Shf.* |
| Random | 207±10 | 55±9 | 66±11 | 809±15 | 264±12 | 356±13 | 816±20 | 315±26 | 463±37 | 816±26 | 434±21 | 693±40 | 812±28 | 385±29 | 588±35 | 812±28 | 392±20 | 594±33 |
| Supervised | 32±12 | 35±8 | 58±11 | 360±28 | 48±8 | 356±28 | 70±14 | 456±33 | 468±33 | 203±34 | 575±31 | 695±50 | 356±42 | 316±33 | 589±20 | 280±36 | 422±52 | 609±38 |
| Cost-Sensitive | 58±29 | 20±11 | 66±26 | 350±33 | 31±5 | 350±34 | 225±52 | 345±38 | 490±81 | 309±43 | 584±69 | 794±67 | 611±51 | 153±16 | 662±43 | 530±36 | 157±17 | 583±39 |
| Thompson Sampling | 80±19 | 62±12 | 97±18 | 423±37 | 78±8 | 356±37 | 216±41 | 521±40 | 560±66 | 345±71 | 705±66 | 849±109 | 507±35 | 427±26 | 687±31 | 494±51 | 450±41 | 661±25 |
| Full Thompson Sampling | 74±16 | 90±12 | 118±13 | 417±24 | 133±17 | 395±23 | 214±38 | 692±29 | 745±46 | 352±48 | 796±31 | 969±46 | 491±54 | 545±49 | 795±27 | 508±40 | 587±26 | 826±17 |
| Epsilon-Greedy | 55±14 | 17±7 | 51±16 | 366±27 | 47±5 | 327±29 | 183±39 | 293±65 | 370±89 | 315±35 | 513±39 | 701±52 | 543±44 | 183±21 | 582±38 | 470±48 | 202±49 | 533±40 |
| Epsilon-Request | 29±12 | 16±6 | 38±8 | 295±24 | 26±4 | 294±24 | 62±16 | 209±31 | 239±37 | 232±30 | 460±34 | 615±52 | 423±30 | 155±18 | 491±18 | 333±23 | 182±32 | 435±22 |
| Pessimistic Bayesian Sampling | 28±9 | 24±8 | 42±12 | 271±17 | 36±6 | 279±15 | 89±28 | 355±34 | 371±45 | 199±33 | 557±28 | 656±39 | 335±50 | 265±20 | 512±33 | 285±39 | 280±33 | 476±25 |
| Bayesian Active Request | 19±8 | 18±7 | 33±5 | 346±15 | 40±8 | 346±15 | 33±10 | 219±24 | 222±25 | 160±20 | 461±29 | 554±29 | 263±31 | 234±30 | 438±21 | 211±37 | 278±28 | 431±24 |
| **UMPIRE** | 9±5 | 3±2 | 12±6 | 239±17 | 24±6 | 239±17 | 22±8 | 74±53 | 85±48 | 128±26 | 326±20 | 411±30 | 185±14 | 86±16 | 248±20 | 139±19 | 82±13 | 203±14 |

Table 6: *Mediator Performance*: Erroneous acceptance, excessive intervention, and abstention shortfall at $t=n$.

## E.4 Sensitivity on Human Error (Source of Gain)

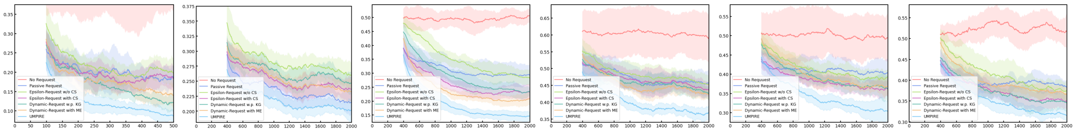

(a) **GaussSine** (b) **HighEnergy** (c) **MotionCapture** (d) **LunarLander** (e) **Alzheimers** (f) **CysticFibrosis**

Figure 39: *System Performance*: Losses. Numbers are plotted as moving average of rolling window of width $n/5$.

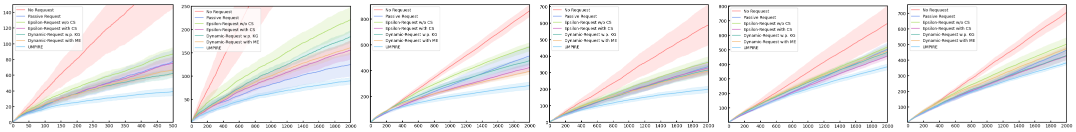

(a) **GaussSine** (b) **HighEnergy** (c) **MotionCapture** (d) **LunarLander** (e) **Alzheimers** (f) **CysticFibrosis**

Figure 40: *System Performance*: Regrets. Numbers are plotted as cumulative sums of system loss less oracle loss.

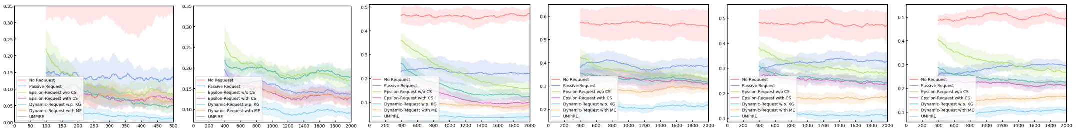

(a) **GaussSine** (b) **HighEnergy** (c) **MotionCapture** (d) **LunarLander** (e) **Alzheimers** (f) **CysticFibrosis**

Figure 41: *System Performance*: Mistakes. Numbers are plotted as moving average of rolling window of width $n/5$.

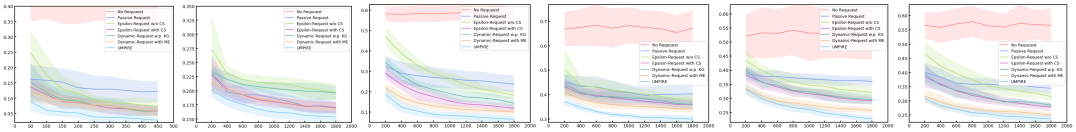

(a) **GaussSine** (b) **HighEnergy** (c) **MotionCapture** (d) **LunarLander** (e) **Alzheimers** (f) **CysticFibrosis**

Figure 42: *Model Performance*: Heldout Mistakes. Models are evaluated on heldout data once every $n/10$ rounds.

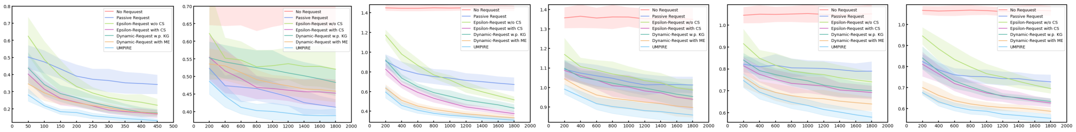

(a) **GaussSine** (b) **HighEnergy** (c) **MotionCapture** (d) **LunarLander** (e) **Alzheimers** (f) **CysticFibrosis**

Figure 43: *Model Performance*: Heldout CrossEnt. Models are evaluated on heldout data once every $n/10$ rounds.

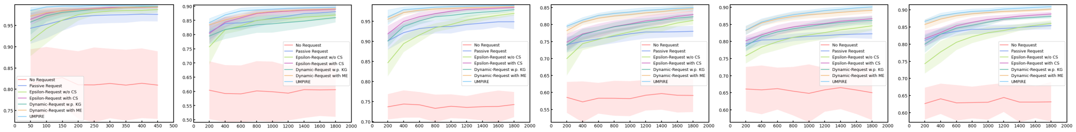

(a) **GaussSine** (b) **HighEnergy** (c) **MotionCapture** (d) **LunarLander** (e) **Alzheimers** (f) **CysticFibrosis**

Figure 44: *Model Performance*: Heldout AUROC. Models are evaluated on heldout data once every $n/10$ rounds.

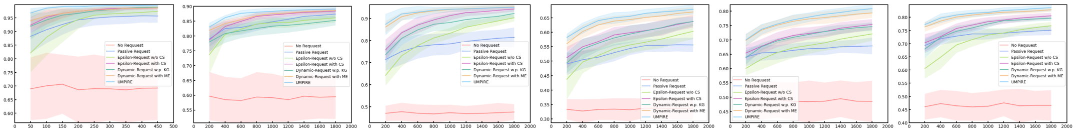

(a) **GaussSine** (b) **HighEnergy** (c) **MotionCapture** (d) **LunarLander** (e) **Alzheimers** (f) **CysticFibrosis**

Figure 45: *Model Performance*: Heldout AUPRC. Models are evaluated on heldout data once every $n/10$ rounds.

| | **GaussSine** | | | **HighEnergy** | | | **MotionCapture** | | | **LunarLander** | | | **Alzheimers** | | | **CysticFibrosis** | | |
|---|---|---|---|---|---|---|---|---|---|---|---|---|---|---|---|---|---|---|
| Benchmark | *Err. Acc.* | *Exc. Int.* | *Abs. Shf.* | *Err. Acc.* | *Exc. Int.* | *Abs. Shf.* | *Err. Acc.* | *Exc. Int.* | *Abs. Shf.* | *Err. Acc.* | *Exc. Int.* | *Abs. Shf.* | *Err. Acc.* | *Exc. Int.* | *Abs. Shf.* | *Err. Acc.* | *Exc. Int.* | *Abs. Shf.* |
| No Requuest | 221±60 | 55±28 | 211±60 | 1051±119 | 76±28 | 890±190 | 955±104 | 428±67 | 1050±68 | 1060±294 | 477±176 | 1211±138 | 1255±125 | 186±101 | 963±165 | 1273±114 | 246±77 | 1033±91 |
| Passive Request | 58±29 | 20±11 | 66±26 | 350±33 | 31±5 | 350±34 | 225±52 | 345±38 | 490±81 | 309±43 | 584±69 | 794±67 | 611±51 | 153±16 | 662±43 | 530±36 | 157±17 | 583±39 |
| Epsilon-Request w/o CS | 49±15 | 26±7 | 58±11 | 399±27 | 38±6 | 356±28 | 149±25 | 394±30 | 468±33 | 292±41 | 509±30 | 695±50 | 457±48 | 265±36 | 589±20 | 474±48 | 314±53 | 609±38 |
| Epsilon-Request with CS | 29±12 | 16±6 | 38±8 | 295±24 | 26±4 | 294±24 | 62±16 | 209±31 | 239±37 | 232±30 | 460±34 | 615±52 | 423±30 | 155±18 | 491±18 | 333±23 | 182±32 | 435±22 |
| Dynamic-Request w.p. KG | 33±8 | 16±8 | 39±8 | 381±16 | 31±7 | 349±14 | 85±20 | 296±35 | 331±26 | 236±33 | 479±32 | 625±38 | 364±33 | 224±31 | 489±20 | 332±34 | 258±31 | 476±21 |
| **UMPIRE** | 9±5 | 3±2 | 12±6 | 239±17 | 24±6 | 239±17 | 22±8 | 74±53 | 85±48 | 128±26 | 326±20 | 411±30 | 185±14 | 86±16 | 248±20 | 139±19 | 82±13 | 203±14 |

Table 7: *Mediator Performance*: Erroneous acceptance, excessive intervention, and abstention shortfall at $t = n$.

### E.5 Complete Sensitivities on $\alpha$ and $k_{\texttt{int}}$ (Performance)

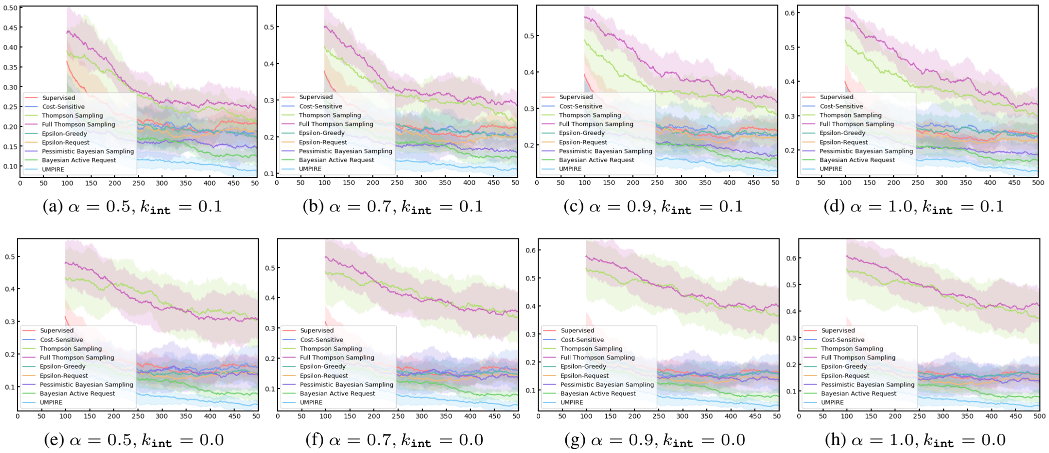

(a) $\alpha = 0.5, k_{\texttt{int}} = 0.1$ (b) $\alpha = 0.7, k_{\texttt{int}} = 0.1$ (c) $\alpha = 0.9, k_{\texttt{int}} = 0.1$ (d) $\alpha = 1.0, k_{\texttt{int}} = 0.1$

(e) $\alpha = 0.5, k_{\texttt{int}} = 0.0$ (f) $\alpha = 0.7, k_{\texttt{int}} = 0.0$ (g) $\alpha = 0.9, k_{\texttt{int}} = 0.0$ (h) $\alpha = 1.0, k_{\texttt{int}} = 0.0$

Figure 46: *System Performance*: Losses. Numbers are plotted as moving average of rolling window of width $n/5$.

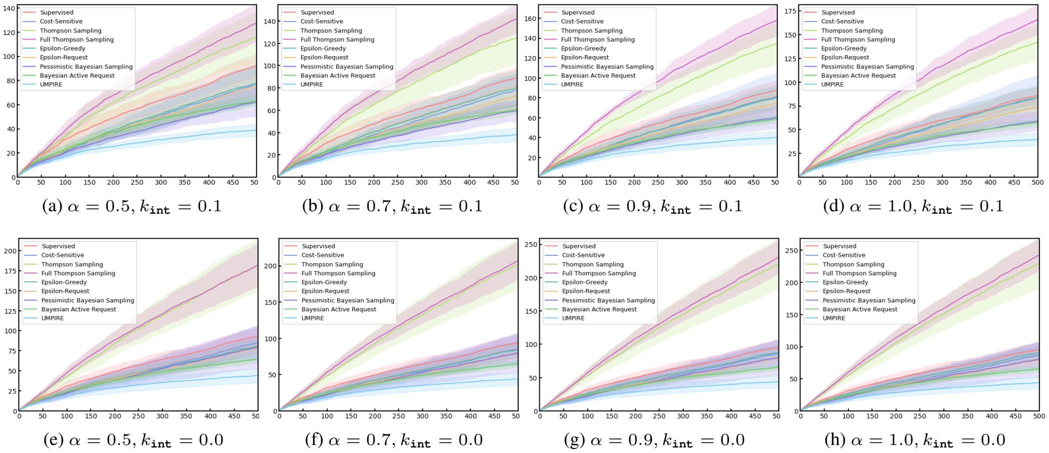

(a) $\alpha = 0.5, k_{\texttt{int}} = 0.1$ (b) $\alpha = 0.7, k_{\texttt{int}} = 0.1$ (c) $\alpha = 0.9, k_{\texttt{int}} = 0.1$ (d) $\alpha = 1.0, k_{\texttt{int}} = 0.1$

(e) $\alpha = 0.5, k_{\texttt{int}} = 0.0$ (f) $\alpha = 0.7, k_{\texttt{int}} = 0.0$ (g) $\alpha = 0.9, k_{\texttt{int}} = 0.0$ (h) $\alpha = 1.0, k_{\texttt{int}} = 0.0$

Figure 47: *System Performance*: Regrets. Numbers are plotted as cumulative sums of system loss less oracle loss.

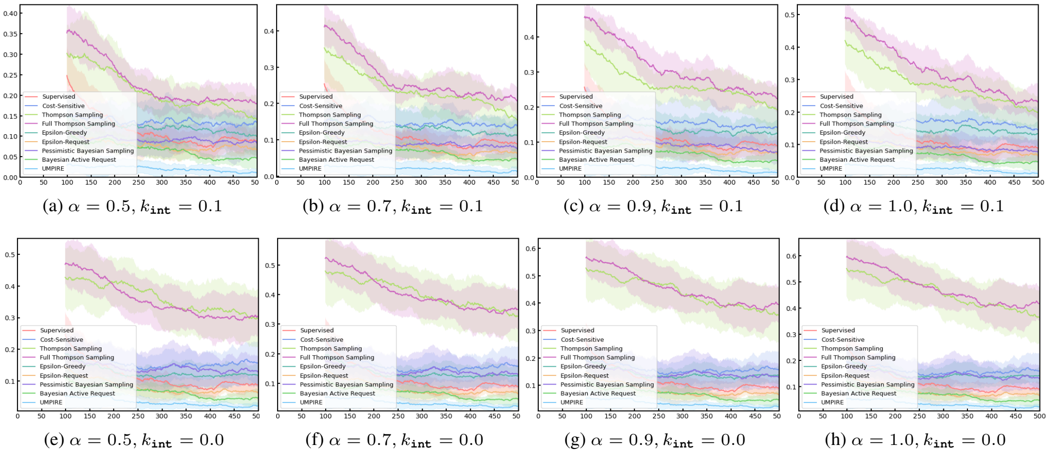

(a) $\alpha = 0.5, k_{\texttt{int}} = 0.1$ (b) $\alpha = 0.7, k_{\texttt{int}} = 0.1$ (c) $\alpha = 0.9, k_{\texttt{int}} = 0.1$ (d) $\alpha = 1.0, k_{\texttt{int}} = 0.1$

(e) $\alpha = 0.5, k_{\texttt{int}} = 0.0$ (f) $\alpha = 0.7, k_{\texttt{int}} = 0.0$ (g) $\alpha = 0.9, k_{\texttt{int}} = 0.0$ (h) $\alpha = 1.0, k_{\texttt{int}} = 0.0$

Figure 48: *System Performance*: Mistakes. Numbers are plotted as moving average of rolling window of width $n/5$.

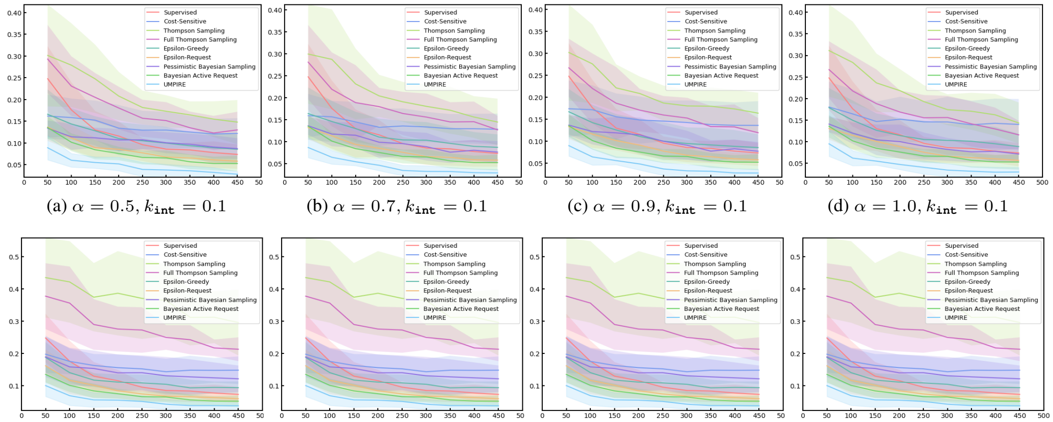

(a) $\alpha = 0.5, k_{\texttt{int}} = 0.1$ (b) $\alpha = 0.7, k_{\texttt{int}} = 0.1$ (c) $\alpha = 0.9, k_{\texttt{int}} = 0.1$ (d) $\alpha = 1.0, k_{\texttt{int}} = 0.1$

(e) $\alpha = 0.5, k_{\texttt{int}} = 0.0$ (f) $\alpha = 0.7, k_{\texttt{int}} = 0.0$ (g) $\alpha = 0.9, k_{\texttt{int}} = 0.0$ (h) $\alpha = 1.0, k_{\texttt{int}} = 0.0$

Figure 49: *Model Performance*: Heldout Mistakes. Models are evaluated on heldout data once every $n/10$ rounds.

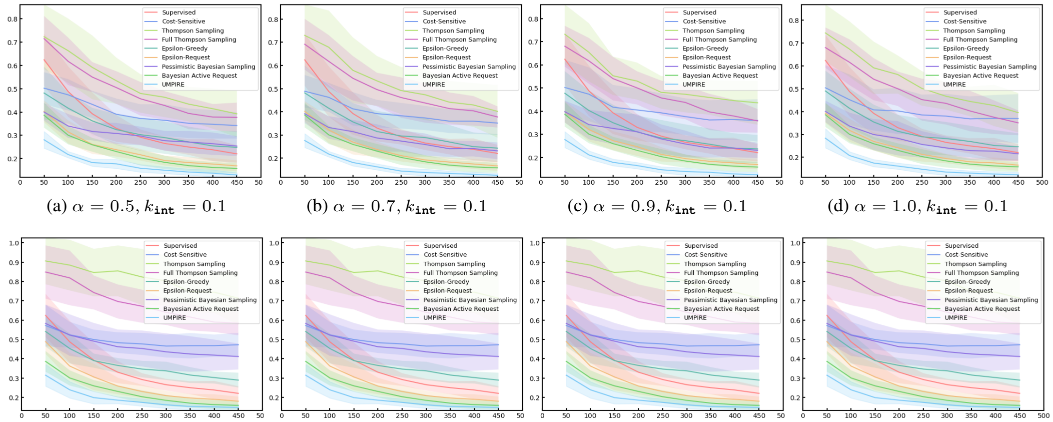

(a) $\alpha = 0.5, k_{\texttt{int}} = 0.1$ (b) $\alpha = 0.7, k_{\texttt{int}} = 0.1$ (c) $\alpha = 0.9, k_{\texttt{int}} = 0.1$ (d) $\alpha = 1.0, k_{\texttt{int}} = 0.1$

(e) $\alpha = 0.5, k_{\texttt{int}} = 0.0$ (f) $\alpha = 0.7, k_{\texttt{int}} = 0.0$ (g) $\alpha = 0.9, k_{\texttt{int}} = 0.0$ (h) $\alpha = 1.0, k_{\texttt{int}} = 0.0$

Figure 50: *Model Performance*: Heldout CrossEnt. Models are evaluated on heldout data once every $n/10$ rounds.

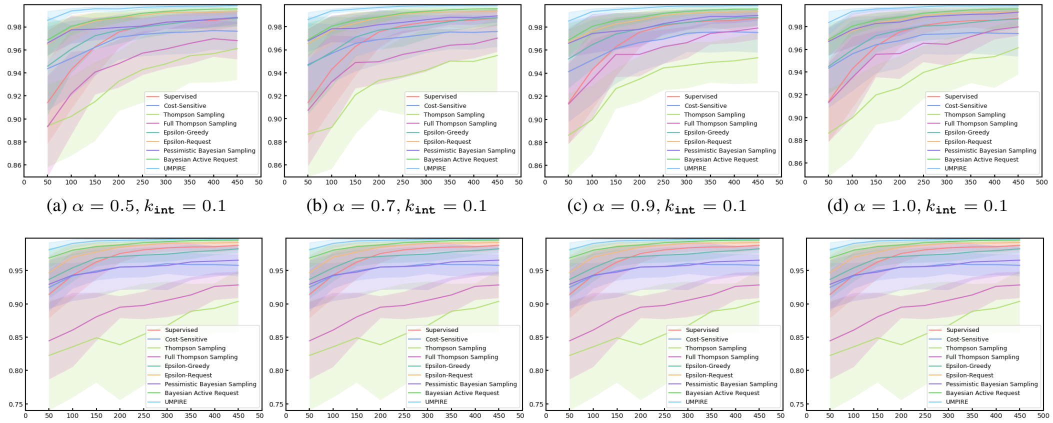

(a) $\alpha = 0.5, k_{\texttt{int}} = 0.1$ (b) $\alpha = 0.7, k_{\texttt{int}} = 0.1$ (c) $\alpha = 0.9, k_{\texttt{int}} = 0.1$ (d) $\alpha = 1.0, k_{\texttt{int}} = 0.1$

(e) $\alpha = 0.5, k_{\texttt{int}} = 0.0$ (f) $\alpha = 0.7, k_{\texttt{int}} = 0.0$ (g) $\alpha = 0.9, k_{\texttt{int}} = 0.0$ (h) $\alpha = 1.0, k_{\texttt{int}} = 0.0$

Figure 51: *Model Performance*: Heldout AUROC. Models are evaluated on heldout data once every $n/10$ rounds.

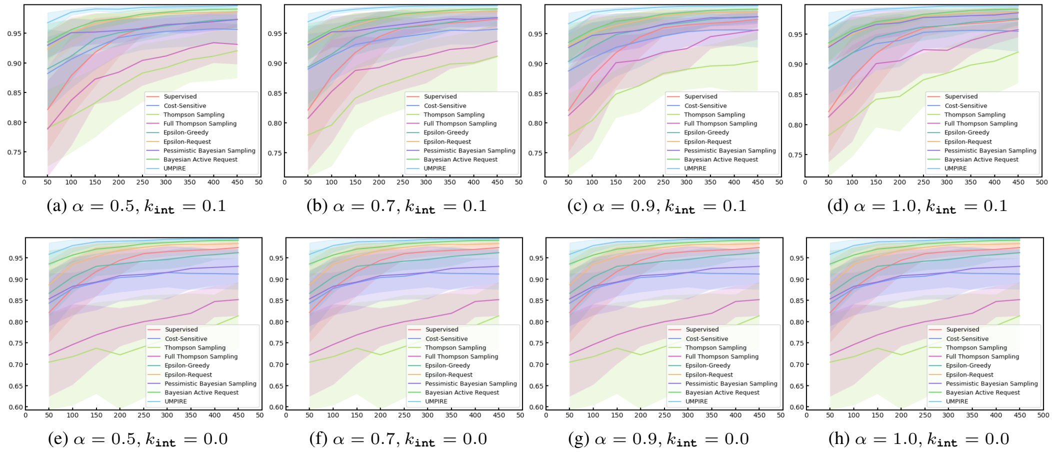

(a) $\alpha = 0.5, k_{\texttt{int}} = 0.1$ (b) $\alpha = 0.7, k_{\texttt{int}} = 0.1$ (c) $\alpha = 0.9, k_{\texttt{int}} = 0.1$ (d) $\alpha = 1.0, k_{\texttt{int}} = 0.1$

(e) $\alpha = 0.5, k_{\texttt{int}} = 0.0$ (f) $\alpha = 0.7, k_{\texttt{int}} = 0.0$ (g) $\alpha = 0.9, k_{\texttt{int}} = 0.0$ (h) $\alpha = 1.0, k_{\texttt{int}} = 0.0$

Figure 52: *Model Performance*: Heldout AUPRC. Models are evaluated on heldout data once every $n/10$ rounds.

### E.6 Complete Sensitivities on $\alpha$ and $k_{\text{int}}$ (Source of Gain)

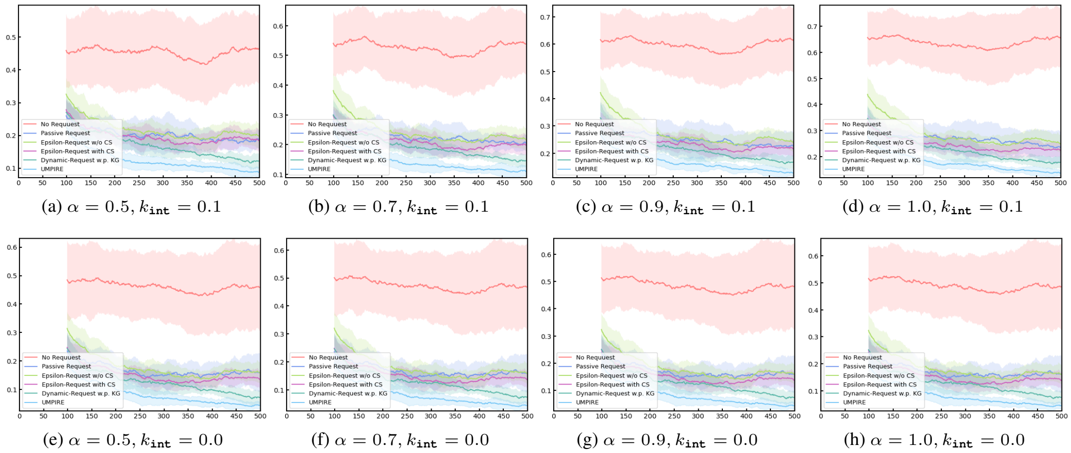

(a) $\alpha = 0.5, k_{\texttt{int}} = 0.1$ (b) $\alpha = 0.7, k_{\texttt{int}} = 0.1$ (c) $\alpha = 0.9, k_{\texttt{int}} = 0.1$ (d) $\alpha = 1.0, k_{\texttt{int}} = 0.1$

(e) $\alpha = 0.5, k_{\texttt{int}} = 0.0$ (f) $\alpha = 0.7, k_{\texttt{int}} = 0.0$ (g) $\alpha = 0.9, k_{\texttt{int}} = 0.0$ (h) $\alpha = 1.0, k_{\texttt{int}} = 0.0$

Figure 53: *System Performance*: Losses. Numbers are plotted as moving average of rolling window of width $n/5$.

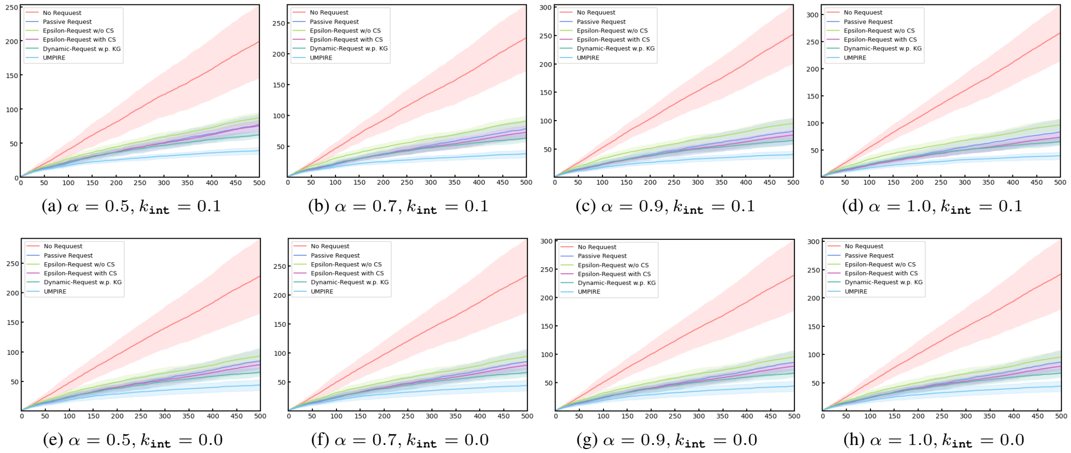

(a) $\alpha = 0.5, k_{\texttt{int}} = 0.1$ (b) $\alpha = 0.7, k_{\texttt{int}} = 0.1$ (c) $\alpha = 0.9, k_{\texttt{int}} = 0.1$ (d) $\alpha = 1.0, k_{\texttt{int}} = 0.1$

(e) $\alpha = 0.5, k_{\texttt{int}} = 0.0$ (f) $\alpha = 0.7, k_{\texttt{int}} = 0.0$ (g) $\alpha = 0.9, k_{\texttt{int}} = 0.0$ (h) $\alpha = 1.0, k_{\texttt{int}} = 0.0$

Figure 54: *System Performance*: Regrets. Numbers are plotted as cumulative sums of system loss less oracle loss.

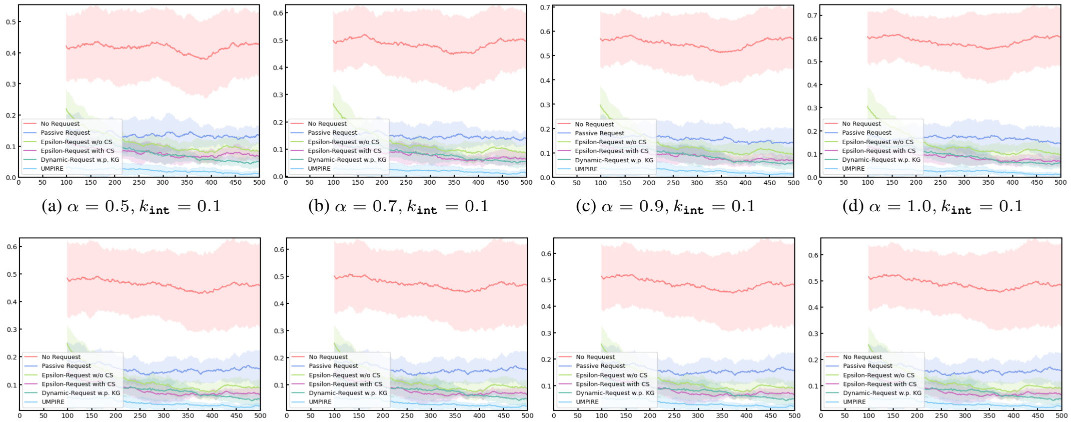

(a) $\alpha = 0.5, k_{\texttt{int}} = 0.1$ (b) $\alpha = 0.7, k_{\texttt{int}} = 0.1$ (c) $\alpha = 0.9, k_{\texttt{int}} = 0.1$ (d) $\alpha = 1.0, k_{\texttt{int}} = 0.1$

(e) $\alpha = 0.5, k_{\texttt{int}} = 0.0$ (f) $\alpha = 0.7, k_{\texttt{int}} = 0.0$ (g) $\alpha = 0.9, k_{\texttt{int}} = 0.0$ (h) $\alpha = 1.0, k_{\texttt{int}} = 0.0$

Figure 55: *System Performance*: Mistakes. Numbers are plotted as moving average of rolling window of width $n/5$.

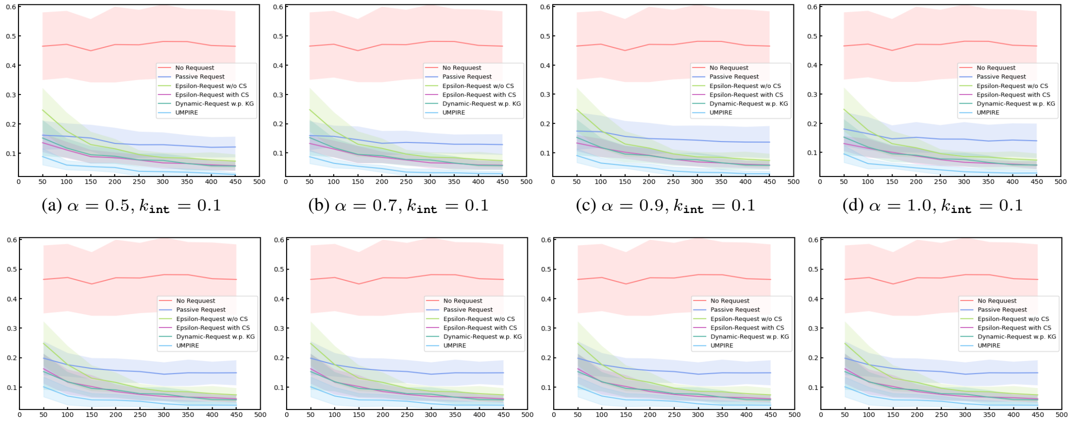

(a) $\alpha = 0.5, k_{\texttt{int}} = 0.1$ (b) $\alpha = 0.7, k_{\texttt{int}} = 0.1$ (c) $\alpha = 0.9, k_{\texttt{int}} = 0.1$ (d) $\alpha = 1.0, k_{\texttt{int}} = 0.1$

(e) $\alpha = 0.5, k_{\texttt{int}} = 0.0$ (f) $\alpha = 0.7, k_{\texttt{int}} = 0.0$ (g) $\alpha = 0.9, k_{\texttt{int}} = 0.0$ (h) $\alpha = 1.0, k_{\texttt{int}} = 0.0$

Figure 56: *Model Performance*: Heldout Mistakes. Models are evaluated on heldout data once every $n/10$ rounds.

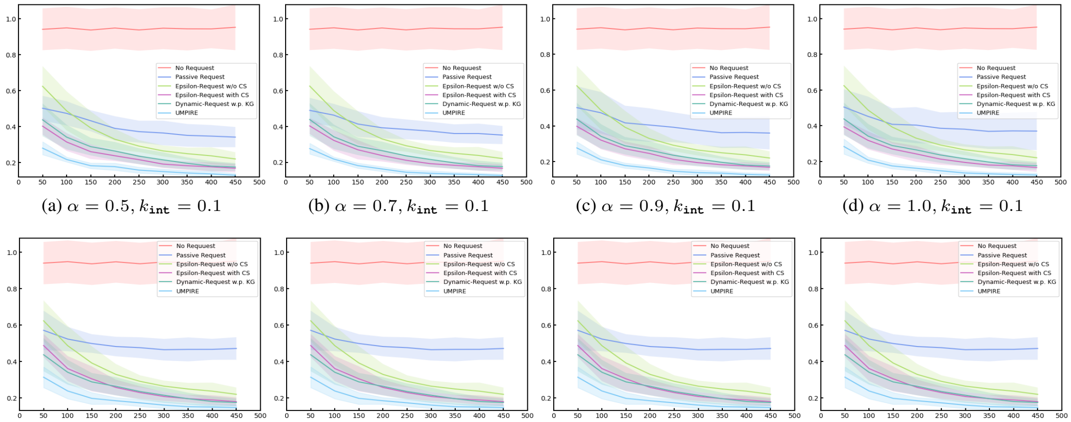

(a) $\alpha = 0.5, k_{\texttt{int}} = 0.1$ (b) $\alpha = 0.7, k_{\texttt{int}} = 0.1$ (c) $\alpha = 0.9, k_{\texttt{int}} = 0.1$ (d) $\alpha = 1.0, k_{\texttt{int}} = 0.1$

(e) $\alpha = 0.5, k_{\texttt{int}} = 0.0$ (f) $\alpha = 0.7, k_{\texttt{int}} = 0.0$ (g) $\alpha = 0.9, k_{\texttt{int}} = 0.0$ (h) $\alpha = 1.0, k_{\texttt{int}} = 0.0$

Figure 57: *Model Performance*: Heldout CrossEnt. Models are evaluated on heldout data once every $n/10$ rounds.

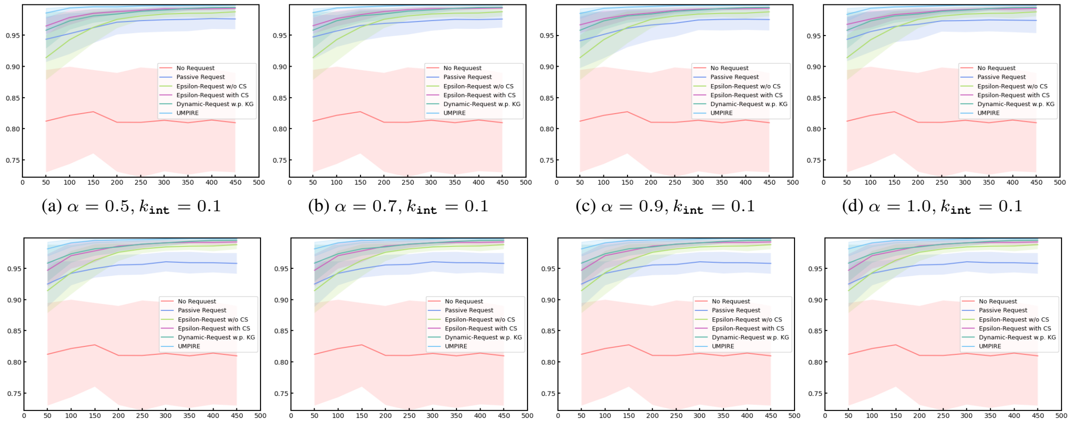

(a) $\alpha = 0.5, k_{\texttt{int}} = 0.1$ (b) $\alpha = 0.7, k_{\texttt{int}} = 0.1$ (c) $\alpha = 0.9, k_{\texttt{int}} = 0.1$ (d) $\alpha = 1.0, k_{\texttt{int}} = 0.1$

(e) $\alpha = 0.5, k_{\texttt{int}} = 0.0$ (f) $\alpha = 0.7, k_{\texttt{int}} = 0.0$ (g) $\alpha = 0.9, k_{\texttt{int}} = 0.0$ (h) $\alpha = 1.0, k_{\texttt{int}} = 0.0$

Figure 58: *Model Performance*: Heldout AUROC. Models are evaluated on heldout data once every $n/10$ rounds.

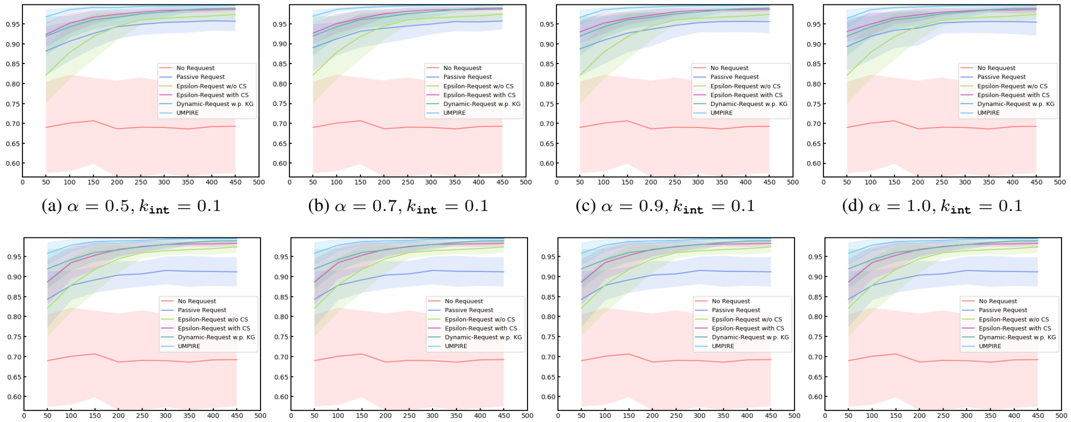

(a) $\alpha = 0.5, k_{\texttt{int}} = 0.1$ (b) $\alpha = 0.7, k_{\texttt{int}} = 0.1$ (c) $\alpha = 0.9, k_{\texttt{int}} = 0.1$ (d) $\alpha = 1.0, k_{\texttt{int}} = 0.1$

(e) $\alpha = 0.5, k_{\texttt{int}} = 0.0$ (f) $\alpha = 0.7, k_{\texttt{int}} = 0.0$ (g) $\alpha = 0.9, k_{\texttt{int}} = 0.0$ (h) $\alpha = 1.0, k_{\texttt{int}} = 0.0$

Figure 59: *Model Performance*: Heldout AUPRC. Models are evaluated on heldout data once every $n/10$ rounds.

## E.7 How Mediation Evolves over Time

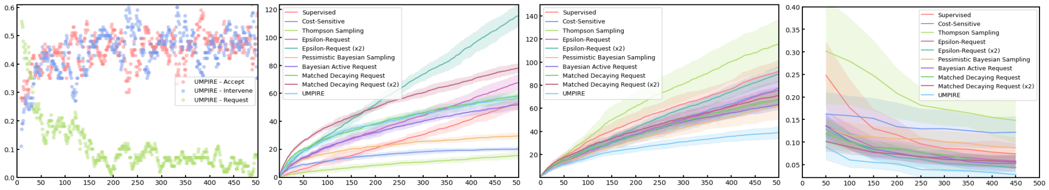

(a) Evolution of Actions (b) Cumulative Requests (c) Cumulative (Sys.) Regret (d) Heldout (Model) Mistakes

Figure 60: Visualization of Evolution of Actions, Cumulative Requests, and System/Model Performances

Intuitively, we would expect a good mediator policy to request more in the beginning, when the model is more likely to learn from expert actions (and more likely to make mistakes otherwise). Figure 60(a) shows how $Z$ evolves over time by visualizing the relative frequencies of each mediator action (i.e. "accept", "intervene", and "request") that UMPIRE issues, using GaussSine as environment. Numbers are plotted as moving averages of windows of length 10 (steps). Moreover, we can also ask how the pattern of "request" actions compares across different methods. Figure 60(b) plots the cumulative progression of request actions for UMPIRE, as well as some other methods for comparison.

Finally, it is worth reiterating here that the bottom-line performance difference between methods (e.g. between UMPIRE and its comparators) is *not* attributable to request frequencies alone—It also depends on *which* samples are being requested. Case in point: Purely based on request frequencies, some methods request less than UMPIRE, some methods request more than UMPIRE, and Matched Decaying Request requests just as frequently as UMPIRE. (Here, we also show an Epsilon-Request "x2" benchmark using twice the ($\epsilon$) rate of requests as the original Epsilon Request, as well as a Matched Decaying Request "x2" benchmark also using twice the ($\epsilon_t$) rate of requests as the original Matched Decaying Request). Yet we see in Figure 60(c)–(d) that UMPIRE still performs better than these comparators, whether they request at more, less, or the same rate. In fact, as we discuss in Section 4.2 and additionally shown in Appendix A.2, UMPIRE's advantage is due to a combination of cost-sensitivity, deliberate exploration, and uncertainty-awareness.

### E.8 Related Work: Human vs. AI to Defer

Literature related to this field can broadly be separated into (1) work that assumes a *machine* is in control, and selectively defers to an expert, and (2) work that assumes the *human* is in control, and selectively relies on machines for help.

The first perspective is often associated with the learning with rejection paradigm, as well as some active learning problem settings, such as those referenced and discussed in Section 2.2. The goal is often to optimize a certain performance metric of the model acting autonomously, with an important choice being when to defer to an expert.

The second perspective is often concerned with how humans themselves should best leverage machines to inform their own behavior in response. For instance, this is associated with "closing the loop" in clinical decision support [74], as well as how to select representative examples to teach the human how a machine learning model operates [102].

Indeed, while these two perspectives are often studied in separate clusters of work, they an and ought to be *complementary*—because in the real world, humans and machines must jointly act as an effective "team"/"system".

In our present work, the ODM objective is to minimize the cumulative *system regret* (in a stream-based setting with abstentive feedback), where an imperfect human is the initial decision-maker, and where a resource-scarce expert is available. In this sense, we are already moving from perspective (1) towards a more holistic view of humans and machines as a team (instead of just measuring model risk alone). In doing so, we focus on how a *mediator* should make suggestions, such that—if its recommendations were accepted—the system regret would be low.

In contrast, some other works have instead started from perspective (2), and then moved towards this more holistic view. In particular, it is important to account for the fact that the human indeed must *choose* whether to accept a model's recommendation, or make decisions on their own [103]—which has important implications for how to design model recommendations in the first place. Thus both perspectives are complementary, and future work would benefit from jointly studying how humans and machines should behave in a mutually-aware fashion [104].

### E.9 Performance w.r.t. Expert Stochasticity

Regarding the performance of UMPIRE in the presence of increasing expert stochasticity, note that the relative advantage between UMPIRE and *any* other benchmark that decreases as noise levels rise, as our estimates of uncertainty become more entangled with noise. This can be observed across the panels of Figures 22, 23, 24, and 25, where most methods begin to "bunch up" more tightly as we read the panels from left to right (beware of the vertical axis scaling). Since Pessimistic Bayesian Sampling generally performs quite well (on GaussSine), it is also true that the relative advantage between UMPIRE and Pessimistic Bayesian Sampling decreases as noise levels rise. However, this phenomenon is *not specific to* Pessimistic Bayesian Sampling. Instead, it is simply that the advantage conferred by UMPIRE's strategy is smaller as the inherent stochasticity of the expert increases.

This is relevant when considering how much stochasticity is present in different real-world settings. For instance, medical diagnosis in particular is known to be a fairly noisy process in the real world—especially in cases where an early diagnosis is required given limited information. In these cases, we would also expect that the advantage conferred by UMPIRE's strategy is smaller. In fact, this is what we can already observe from the performance results: We see slightly smaller advantages for UMPIRE in the Alzheimers and CysticFibrosis environments, relative to other benchmarks.

### E.10 Visualizing the Adjustment Factor

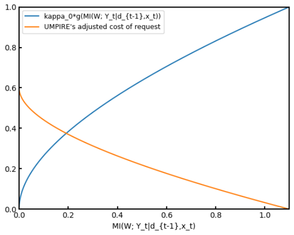

The right-hand-side of Equation 6 is a function of the mutual information ("MI") term $\mathbb{I}[W; Y_t|d_{t-1}, x_t]$, which represents how much the epistemic uncertainty in the model policy is expected to decrease if $Y_t \sim p(\cdot|d_{t-1}, x_t)$ is revealed. Here, we plot $\kappa_0 g(\mathbb{I}[W; Y_t|d_{t-1}, x_t])$ as a function of the inside MI term (using $m = 3$ as in the GaussSine environment). We confirm that it is monotonically increasing, which is in line with our motivation to "translate" the expected decrease in epistemic uncertainty into an upper bound on expected improvement in model risk. We also plot the resulting adjusted cost of request $\bar{k}_{\text{req}}$ (using the base value $k_{\text{req}} = 0.6$ as in the GaussSine environment). We see that this means $\bar{k}_{\text{req}}$ is low in the beginning when the MI term is high, whence UMPIRE behaves like standard incremental learning. In the limit of a perfect model, $\bar{k}_{\text{req}}$ converges to $k_{\text{req}}$ (towards the left side of the graph), whence UMPIRE behaves like the optimal greedy mediator.

### E.11 Applications of the ODM Framework

In addition to clinical decision support, the ODM problem setting is applicable to any scenario where "imperfect" decision-makers are the front-line decision-makers, and "oracle" decision-makers are available as expert supervision—albeit with limited availability, and where learning feedback is abstentive. This situation arises in many settings where the responsibility for a decision must ultimately fall on a *person* (i.e. the imperfect human or the expert), but a *machine* is available for learning and issuing recommendations. Some more examples, in addition to clinical decision support:

**Product Inspection**: A junior employee signs off on the quality of a product batch. The mediator can decide to (1) accept the sign-off *as is*, or (2) recommend a re-inspection due to a disagreeing autonomous prediction as to product quality, or (3) recommend that a more senior employee take over and issue their more qualified assessment.

**Content Moderation**: A user in a social network can report content violations in real time. The mediator can decide to (1) accept and act on the report, or (2) recommend that the user re-classify the content due to a disagreeing assessment as to its appropriateness, or (3) recommend that an internal moderator take over and issue their judgement.

**Spoken-Dialog System**: A customer selects a possibly-nonsensical option in a spoken-dialog system. The mediator can decide to (1) accept the user's option, or (2) recommend that the user re-select an option from the same menu, or (3) re-route the customer to a phone conversation with an actual (human) customer representative to continue the work.

Finally, note that ODM is also applicable in settings where there is no imperfect human involved, so the machine makes decisions with selective expert feedback. Consider setting $k_{\text{int}} = 0$ in ODM: This effectively recovers such a setting, where a machine interacts with an expert (i.e. the imperfect human becomes "redundant"). Note that this does not alter the "hardness" of the ODM problem, which is distinguished by the fact that expert feedback is costly and abstentive.

### E.12 Limitations of the ODM Framework

There are two main limitations of our analysis using the ODM framework:

First, ODM is an *online learning* framework. In general, it is known that online learning may not perform well during the early time steps when an online learner's decisions are largely exploratory, especially if learning proceeds "from scratch". In this sense, UMPIRE as a solution is also not immune to this challenge. Therefore, future work would benefit from examining the potential to *not* learn from scratch—e.g. to "warm-start" a learner using existing data, which can be done using a variety of methods from the extensive literature on imitation learning.

Second, we must recognize that there are *two sides* to human-machine interactions: While ODM focuses on how machines should best propose recommendations to humans, there is also the complementary aspect of how/whether humans actually incorporate such recommendations into their behavior. Ignoring this second aspect may lead to models that are accurate but not necessarily proposing recommendations that are most likely to be complied with—which would severely undermine the practical utility of such a model. Therefore, future work would also benefit from *jointly* studying how humans and machines should behave in a "mutually-aware" fashion.

## References

[1] Gernmanno Teles, Joel JPC Rodrigues, Kashif Saleem, Sergei Kozlov, and Ricardo AL Rabêlo. Machine learning and decision support system on credit scoring. *Neural Computing and Applications*, 32(14):9809–9826, 2020.

[2] Bernhard Kratzwald, Suzana Ilić, Mathias Kraus, Stefan Feuerriegel, and Helmut Prendinger. Deep learning for affective computing: Text-based emotion recognition in decision support. *Decision Support Systems*, 115:24–35, 2018.

[3] Alistair EW Johnson, Mohammad M Ghassemi, Shamim Nemati, Katherine E Niehaus, David A Clifton, and Gari D Clifford. Machine learning and decision support in critical care. *Proceedings of the IEEE*, 104(2):444–466, 2016.

[4] Daniel Jarrett, Alihan Hüyük, and Mihaela Van Der Schaar. Inverse decision modeling: Learning interpretable representations of behavior. *International Conference on Machine Learning (ICML)*, 2021.

[5] Alihan Hüyük, Daniel Jarrett, Cem Tekin, and Mihaela van der Schaar. Explaining by imitating: Understanding decisions by interpretable policy learning. *International Conference on Learning Representations (ICLR)*, 2021.

[6] Constantin A Rothkopf and Christos Dimitrakakis. Preference elicitation and inverse reinforcement learning. *Joint European conference on machine learning and knowledge discovery in databases (ECML)*, 2011.

[7] Iván Sánchez Fernández, Arnold J Sansevere, Marina Gaínza-Lein, Kush Kapur, and Tobias Loddenkemper. Machine learning for outcome prediction in electroencephalograph (eeg)-monitored children in the intensive care unit. *Journal of child neurology*, 33(8):546–553, 2018.

[8] Bryan Lim and Mihaela van der Schaar. Disease-atlas: Navigating disease trajectories using deep learning. In *Machine Learning for Healthcare Conference*, pages 137–160. PMLR, 2018.

[9] Ahmad EL Sallab, Mohammed Abdou, Etienne Perot, and Senthil Yogamani. Deep reinforcement learning framework for autonomous driving. *Electronic Imaging*, 2017(19):70–76, 2017.

[10] Tim Lustberg, Johan van Soest, Mark Gooding, Devis Peressutti, Paul Aljabar, Judith van der Stoep, Wouter van Elmpt, and Andre Dekker. Clinical evaluation of atlas and deep learning based automatic contouring for lung cancer. *Radiotherapy and Oncology*, 126(2):312–317, 2018.

[11] Katerina Lepenioti, Minas Pertselakis, Alexandros Bousdekis, Andreas Louca, Fenareti Lampathaki, Dimitris Apostolou, Gregoris Mentzas, and Stathis Anastasiou. Machine learning for predictive and prescriptive analytics of operational data in smart manufacturing. In *International Conference on Advanced Information Systems Engineering*, pages 5–16. Springer, 2020.

[12] Eyke Hüllermeier. Prescriptive machine learning for automated decision making: Challenges and opportunities. *arXiv preprint arXiv:2112.08268*, 2021.

[13] Samuele Lo Piano. Ethical principles in machine learning and artificial intelligence: cases from the field and possible ways forward. *Nature*, 7(1):1–7, 2020.

[14] Nina Schwalbe and Brian Wahl. Artificial intelligence and the future of global health. *The Lancet*, 395(10236):1579–1586, 2020.

[15] Emanuele Neri, Francesca Coppola, Vittorio Miele, Corrado Bibbolino, and Roberto Grassi. Artificial intelligence: Who is responsible for the diagnosis?, 2020.

[16] Abdullah Awaysheh, Jeffrey Wilcke, François Elvinger, Loren Rees, Weiguo Fan, and Kurt L Zimmerman. Review of medical decision support and machine-learning methods. *Veterinary pathology*, 56(4):512–525, 2019.

[17] Daniel Jarrett, Eleanor Stride, Katherine Vallis, and Mark J Gooding. Applications and limitations of machine learning in radiation oncology. *The British journal of radiology*, 92(1100):20190001, 2019.

[18] Saif Khairat, David Marc, William Crosby, Ali Al Sanousi, et al. Reasons for physicians not adopting clinical decision support systems: critical analysis. *JMIR medical informatics*, 6(2):e8912, 2018.

[19] Bennett P Leifer. Early diagnosis of alzheimer's disease: clinical and economic benefits. *Journal of the American Geriatrics Society*, 51(5s2):S281–S288, 2003.

[20] Susanne G Mueller, Michael W Weiner, Leon J Thal, Ronald C Petersen, Clifford R Jack, William Jagust, John Q Trojanowski, Arthur W Toga, and Laurel Beckett. Ways toward an early diagnosis in alzheimer's disease: the alzheimer's disease neuroimaging initiative (adni). *Alzheimer's & Dementia*, 1(1):55–66, 2005.

[21] Corinna Cortes, Giulia DeSalvo, and Mehryar Mohri. Learning with rejection. In *International Conference on Algorithmic Learning Theory*, pages 67–82. Springer, 2016.

[22] Harish G Ramaswamy, Ambuj Tewari, and Shivani Agarwal. Consistent algorithms for multiclass classification with an abstain option. *Electronic Journal of Statistics*, 12(1):530–554, 2018.

[23] Chenri Ni, Nontawat Charoenphakdee, Junya Honda, and Masashi Sugiyama. On the calibration of multiclass classification with rejection. *Advances in Neural Information Processing Systems*, 32, 2019.

[24] Hussein Mozannar and David Sontag. Consistent estimators for learning to defer to an expert. In *International Conference on Machine Learning*, pages 7076–7087. PMLR, 2020.

[25] Nontawat Charoenphakdee, Zhenghang Cui, Yivan Zhang, and Masashi Sugiyama. Classification with rejection based on cost-sensitive classification. In *International Conference on Machine Learning*, pages 1507–1517. PMLR, 2021.

[26] Kilian Hendrickx, Lorenzo Perini, Dries Van der Plas, Wannes Meert, and Jesse Davis. Machine learning with a reject option: A survey. *arXiv preprint arXiv:2107.11277*, 2021.

[27] Gergely Neu and Nikita Zhivotovskiy. Fast rates for online prediction with abstention. In *Conference on Learning Theory*, pages 3030–3048. PMLR, 2020.

[28] Amin Sayedi, Morteza Zadimoghaddam, and Avrim Blum. Trading off mistakes and don't-know predictions. *Advances in Neural Information Processing Systems*, 23, 2010.

[29] Corinna Cortes, Giulia DeSalvo, Claudio Gentile, Mehryar Mohri, and Scott Yang. Online learning with abstention. In *international conference on machine learning*, pages 1059–1067. PMLR, 2018.

[30] Chicheng Zhang and Kamalika Chaudhuri. The extended littlestone's dimension for learning with mistakes and abstentions. In *Conference on Learning Theory*, pages 1584–1616. PMLR, 2016.

[31] Les Atlas, David Cohn, and Richard Ladner. Training connectionist networks with queries and selective sampling. *Advances in neural information processing systems*, 2, 1989.

[32] David Cohn, Les Atlas, and Richard Ladner. Improving generalization with active learning. *Machine learning*, 15(2):201–221, 1994.

[33] Sanjoy Dasgupta, Daniel J Hsu, and Claire Monteleoni. A general agnostic active learning algorithm. *Advances in neural information processing systems*, 20, 2007.

[34] Alina Beygelzimer, Sanjoy Dasgupta, and John Langford. Importance weighted active learning. In *Proceedings of the 26th annual international conference on machine learning*, pages 49–56, 2009.

[35] Burr Settles. Active learning, 2012.

[36] Giulia DeSalvo, Claudio Gentile, and Tobias Sommer Thune. Online active learning with surrogate loss functions. *Advances in Neural Information Processing Systems*, 34, 2021.

[37] Shubhanshu Shekhar, Mohammad Ghavamzadeh, and Tara Javidi. Active learning for binary classification with abstention. *arXiv preprint arXiv:1906.00303*, 2019.

[38] Nikita Puchkin and Nikita Zhivotovskiy. Exponential savings in agnostic active learning through abstention. In *Conference on Learning Theory*, pages 3806–3832. PMLR, 2021.

[39] Shubhanshu Shekhar, Mohammad Ghavamzadeh, and Tara Javidi. Active learning for classification with abstention. *IEEE Journal on Selected Areas in Information Theory*, 2(2):705–719, 2021.

[40] Yinglun Zhu and Robert Nowak. Efficient active learning with abstention. *arXiv preprint arXiv:2204.00043*, 2022.

[41] Kareem Amin, Giulia DeSalvo, and Afshin Rostamizadeh. Learning with labeling induced abstentions. *Advances in Neural Information Processing Systems*, 34, 2021.

[42] Wei Chu, Lihong Li, Lev Reyzin, and Robert Schapire. Contextual bandits with linear payoff functions. In *Proceedings of the Fourteenth International Conference on Artificial Intelligence and Statistics*, pages 208–214. JMLR Workshop and Conference Proceedings, 2011.

[43] Emilie Kaufmann, Olivier Cappé, and Aurélien Garivier. On bayesian upper confidence bounds for bandit problems. In *Artificial intelligence and statistics*, pages 592–600. PMLR, 2012.

[44] Benedict C May, Nathan Korda, Anthony Lee, and David S Leslie. Optimistic bayesian sampling in contextual-bandit problems. *Journal of Machine Learning Research*, 13:2069–2106, 2012.

[45] Shipra Agrawal and Navin Goyal. Thompson sampling for contextual bandits with linear payoffs. In *International conference on machine learning*, pages 127–135. PMLR, 2013.

[46] Daniel J Russo, Benjamin Van Roy, Abbas Kazerouni, Ian Osband, Zheng Wen, et al. A tutorial on thompson sampling. *Foundations and Trends® in Machine Learning*, 11(1):1–96, 2018.

[47] Tor Lattimore and Csaba Szepesvári. *Bandit algorithms*. Cambridge University Press, 2020.

[48] Alihan Hüyük, Daniel Jarrett, and Mihaela van der Schaar. Inverse contextual bandits: Learning how behavior evolves over time. *arXiv preprint arXiv:2107.06317*, 2021.

[49] Linqi Song and Jie Xu. A contextual bandit approach for stream-based active learning. *arXiv preprint arXiv:1701.06725*, 2017.

[50] András Antos, Varun Grover, and Csaba Szepesvári. Active learning in multi-armed bandits. In *International conference on algorithmic learning theory*. Springer, 2009.

[51] Alexandra Carpentier, Alessandro Lazaric, Mohammad Ghavamzadeh, Rémi Munos, and Peter Auer. Upper-confidence-bound algorithms for active learning in multi-armed bandits. In *International Conference on Algorithmic Learning Theory*. Springer, 2015.

[52] Linqi Song, Jie Xu, and Congduan Li. Active learning for streaming data in a contextual bandit framework. In *Proceedings of the 2019 5th International Conference on Computing and Data Engineering*, pages 29–35, 2019.

[53] David P Helmbold, Nick Littlestone, and Philip M Long. Apple tasting and nearly one-sided learning. In *Proceedings., 33rd Annual Symposium on Foundations of Computer Science*, pages 493–502. IEEE Computer Society, 1992.

[54] David P Helmbold, Nicholas Littlestone, and Philip M Long. Apple tasting. *Information and Computation*, 161(2):85–139, 2000.

[55] James A Grant and David S Leslie. Apple tasting revisited: Bayesian approaches to partially monitored online binary classification. *arXiv preprint arXiv:2109.14412*, 2021.

[56] Sarah Wassermann, Thibaut Cuvelier, and Pedro Casas. Ral-improving stream-based active learning by reinforcement learning. In *European Conference on Machine Learning and Principles and Practice of Knowledge Discovery in Databases (ECML-PKDD) Workshop on Interactive Adaptive Learning (IAL)*, 2019.

[57] Ravi Ganti and Alexander G Gray. Building bridges: Viewing active learning from the multi-armed bandit lens. *arXiv preprint arXiv:1309.6830*, 2013.

[58] Djallel Bouneffouf, Romain Laroche, Tanguy Urvoy, Raphael Féraud, and Robin Allesiardo. Contextual bandit for active learning: Active thompson sampling. In *International Conference on Neural Information Processing*, pages 405–412. Springer, 2014.

[59] David JC MacKay. Information-based objective functions for active data selection. *Neural computation*, 4(4):590–604, 1992.

[60] Neil Houlsby, Ferenc Huszár, Zoubin Ghahramani, and Máté Lengyel. Bayesian active learning for classification and preference learning. *arXiv preprint arXiv:1112.5745*, 2011.

[61] Geoff Pleiss, Jacob R. Gardner, Kilian Q. Weinberger, Andrew Gordon Wilson, and Max Balandat. Exact gp regression on classification labels. *GPyTorch Examples*, 2020.

[62] RK Bock, A Chilingarian, M Gaug, F Hakl, Th Hengstebeck, M Jiřina, J Klaschka, E Kotrč, P Savický, S Towers, et al. Methods for multidimensional event classification: a case study using images from a cherenkov gamma-ray telescope. *Nuclear Instruments and Methods in Physics Research Section A: Accelerators, Spectrometers, Detectors and Associated Equipment*, 516(2-3):511–528, 2004.

[63] Andrew Gardner, Jinko Kanno, Christian A Duncan, and Rastko Selmic. Measuring distance between unordered sets of different sizes. In *Proceedings of the IEEE conference on computer vision and pattern recognition*, pages 137–143, 2014.

[64] Greg Brockman, Vicki Cheung, Ludwig Pettersson, Jonas Schneider, John Schulman, Jie Tang, and Wojciech Zaremba. Openai gym. *OpenAI*, 2016.

[65] John Schulman, Sergey Levine, Pieter Abbeel, Michael Jordan, and Philipp Moritz. Trust region policy optimization. *International Conference on Machine Learning (ICML)*, 2015.

[66] Antonin Raffin. Rl baselines zoo: A collection of pre-trained reinforcement learning agents. `https://github.com/araffin/rl-baselines-zoo`, 2018.

[67] Laurel A Beckett, Michael C Donohue, Cathy Wang, et al. The alzheimer's disease neuroimaging initiative phase 2: Increasing the length, breadth, and depth of our understanding. *Alzheimer's & Dementia*, 11(7):823–831, 2015.

[68] David Taylor-Robinson, Olia Archangelidi, Siobhán B Carr, Rebecca Cosgriff, Elaine Gunn, Ruth H Keogh, Amy MacDougall, Simon Newsome, Daniela K Schlüter, Sanja Stanojevic, et al. Data resource profile: the uk cystic fibrosis registry. *International journal of epidemiology*, 47(1):9–10e, 2018.

[69] Federico P Gómez and Roberto Rodriguez-Roisin. Global initiative for chronic obstructive lung disease (gold) guidelines for chronic obstructive pulmonary disease. *Current opinion in pulmonary medicine*, 8(2):81–86, 2002.

[70] Carl Edward Rasmussen and Christopher KI Williams. Gaussian processes for machine learning. 2006. *Cited on*, page 95, 2014.

[71] Jacob R Gardner, Geoff Pleiss, David Bindel, Kilian Q Weinberger, and Andrew Gordon Wilson. Gpytorch: Blackbox matrix-matrix gaussian process inference with gpu acceleration. In *Advances in Neural Information Processing Systems*, 2018.

[72] Dimitrios Milios, Raffaello Camoriano, Pietro Michiardi, Lorenzo Rosasco, and Maurizio Filippone. Dirichlet-based gaussian processes for large-scale calibrated classification. *Advances in Neural Information Processing Systems*, 31, 2018.

[73] Baptiste Vasey, Stephan Ursprung, Benjamin Beddoe, Elliott H Taylor, Neale Marlow, Nicole Bilbro, Peter Watkinson, and Peter McCulloch. Association of clinician diagnostic performance with machine learning–based decision support systems: a systematic review. *JAMA network open*, 4(3):e211276–e211276, 2021.

[74] Yuchao Qin, Fergus Imrie, Alihan Hüyük, Daniel Jarrett, Mihaela van der Schaar, et al. Closing the loop in medical decision support by understanding clinical decision-making: A case study on organ transplantation. *Advances in Neural Information Processing Systems*, 34, 2021.

[75] Yarin Gal, Riashat Islam, and Zoubin Ghahramani. Deep bayesian active learning with image data. In *International Conference on Machine Learning*, pages 1183–1192. PMLR, 2017.

[76] Andreas Kirsch, Joost Van Amersfoort, and Yarin Gal. Batchbald: Efficient and diverse batch acquisition for deep bayesian active learning. *Advances in neural information processing systems*, 32, 2019.

[77] Andrew Jesson, Panagiotis Tigas, Joost van Amersfoort, Andreas Kirsch, Uri Shalit, and Yarin Gal. Causal-bald: Deep bayesian active learning of outcomes to infer treatment-effects from observational data. *Advances in Neural Information Processing Systems*, 34, 2021.

[78] Hideaki Ishibashi and Hideitsu Hino. Stopping criterion for active learning based on deterministic generalization bounds. In *International Conference on Artificial Intelligence and Statistics*, pages 386–397. PMLR, 2020.

[79] Gábor Bartók and Csaba Szepesvári. Partial monitoring with side information. In *International Conference on Algorithmic Learning Theory*, pages 305–319. Springer, 2012.

[80] Johannes Kirschner, Tor Lattimore, and Andreas Krause. Information directed sampling for linear partial monitoring. In *Conference on Learning Theory*, pages 2328–2369. PMLR, 2020.

[81] Hongju Park and Mohamad Kazem Shirani Faradonbeh. Analysis of thompson sampling for partially observable contextual multi-armed bandits. *IEEE Control Systems Letters*, 6:2150–2155, 2021.

[82] Guy Tennenholtz, Uri Shalit, Shie Mannor, and Yonathan Efroni. Bandits with partially observable confounded data. In *Uncertainty in Artificial Intelligence*, pages 430–439. PMLR, 2021.

[83] Rohin Shah, Pedro Freire, Neel Alex, Rachel Freedman, Dmitrii Krasheninnikov, Lawrence Chan, Michael D Dennis, Pieter Abbeel, Anca Dragan, and Stuart Russell. Benefits of assistance over reward learning. 2020.

[84] Allan Dafoe, Edward Hughes, Yoram Bachrach, Tantum Collins, Kevin R McKee, Joel Z Leibo, Kate Larson, and Thore Graepel. Open problems in cooperative ai. *arXiv preprint arXiv:2012.08630*, 2020.

[85] Dorsa Sadigh, Anca D Dragan, Shankar Sastry, and Sanjit A Seshia. *Active preference-based learning of reward functions*. 2017.

[86] Sören Mindermann, Rohin Shah, Adam Gleave, and Dylan Hadfield-Menell. Active inverse reward design. *arXiv preprint arXiv:1809.03060*, 2018.

[87] Erdem Bıyık, Malayandi Palan, Nicholas C Landolfi, Dylan P Losey, and Dorsa Sadigh. Asking easy questions: A user-friendly approach to active reward learning. *arXiv preprint arXiv:1910.04365*, 2019.

[88] Nils Wilde, Dana Kulić, and Stephen L Smith. Active preference learning using maximum regret. In *2020 IEEE/RSJ International Conference on Intelligent Robots and Systems (IROS)*, pages 10952–10959. IEEE, 2020.

[89] Dylan Hadfield-Menell, Stuart J Russell, Pieter Abbeel, and Anca Dragan. Cooperative inverse reinforcement learning. *Advances in neural information processing systems*, 29, 2016.

[90] Dhruv Malik, Malayandi Palaniappan, Jaime Fisac, Dylan Hadfield-Menell, Stuart Russell, and Anca Dragan. An efficient, generalized bellman update for cooperative inverse reinforcement learning. In *International Conference on Machine Learning*, pages 3394–3402. PMLR, 2018.

[91] Mark Woodward, Chelsea Finn, and Karol Hausman. Learning to interactively learn and assist. In *Proceedings of the AAAI conference on artificial intelligence*, volume 34, pages 2535–2543, 2020.

[92] Dylan Hadfield-Menell. The principal-agent alignment problem in artificial intelligence. 2021.

[93] Umaa Rebbapragada, Carla E Brodley, Damien Sulla-Menashe, and Mark A Friedl. Active label correction. In *2012 IEEE 12th International Conference on Data Mining*, pages 1080–1085. IEEE, 2012.

[94] Ruth Urner, Shai Ben David, and Ohad Shamir. Learning from weak teachers. In *Artificial intelligence and statistics*, pages 1252–1260. PMLR, 2012.

[95] Jan Kremer, Fei Sha, and Christian Igel. Robust active label correction. In *International conference on artificial intelligence and statistics*, pages 308–316. PMLR, 2018.

[96] Mattia Zeni, Wanyi Zhang, Enrico Bignotti, Andrea Passerini, and Fausto Giunchiglia. Fixing mislabeling by human annotators leveraging conflict resolution and prior knowledge. *Proceedings of the ACM on Interactive, Mobile, Wearable and Ubiquitous Technologies*, 3(1):1–23, 2019.

[97] Andrea Bontempelli, Stefano Teso, Fausto Giunchiglia, and Andrea Passerini. Learning in the wild with incremental skeptical gaussian processes. *arXiv preprint arXiv:2011.00928*, 2020.

[98] Stefano Teso, Andrea Bontempelli, Fausto Giunchiglia, and Andrea Passerini. Interactive label cleaning with example-based explanations. *Advances in Neural Information Processing Systems*, 34, 2021.

[99] Chicheng Zhang and Kamalika Chaudhuri. Active learning from weak and strong labelers. *Advances in Neural Information Processing Systems*, 28, 2015.

[100] Songbai Yan, Kamalika Chaudhuri, and Tara Javidi. Active learning from imperfect labelers. *Advances in Neural Information Processing Systems*, 29, 2016.

[101] Shalmali Joshi, Sonali Parbhoo, and Finale Doshi-Velez. Pre-emptive learning-to-defer for sequential medical decision-making under uncertainty. *arXiv preprint arXiv:2109.06312*, 2021.

[102] Hussein Mozannar, Arvind Satyanarayan, and David Sontag. Teaching humans when to defer to a classifier via exemplars. In *Proceedings of the AAAI Conference on Artificial Intelligence*, volume 36, pages 5323–5331, 2022.

[103] Gagan Bansal, Besmira Nushi, Ece Kamar, Eric Horvitz, and Daniel S Weld. Is the most accurate ai the best teammate? optimizing ai for teamwork. In *Proceedings of the AAAI Conference on Artificial Intelligence*, volume 35, pages 11405–11414, 2021.

[104] Gagan Bansal, Besmira Nushi, Ece Kamar, Daniel S Weld, Walter S Lasecki, and Eric Horvitz. Updates in human-ai teams: Understanding and addressing the performance/compatibility tradeoff. In *Proceedings of the AAAI Conference on Artificial Intelligence*, volume 33, pages 2429–2437, 2019.